UNIVERSITY OF CALIFORNIA, SAN DIEGO

Investigating the Role of Turn Motif and Activation Loop Phosphorylation in the Regulation of PKA Structure and Function

A dissertation submitted in partial satisfaction of the requirements for the degree

Doctor of Philosophy

in

Chemistry

by

Jon Martin Steichen

Committee in charge:

Professor Susan S. Taylor, Chair
Professor Daniel Donoghue
Professor Ulrich Muller
Professor Alexandra Newton
Professor Kimberly Prather

2012

The Dissertation of Jon Martin Steichen is approved, and it is acceptable in quality and form for publication on microfilm and electronically:

_____

_____

_____

_____

_____

Chair

University of California, San Diego

2012

DEDICATION

For my parents

TABLE OF CONTENTS

LIST OF ABBREVIATIONS

Å. Angstrom

AGC. Group of kinases including PKA, PKG, and PKC

AKAP. A-kinase anchoring protein

AMP-PNP. Adenylyl-imidodiphosphate

AST. Active site tether

ATP. Adenosine triphosphate

cAMP. Adenosine 3',5'-cyclic monophosphate

CLT. C-lobe tether

C-subunit. The Catalytic Subunit of PKA

C-terminus. Carboxy-terminus

D/D. Dimerization Docking domain

DNA. Deoxyribonucleic Acid

DTT. Dithiothreitol

E. coli. *Escherichia coli*

EDTA. Ethylenediaminetetraacetic acid

EGTA. [ethylenebis(oxyethylenenitrilo)] tetraacetic acid

HM. Hydrophobic motif

IP20. Residues 5-24 of PKI

kDa. Kilodaltons

MES. 2-(N-morpholino) ethanesulfonic acid

mg. milligram

µL. Microliter

$MgCl_2$. Magnesium chloride

mM. millimoles/liter

MOPS. 3-(N-morpholino) propanesulfonic acid

NaCl. Sodium chloride

NLT. N-lobe tether

N-terminus. Amino-terminus

PAGE. Polyacrylamide gel electrophoresis

PBS. Phosphate buffered saline

PDB. Protein data bank

PDK1. Phosphoinositide-dependent protein kinase

PKA. Protein Kinase A or cyclic-AMP Dependent Protein Kinase

PKC. Protein kinase C

PKI. Protein kinase A inhibitor

RSK. p90 ribosomal S6 kinase

R-subunit. The Regulatory Subunit of PKA

SDS. Sodium dodecyl sulfate

TBS. Tris-buffered saline

Tris. Tris Hydroxymethylaminoethane

TM. Turn motif

WT. Wild type

LIST OF FIGURES

LIST OF TABLES

ACKNOWLEDGEMENTS

I would like to thank my advisor, Dr. Susan Taylor for providing direction, constant support and encouragement, and a lot of freedom to explore numerous areas of research, which helped me in broadening my scientific understanding. I also would like to thank her for encouraging me to attend numerous scientific meetings throughout the world, which has given me exposure to several areas of research outside my immediate field, and allowed me to experience other cultures around the globe.

I wish to thank my thesis committee members, Dr. Daniel Donoghue, Dr. Ulrich Muller, Dr. Alexandra Newton, and Dr. Kimberly Prather, for giving me lots of helpful ideas during committee meetings as well as in the numerous talks that I presented throughout graduate school.

I greatly appreciate all the help received from Dr. Elizabeth Komives throughout graduate school. She has always been there to help me trouble shoot any biophysical chemistry experiment. Thanks are also due to Dr. Virgil Woods and Dr. Sheng Li for all the assistance with H/D exchange experiments, and Dr. Joseph Adams with kinetic studies.

Thanks to all the current and former members of the Taylor lab who have helped me with my research and made my graduate school experience fun and memorable. I am grateful to Jie Yang who has been a great mentor and taught me almost every experimental technique that I know today. Additionally, she inspired me

in many ways and provided me much moral support whenever I needed that helped me to become a better person. Manjula Darshi has been my best friend since joining the lab five years ago and has always been there whenever I needed, whether it is just walking for a cup of coffee, analyzing my gels or helping with stressful presentations. Mike Kuchinskas was always fun to spend time with, in the lab or outside the lab during hiking trips and he also taught me crystallography and provided me a lot of help with the R194A structure. Adam has been a great bay mate and friend, and it is always fun to beat him in a game of pool. Having Kristina work in the bay in this last year provided plenty of entertainment that made research fun and simple. Hiruy has become a good friend in the past year and it's great to discuss ideas with him about science in the lab and more interesting topics outside the lab. Chris Eggers could answer any of my questions when nobody else had answers. Sarma and Jian were always there to help me with crystallography problems.

I would also like to thank all other members of the Taylor lab who have helped me out along the way including Mira, Michele, Angie, Mike Deal, Cecilia, C.J. Allison, Alexandr, Sventja, Jeff, Ronit, Malik, and Phil. Special word of thanks to all the administrative assistants: Juniper Pennypacker, Carolyn Huttenmaier, Cindy Boulton and Grace Liu for their timely help during my stay in the Taylor lab.

I would also like to thank my friends from the Chemistry Department and BMS program, Brian Fuglestad, Rich Fair, Jeff Brodin and Loren Brown for late night hangouts, often needed outside the lab.

Last but never the least, I am forever indebted to my parents Edward and Agnes, sister Jenny, and brother Matthew for their constant support and love in all of

the, sometimes short lived careers, that I chose. They always believed in me and provided me with all the help whenever I needed and encouraged me to do my best in every aspect of life.

Chapter 1, in part, has been accepted for publication as Evolution of the eukaryotic protein kinases as dynamic molecular switches. Taylor, S.S., Keshwani, M.M., Steichen, J.M., Kornev, A.P. *Philosophical Transactions B*. The dissertation author was a secondary author of this work.

Chapter 2, in part, was published as Global Consequences of Activation Loop Phosphorylation on Protein Kinase A. Steichen JM, Iyer GH, Li S, Saldanha SA, Deal MS, Woods VL Jr, Taylor SS. *J. Biol. Chem*. 2010 Feb 5; 285(6):3825-32. The dissertation author was the primary investigator and author of this work.

Chapter 3 in its entirety was published in Structural Basis for the Regulation of Protein Kinase A by Activation Loop Phosphorylation. Steichen JM, Kuchinskas M, Keshwani MM, Yang J, Adams JA, Taylor SS. *J. Biol. Chem*. 2012 Apr 27;287(18):14672-80. The dissertation author was the primary investigator and author of this work.

Chapter 5, in part, was published as A conserved Glu-Arg salt bridge connects co-evolved motifs that define the eukaryotic protein kinase fold. Yang, J., Wu, J., Steichen, J.M., Kornev, A., Deal, M.S., Li, S., Sankaran, B., Woods, V.L. Jr, and Taylor, S.S. *J. Mol. Biol*. 2012. Jan 27: 415(4):666-679. The dissertation author was a secondary investigator and author of this work.

VITA

Education

2012 Ph.D., Chemistry
University of California, San Diego

2010 M.S., Chemistry
University of California, San Diego

2006 B.S., Biochemistry
University of Wisconsin, Madison

Publications

Taylor, S.S., Keshwani, M.M., **Steichen, J.M.**, Kornev, A.P. Evolution of the eukaryotic protein kinases as dynamic molecular switches. ***Philosophical Transactions B*** (Accepted for publication).

Bastidas, A.C., Deal, M.S., **Steichen, J.M.**, Keshwani, M.M., and Taylor, S.S. Role of N-terminal myristylation in the structure and regulation of cAMP-dependent protein kinase. J. Mol. Biol. 2012. May 19

Steichen, J.M., Kuchinskas, M., Keshwani, M.M., Yang, J., Adams, J.A., and Taylor, S.S. Structural basis for the regulation of protein kinase A by activation loop phosphorylation. ***J. Biol. Chem.*** 2012. April 27: 287(18):14672-80.

Yang, J., Wu, J., **Steichen, J.M.**, Kornev, A., Deal, M.S., Li, S., Sankaran, B., Woods, V.L. Jr, and Taylor, S.S. A conserved Glu-Arg salt bridge connects co-evolved motifs that define the eukaryotic protein kinase fold. ***J. Mol. Biol.*** 2012. Jan 27: 415(4):666-679.

Steichen, J.M., Iyer, G.H., Li, S., Saldanha, S.A., Deal, M.S., Woods, V.L. Jr, and Taylor, S.S. Global consequences of activation loop phosphorylation on protein kinase A. ***J. Biol. Chem.*** 2010. Feb 5: 285(6):3825-3832.

Steichen, J.M., Petty, R.V., and Sharkey, T.D. Domain characterization of a 4-α-glucanotransferase essential for maltose metabolism in photosynthetic leaves. ***J. Biol. Chem.*** 2008. July 25: 283(30):20797-20804

Lu, Y., **Steichen, J.M**., Yao, J., and Sharkey, T.D. The role of cytosolic alpha-glucan phosphorylase in maltose metabolism and the comparison of amylomaltase in *Arabidopsis* and *Escherichia coli*. ***Plant physiology***. 2006 Nov: 142(3):878-889.

Lu, Y., **Steichen, J.M**., Weise, S.E., and Sharkey, T.D. Cellular and organ level localization of maltose in maltose-excess *Arabidopsis* mutants. ***Planta***. 2006 Sep: 224(4):935-943.

ABSTRACT OF THE DISSERTATION

Investigating the Role of Turn Motif and Activation Loop Phosphorylation in the Regulation of PKA Structure and Function

by

Jon Martin Steichen

Doctor of Philosophy in Chemistry

University of California, San Diego, 2012

Professor Susan S. Taylor, Chair

The catalytic (C) subunit of cAMP-dependent protein kinase (PKA) is a member of the AGC group of protein kinases. PKA has served as a structural and biochemical prototype for understanding the protein kinase superfamily. In cells, PKA is regulated primarily by three different mechanisms: cAMP binding to the regulatory subunits, PKI, and phosphorylation on the turn motif and activation loop. The main

focus of this dissertation was to investigate the role of turn motif and activation loop phosphorylation on the regulation of PKA structure and function.

The molecular basis for activation loop (Thr197) phosphorylation was explored using biochemical and structural methods. An X-ray crystal structure of the unphosphorylated C-subunit revealed that the N- and C-lobes of the kinase were separated and there was a dramatic loss in hydrogen bonding at the active site. These changes were correlated with a decrease in activity, loss of stability, and increased dynamics of the enzyme as measured by hydrogen/deuterium exchange.

Next, the role of turn motif (Ser338) phosphorylation in the C-terminal tail of PKA was investigated by structural and biochemical methods. Even though the structure of the unphosphorylated protein was similar to wild type PKA, our studies showed that the phosphorylation at the turn motif was a necessary precursor for activation loop phosphorylation, and is essential for maintaining normal PKA activity in mammalian cells.

Finally, the phosphoinositide-dependent protein kinase (PDK1) is known to phosphorylate the activation loops of numerous AGC kinases. We sought to determine the molecular basis for substrate recognition and activation loop phosphorylation by PDK1. An internal Glu-Arg salt bridge was found to be a critical nonlinear recognition motif in all PDK1 substrates tested. This salt bridge is highly conserved and disease-associated SNPs at the Glu and Arg positions have been found in numerous protein kinases indicating that this may be a common recognition motif in the protein kinase superfamily.

Chapter 1

Introduction

Signal transduction is pivotal for almost all fundamental cellular processes- metabolism, migration, proliferation and apoptosis, to name a few. Deregulation in these pathways has been linked to a variety of human diseases (Hunter, 2000). Control of cell signaling occurs at many levels. The most common include binding of metabolites, co-factors or chemical messengers that allosterically modulate the activity of the enzymes and trigger the network of signaling cascades. Binding of hormones or ligands (first messengers) to cell surface receptors initiate a series of events, which leads to generation of the 'second messengers' that relays signals into the cell, eliciting a physiological response. These molecules greatly amplify the strength of the signal from the receptors to the target molecules inside the cell, and thus play a prominent role in the signaling cascade. Some of the principle second messengers are cyclic adenosine monophosphate (cAMP), cyclic guanidine monophosphate (cGMP), calcium ion (Ca^{+2}), inositol 1,4,5-trisphosphate (IP3), Diacyl glycerol (DAG) and nitric oxide (NO). In addition to this, post-translational modification and protein-protein interactions contribute to the cell signaling events. Protein phosphorylation, dephosphorylation, ubiquitination, acetylation, myristylation, palmytylation, sulfonation, and neddylation are some of the post-translational modifications that are important in regulating signaling events at the molecular levels. Among these, protein phosphorylation/dephosphorylation is the most commonly studied area since it is central to the regulation of most aspects of cellular processes and it is discussed in detail in the following section.

1.1 Protein Phosphorylation

The reversible, covalent attachment of a phosphate group to a protein, known as protein phosphorylation, was first identified as a regulatory mechanism for protein activity in the 1950s from the work of Eddie Fisher and Ed Krebs. They showed that the activation of glycogen phosphorylase *b* to glycogen phosphorylase *a* was dependent on a protein together with ATP (Fischer and Krebs, 1955). The phosphorylation of a protein can have a wide variety of effects in the cell ranging from altering the activity of an enzyme to providing docking sites for other proteins to increasing/decreasing the stability of a protein. Phosphorylation provides the molecular basis for a vast network of signal transduction pathways. It has been estimated that approximately 30% of proteins can be modified by phosphorylation in eukaryotic cells at some stage and thus they are one of the most significant driving forces of signal transduction (Olsen et al., 2006; Ptacek et al., 2005). Protein phosphorylation is catalyzed by a family of enzymes known as the protein kinases. The human genome contains 518 protein kinases, described in 2002 as the human kinome (**Fig. 1.1**), which makes up ~2% of the genome (Manning et al., 2002). In addition to the 518 protein kinases, the human genome contains 1,543 signalling receptors and ~150 protein phosphatases, which can reverse the action of kinases by removing phosphate groups (Papin et al., 2005). Thus, with an estimated 25,000 genes in the human genome, nearly 10% may contribute to the regulation of proteins by phosphorylation.

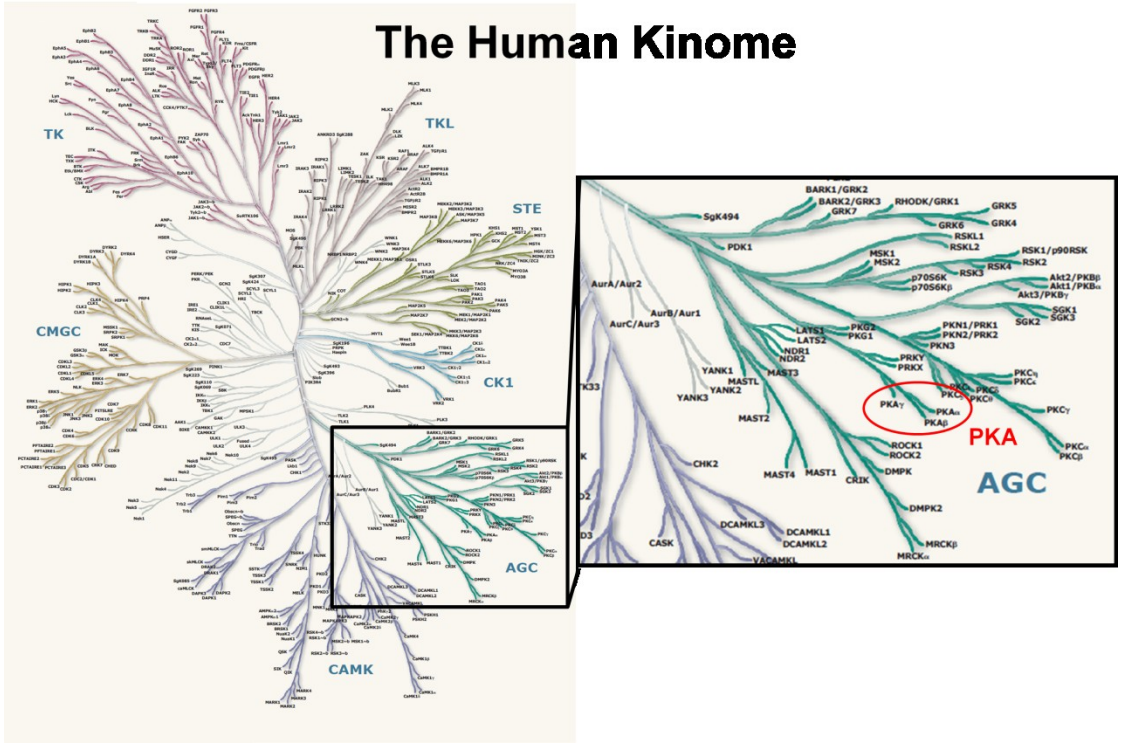

Figure 1.1. The Human Kinome. The seven major groups of the human kinome are shown with the AGC group highlighted. PKA as well as ~60 other Ser/Thr kinases belong to the AGC group. Taken from Manning et al. (2002) *Science* 298:1912.

1.2 Protein Kinases

Protein kinases are the class of enzymes that catalyze the transfer of the gamma phosphate from ATP to the hydroxyl group of a serine, threonine, or tyrosine residue on the substrate protein. There are two main subcategories of protein kinases based on the chemical reactions they catalyze. The Ser/Thr protein kinases phosphorylate serine or threonine side chains and the Tyr kinases phosphorylate tyrosine side chains. The dual-specific protein kinases are capable of phosphorylating Ser, Thr, or Tyr residues (Dhanasekaran and Premkumar Reddy, 1998). In addition to this, there are catalytically inactive proteins retaining the conserved kinase fold but lacking key catalytic residues, known as pseudokinases (Scheeff et al., 2009). Because of their lack of kinase activity, the biological function of this family has been unclear. However, some are considered as protein scaffolds bringing together the components of signaling networks, as well as being allosteric activators of protein kinases (Zeqiraj and van Aalten, 2010). Additionally, there are histidine-specific protein kinases in prokaryotes, fungi, and plants but these are structurally unrelated to the eukaryotic protein kinase superfamily (Wolanin et al., 2002). In humans, relative amounts of phosphorylation on serine, threonine, and tyrosine is approximately 86, 12, and 2% respectively (Olsen et al., 2006). Although tyrosine phosphorylation is less common than serine and threonine, many cytoplasmic oncoproteins possess Tyr kinase activity. Additionally, membrane receptors for growth factors are also Tyr kinases making them important targets for cancer therapy (Gschwind et al., 2004).

The human kinome has been classified into seven major groups based on evolutionary relationships (**Fig. 1.1**): AGC [including protein kinase A (PKA), protein

kinase G (PKG), and protein kinase C (PKC)], CaMK (Ca^{+2}/calmodulin-regulated kinases), CK1 (casein kinase 1), CMGC [including cyclin-dependent kinases (CDKs), mitogen-activated protein kinases (MAPKs), glycogen synthase kinase (GSK), and CDK-like kinases], STE (related to yeast sterile kinases), TK (tyrosine kinases), and TKL (tyrosine-kinase like). Additionally, there are aPKs (atypical protein kinases) that lack the kinase fold but are reported to have kinase activity.

Given the important role of protein phosphorylation in signal transduction and protein kinases being key regulators of most cellular pathways it is not surprising that over 180 protein kinases have been associated with human disease (http://www.cellsignal.com/reference/kinase_disease.html). Diseases range from numerous types of cancer, cardiovascular disease, diabetes, neurodegenerative disease, epilepsy, blindness, developmental diseases, inflammation, and others. Protein kinases have now become the second most important group of drug targets after G-protein coupled receptors (GPCRs) (Cohen, 2002; Johnson, 2009). Currently there are ~20 FDA approved drugs which target protein kinases with the vast majority targeting tyrosine kinases. Because all kinases require ATP in order to function, a common strategy for drug/inhibitor design has been to target the ATP binding pocket. The major problem associated with this strategy is that, with such a large protein family, inhibitors that target the ATP binding pocket lack specificity (**Fig. 1.2**). When comparing protein kinases in their active states, the active sites are remarkably similar. However, a comparison of the inactive states has shown a much greater degree of

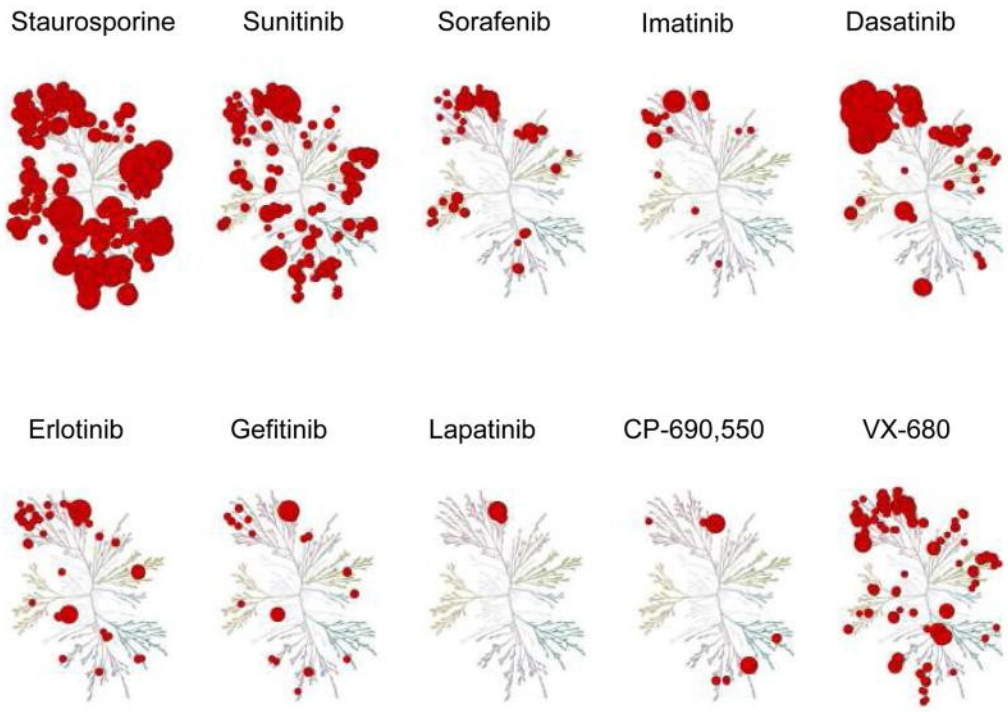

Figure 1.2. The inhibitor specificity maps of the various protein kinase inhibitors. The larger the diameter of the circle the stronger the inhibition. Taken from Ghoreschi et al. (2009) *Nature immunology* 10, 356-360.

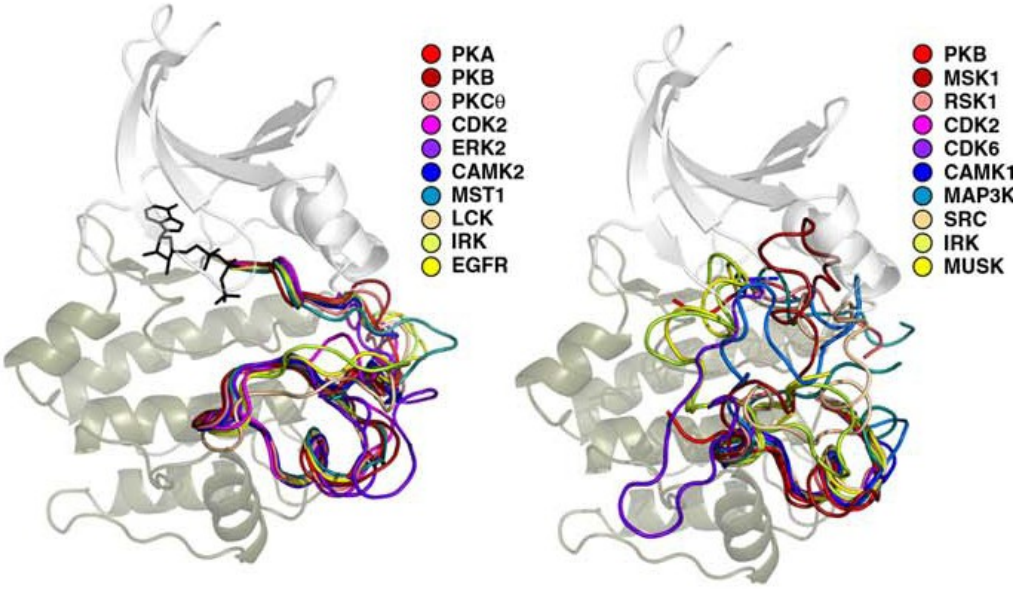

Figure 1.3. Structural alignment of active (left) and inactive (right) kinases. Alignment of kinases in their active states and inactive states shows the activation loop is very similar in the active kinases but takes on diverse orientations in the inactive states. Taken from Taylor et al. (2011) *Trends Biochem Sci*. Feb; 36(2) 65-77.

diversity between kinases (**Fig. 1.3**) and this property has led to the idea that targeting the inactive states of kinases may provide greater specificity for inhibitors. Additionally, because there is now a significant "structural" kinome available that contains over 150 unique protein kinases, many of the general features of the eukaryotic protein kinase superfamily as well as features that are associated with each subfamily have been elucidated. This has allowed for the design of inhibitors with higher selectivity and some inhibitors have already been developed which can bind selectively to the inactive state, such as imatinib, an inhibitor of Bcr-Abl.

1.3 cAMP-Dependent Protein Kinase (Protein Kinase A)

cAMP-dependent protein kinase, also called protein kinase A or PKA is a member of the AGC group of protein kinases. The AGC kinases make up a well studied group that contain about 60 Ser/Thr protein kinases which include PKA, PKG, and PKC among others. This group of proteins shares a high degree of sequence similarity in their catalytic domains, however they differ in the organization of regulatory domains. For example, while the catalytic and regulatory domains of PKC and PKG are fused, they are distinct proteins for PKA. This makes PKA an excellent model system to study the individual components. In cells, PKA exists as a tetrameric holoenzyme composed of two catalytic (C) subunits and two regulatory (R) subunits (**Fig. 1.4**). The R-subunits function as receptors for cAMP, and serve to inhibit the C-subunits in the absence of cAMP. cAMP is generated from adenylyl cyclase in response to ligand induced activation of GPCRs (Ross et al., 1977). PKA is activated

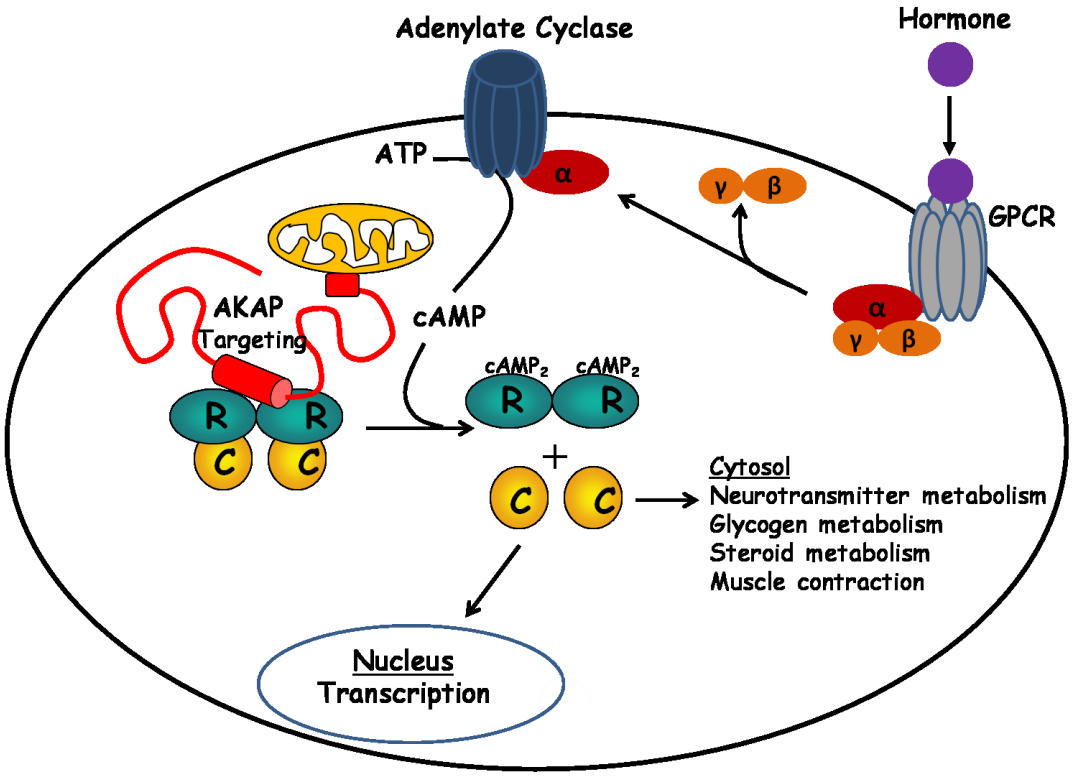

Figure 1.4. cAMP dependent activation of PKA in cells. PKA exists as a tetramer in cells composed of two R-subunits and two C-subunits. It is activated when cAMP binds to the R-subunits releasing the C-subunits. The holoenzyme complex is localized within the cell by binding to AKAPs.

through the binding of cAMP to the R-subunits, resulting in dissociation of the holoenzyme, release of the active C-subunits, and subsequent phosphorylation of downstream substrates like ion channels, key metabolic enzymes and transcription factors. In humans, there are three isoforms of the C-subunit (Cα, Cβ, Cγ), which differ primarily at the N-terminus of the protein and there are four functionally non-redundant R-subunits (RIα, RIβ, RIIα, RIIβ). The C-subunit also requires phosphorylation at its activation loop for full activity. This will be addressed in more detail in later sections of this chapter.

The localization and targeting of PKA to a specific set of substrates in the cell is achieved by binding of the R-subunits to scaffolding proteins, the best known being the A Kinase Anchoring Proteins (AKAPs) (Wong and Scott, 2004). The AKAPs are characterized by an amphipathic helix that binds with high affinity to the dimerization/docking (D/D) domain of the R-subunits (Sarma et al., 2010). In addition to PKA, AKAPs have also been known to assemble other signaling proteins including phosphatases, phosphodiesterases, adenylyl cyclases, and GTPases (Beene and Scott, 2007). Thus, AKAPs regulate PKA activity spatially and temporally through assembly of multimeric signaling scaffolds that include upstream activators, negative regulators, specific substrates and other signaling enzymes. Therefore, the cAMP signaling network is defined by the GPCRs, PKAs, and AKAPs expressed in each cell.

The domain organization of the R-subunits consists of a stable dimerization/docking domain at the N-terminus, followed by a flexible linker that is classified as an intrinsically disordered region (IDR). Embedded within the linker is an inhibitor site (IS) that resembles a substrate and docks to the active site cleft in the

C-subunit, and blocks access to other substrates. At the C-terminus are two cyclic nucleotide binding (CNB) domains. The very stable helical dimerization domain is multi-functional. In addition to creating a stable dimer, it serves as a docking site for AKAPs.

In addition to the R-subunits, the catalytic subunit is also inhibited by the small heat-stable inhibitor of protein kinase A (PKI). PKI is a 77 amino acid protein that is widely expressed in many cell types. It binds to the active site cleft like a pseudosubstrate and inhibits the activity of the C-subunit. It has also been shown to export the C-subunit from the nucleus to the cytosol (Fantozzi et al., 1994). A 20-amino acid peptide (residues 5-24) from PKI binds with high affinity to the C-subunit and has been instrumental in obtaining high resolution X-ray crystal structures of the C-subunit (Knighton et al., 1991b). The PKA co-crystallized with PKI was the first protein kinase to be crystallized and this structure not only defined the overall architecture of the kinase core, but also revealed how a protein kinase recognizes substrates. Using PKA as a model has defined how our understanding of the structure and regulation of one protein kinase can serve as a proto-type for the overall family.

Our understanding of PKA signaling has improved significantly over the years not only because more than 100 crystal structures of the C-subunit have been deposited in the protein data bank but also complexes between the R- and C-subunits (**Fig. 1.5**). The structure of an R:C complex (Kim et al., 2005) showed not only how the IS docked to the active site cleft of the C-subunit but also how the inhibition could be allosterically released by cAMP binding to the CNB domain. Recently the X-ray

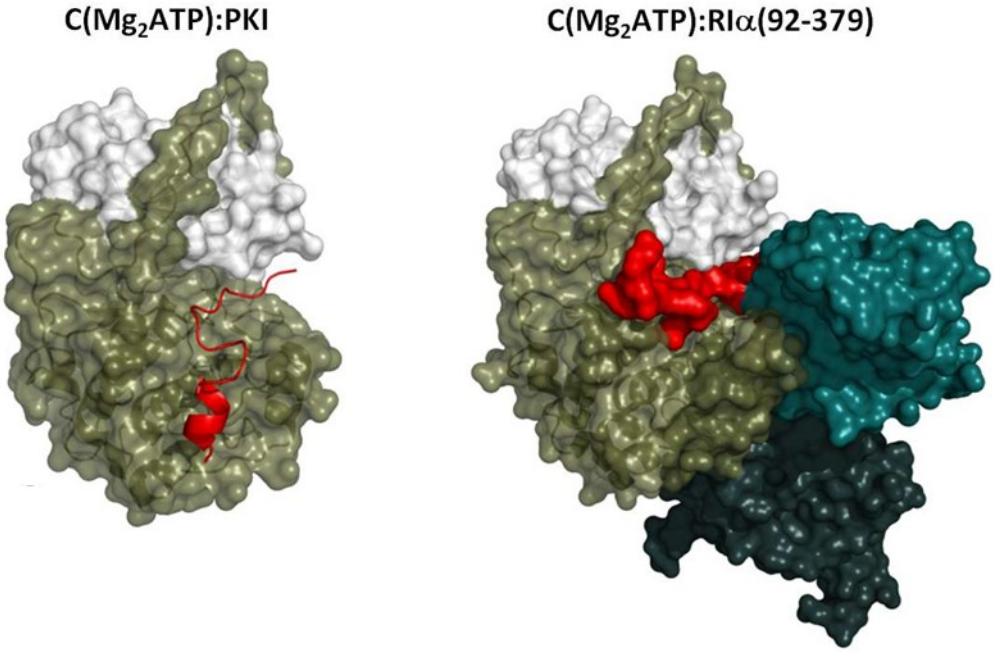

Figure 1.5. Crystal structure of PKA C-subunit in complex with PKI (left) and R1α (right). PKA C-subunit (olive and gray) bound to residues 5-24 of PKI (red). C-subunit bound to the regulatory subunit-I with inhibitor site (red), CNB-A (teal), and CNB-B (dark gray).

crystal structure of two tetrameric holoenzymes (RIβ and RIIβ) have been solved and it was found that each tetrameric holoenzyme has a unique quaternary structure in spite of the highly conserved domain organization of each R-subunit and the very similar tertiary structure of each heterodimer (Ilouz and Taylor, unpublished data) (Zhang et al., 2012). These differences, first predicted by small angle X-ray scattering studies (Heller et al., 2004; Vigil et al., 2006), are now confirmed with these recent holoenzyme structures. The RIIβ holoenzyme (Zhang et al., 2012), for example, is strikingly different from the RIα holoenzyme model (Boettcher et al., 2011). These differences support the idea that the PKA catalytic subunit is assembled as part of four functionally distinct holoenzyme complexes that are then localized to discrete foci in the cell where they are dedicated to the phosphorylation of a specific substrate or set of substrates that are co-localized in close proximity through scaffold and targeting proteins.

1.4 Eukaryotic Protein Kinase Core

The eukaryotic protein kinase superfamily is defined by a conserved kinase core. This core consists of a bilobal structure of approximately 250 residues that contains most of the essential machinery for catalysis and for scaffolding, the two functions that are essential for downstream signaling (**Fig. 1.6**). Scattered throughout the core are specific conserved sequence motifs that were classified early on into 12 subdomains by Hanks and Hunter (Hanks and Hunter, 1995). Once the crystal structure of PKA was solved, these motifs could be defined in terms of their putative function (Knighton et al., 1991a; Knighton et al., 1991b). Each lobe is made up of

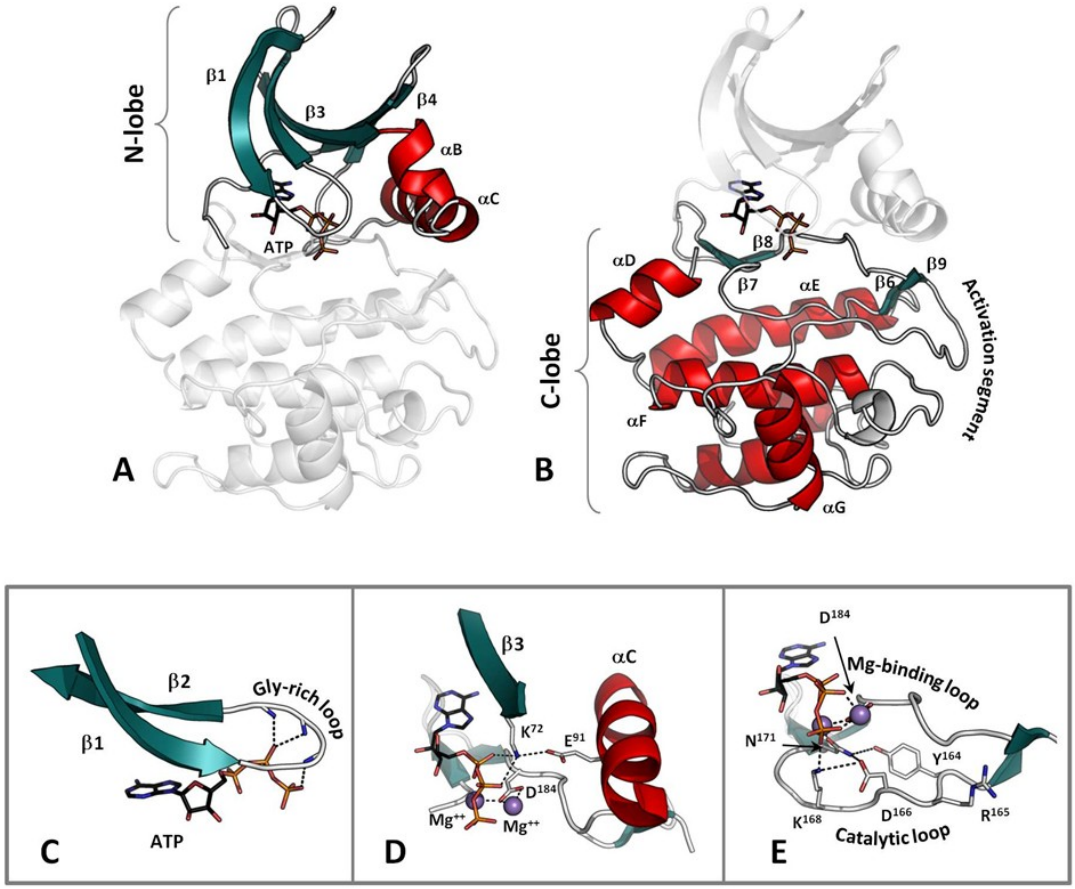

Figure 1.6. Structure of protein kinase A C-subunit showing the conserved core of the eukaryotic protein kinases. The bottom panels (C-E) highlight functional motifs in the N-lobe (C) and the C-lobe (D and E). Helices are shown in red; β-strands in teal. **A**) The N-lobe contains five β-strands and a large αC-helix. **B**) The C-lobe is mostly helical with a large Activation segment. A four stranded β-sheet rests on the helical core and forms one surface of the active site cleft. ATP is bound in the cleft between the two lobes. **C**) The phosphates of ATP are positioned by a conserved Glycine-rich loop between the β1 and β2-strands. **D**) Conserved residues Lys72 from β3-strand, Glu91 from the αC-helix, and Asp164 from the DFG-motif in the Activation segment where Mg^{++} ions are show as tan balls **E**) The Catalytic Loop also contains a set of catalytically important residues: Asp166, Lys168, Asn171.

helical and beta subdomains, and the active site cleft is formed by the two lobes converging to form a deep cleft where the adenine ring of ATP is bound. In this configuration, which is quite distinct from the Walker motif that is associated with most other ATP binding proteins (Ramakrishnan et al., 2002), the γ-phosphate is positioned at the outer edge of the cleft where phosphoryl transfer takes place. Catalysis is mediated by opening and closing of the active site cleft allowing for transfer of the phosphate and then release of the nucleotide.

The N-terminal lobe (N-lobe) consists of a five-stranded anti-parallel beta sheet, which is an essential part of the ATP binding mechanism (**Fig. 1.6A**). Between β3 and β4 is the single conserved helix, the αC-helix. β-strands 1 and 2 are joined by a glycine-rich loop, and this loop packs on top of the ATP with a backbone amide at the tip of the loop anchoring the γ-phosphate and positioning it for phosphoryl transfer (**Fig. 1.6C**). β-strand 3 contains an essential Lys (Lys72 in PKA) that couples to a conserved Glu (Glu91 in PKA) in the αC-helix (**Fig. 1.6D**). The conserved helical subdomain in the N-lobe of PKA and other AGC kinases contains a short αB-helix and a long αC-helix. The αB-helix is not conserved in all kinases, but the αC-helix is an essential conserved feature of every protein kinase. When a kinase is in an active conformation, the N-terminus of the αC-helix typically interacts with the activation loop phosphate, while the C-terminus is part of the hinge at the base of the active site cleft.

In contrast to the N-lobe, the C-terminal lobe (C-lobe) is mostly helical and quite stable (**Fig. 1.6B**). The αE, αF, and αH helices, based on hydrogen deuterium

exchange, for example, are very stable and do not exchange much with solvent even after several days (Yang et al., 2005). Resting on the helical core is a four-stranded β sheet, which contains most of the remaining catalytic residues (**Fig. 1.6E**). This β sheet forms the bottom surface of the active site cleft as seen in the classic view of a protein kinase. Between β-strands 6 and 7 lies the catalytic loop (H/YRDXKXXN), which corresponds to subdomain VIb. This segment contains many of the key residues that direct the γ-phosphate of ATP to the protein substrate as well as the catalytic base Asp166 which positions the substrate serine for catalysis. Between β-strands 8 and 9, referred to as the magnesium positioning loop, is the DFG motif where a conserved aspartate (Asp184 in PKA) binds to the catalytic magnesium ions. Although substrates can be tethered to either the N-lobe or the C-lobe or through a flanking domain or linker in a way that positions the P-site to serve as the acceptor for the γ-phosphate, most are tethered to the C-lobe. This peptide containing the phosphorylation site (Ser, Thr, or Tyr) lies along the outer surface of the C-lobe near the active site cleft.

The Activation Loop - The eukaryotic protein kinases are distinguished from the closely related eukaryotic-like kinases by the presence of a loop surrounding the active site cleft called the activation loop. As the name implies, this is a key site regulating the activation of nearly every eukaryotic protein kinase (**Fig. 1.7**). The activation loop is highly dynamic and is typically assembled in its active conformation by the addition of a phosphate that is mediated by either *cis* or *trans* autophosphorylation or by the action of a heterologous activating kinase (*trans*). In the

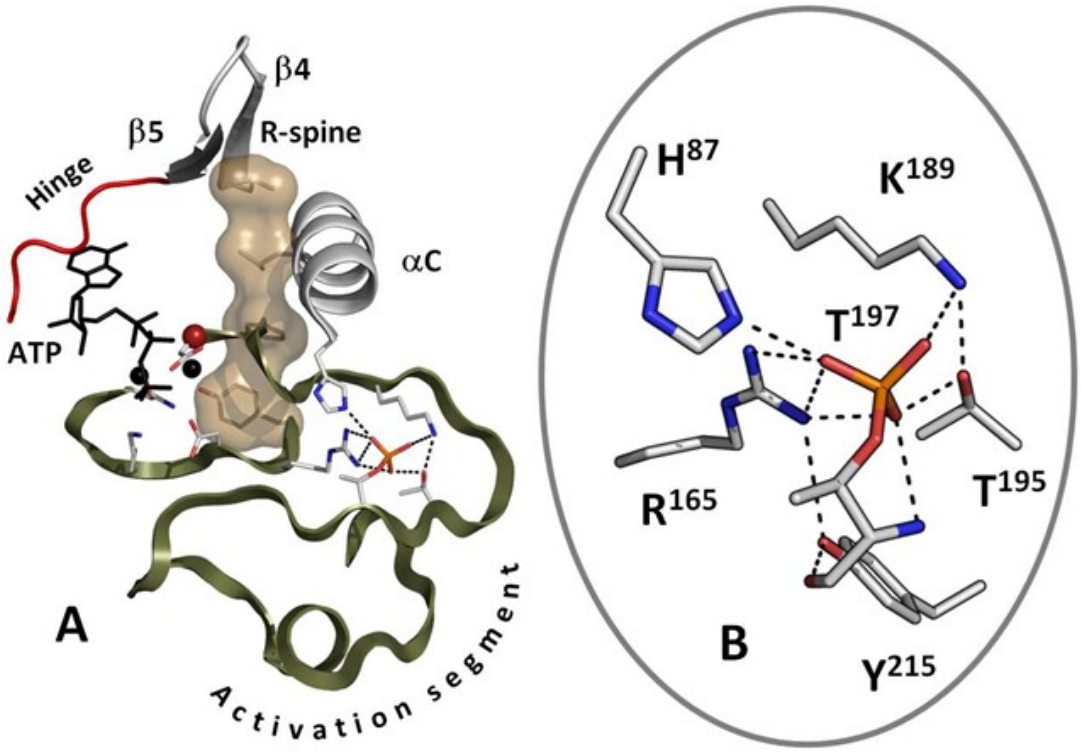

Figure 1.7. The activation loop of PKA depicting the network of interactions mediated by the phosphate at Thr197. (**A**) The activation loop bridges the magnesium positioning loop to the catalytic loop and the N-lobe to the C-lobe. (**B**) A conserved activating phosphorylation site in the activation loop makes hydrogen bonding interactions to four side chains from different regions of the kinase.

phosphorylated state, the activation loop bridges two important catalytic features of the active site; the catalytic loop and the magnesium positioning loop. Additionally, it bridges the small lobe to the large lobe of the kinase, and the C-terminus of the activation loop connects to the substrate binding loop. This activation by phosphorylation is a characteristic feature of most eukaryotic protein kinases, and while the effects of adding phosphate to the activation loop are essentially the same for every protein kinase (*i.e.,* the active sites of the phosphorylated kinases are highly similar) the kinases in their unphosphorylated states are structurally variable. At present, the structures of the unphosphorylated protein kinases are unpredictable based on sequence information alone in contrast to the phosphorylated states. Although there are several conserved mechanisms of inactivation that occur throughout the protein kinase family, these mechanisms do not always fit into evolutionary groups. Instead, the ancestral kinase may have had the capacity for all forms of inactivation and a few select mutations have stabilized different inactive structural conformations for each kinase. In other words, it may take only a few mutations to convert a kinase from one mode of inactivation to another. This suggests that the rules that regulate inactivation could be elucidated using bioinformatics techniques. The first mechanism is the DFG-in to DFG-out conformational change. This involves a conformational change in the Phe from the magnesium positioning loop (Phe185 in PKA). In the phosphorylated active state the Phe is packed in a hydrophobic pocket (DFG-in) while in the inactive state the Phe comes out of the pocket (DFG-out) and in some cases packs into the ATP binding pocket. This mechanism is seen in the Ser/Thr kinase Akt (Yang et al., 2002) and the Tyr kinase Abl (Schindler et al., 2000). A second mode of inactivation is a

shift in the αC-helix from the N-lobe away from the active site. The αC-helix contains the Glu from the catalytically essential Glu-Lys salt bridge described above. Shifting the αC-helix away from the active site breaks the salt bridge and inactivates the kinase. This mode of inactivation is seen in the Tyr kinase c-Src (Xu et al., 1999). Similarly, in some kinases the αC-helix becomes disordered in the unphosphorylated state also breaking the Glu-Lys salt bridge such as in the Ser/Thr kinase Akt (Yang et al., 2002). Notably, Abl and c-Src are closely related kinases whereas Akt is distantly related from both of them. A third mechanism of inactivation involves the decoupling of the N- and C-lobes of the kinase. This allows for a greater degree of rotation of the two lobes of the kinase and because the active site lies at the interface of the two lobes this increase in flexibility may decrease the fraction of protein in the active conformation. This occurs in the Ser/Thr protein kinase p38 MAP Kinase (Wilson et al., 1996). The three mechanisms for inactivation are not mutually exclusive and some kinases are inactivated by multiple mechanisms. Some unphosphorylated protein kinases do not show any major structural changes compared to the phosphorylated state yet functionally they are inactive without phosphorylation (Komander et al., 2005). This may reflect dynamic changes and/or the conditions under which these kinases were crystallized. The different structural changes associated with dephosphorylation of the activation loop are also reflected in the differences in behavior of the inactive kinases. While some kinases are completely inactive in the absence of activation loop phosphorylation, others show moderate to severe decreases in activity. It has been shown that dephosphorylation of the activation loop causes a decrease in the rate of phosphoryl transfer in several protein kinases including PKA

(Adams, 2003). A few kinases do not require phosphorylation for their activation. These kinases generally lack a conserved arginine in the catalytic loop (Arg165 in PKA) which makes hydrogen bonding interactions with the activation loop phosphate (Johnson et al., 1996). In PKA phosphorylation of the activation loop occurs by an intermolecular autophosphorylation reaction when the enzyme is expressed in bacteria (Iyer et al., 2005b; Yonemoto et al., 1997). In mammalian cells, however, the protein kinase that phosphorylates the activation loop of PKA has not been unambiguously identified. Studies have shown that phosphorylation occurs rapidly after translation (Cauthron et al., 1998; Cheng et al., 1998) and may be dependent on PDK1 in some cell types (Moore et al., 2002; Nirula et al., 2006). *In vitro*, biochemical studies of the unphosphorylated C-subunit of PKA are limited due to the instability that is caused by mutating the phosphorylation site (Adams et al., 1995; Iyer et al., 2005a; Yonemoto et al., 1997).

Regulatory and Catalytic Spines - A rigorous comparison of many protein kinase structures, both active and inactive, revealed that the protein fold is built around a stable yet dynamic hydrophobic core that is made up of three essential elements – a single hydrophobic helix that spans the large lobe (αF-Helix) and two hydrophobic spines that are each made up of noncontiguous residues from both lobes (**Fig. 1.8**). The comparison of active and inactive kinases, revealed that every active kinase had a contiguous hydrophobic spine that is made up of two residues from the N-lobe and two from the C-lobe. Because this spine is often broken in the inactive kinases, it was referred to as a "Regulatory" spine or R-spine. Typically the R-spine is assembled as a

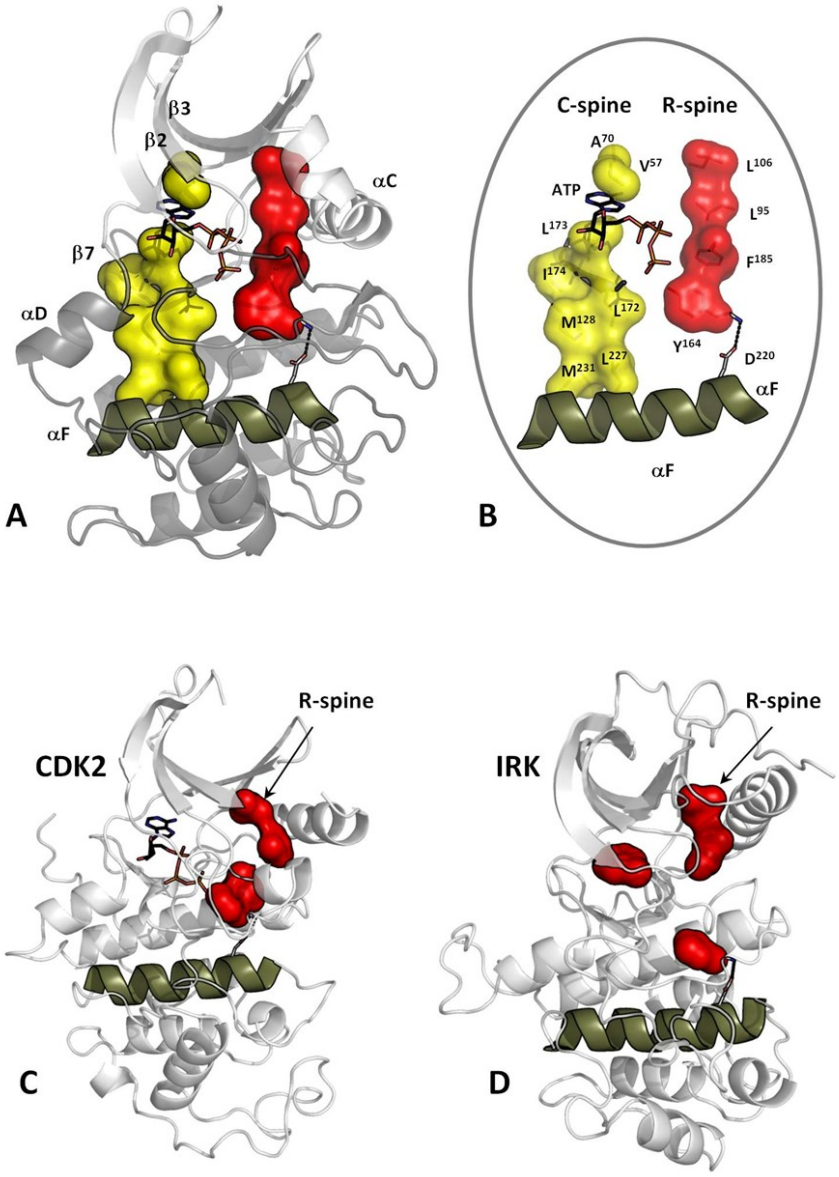

Figure 1.8. Hydrophobic Spines define the internal architecture of the eukaryotic protein kinases. **A)** Two hydrophobic spines span the two lobes of the kinase core and provide a firm but flexible connection between the N- and C-lobes **B**) The regulatory spine (R-spine) contains four residues from different kinase subdomains and is anchored to the αF-helix by conserved Asp220. The catalytic spine (C-spine) is completed by ATP. **C-D**) In the inactive state the R-spine is typically disassembled. Disassembly of the R-spine can be achieved in different ways: by movement of the αC-helix like in Cyclin-dependent kinase 2 (**C**) or by movement of the Activation segment like in Insulin receptor kinase (**D**).

consequence of phosphorylation of the activation loop that joins β strand 9 to the αF-helix. In many kinases this causes the DFG motif that lies between β-strands 8 and 9 to "flip" so that the Phe (Phe185 in PKA) is positioned to complete the spine, and leaving the Asp positioned to interact with one of the ATP bound magnesium ions. The four non-contiguous residues that are aligned in every active kinase are the His from the HRD motif in the catalytic loop that bridges β strands 6 and 7. In PKA and some of the other AGC kinases this His is replaced with a Tyr (Tyr164), but in each case, this hydrophobic residue is packed against Phe185 from the DFG motif. In the N-lobe of PKA the two hydrophobic R-spine residues are Leu97 in the αC-helix and Leu104 in β-strand 5. These two residues are not only linked to the C-lobe through the R-spine but also serve to anchor the beta and helical subdomains in the N-lobe together (Taylor and Kornev, 2011).

Additionally another hydrophobic spine that runs parallel to the R-spine was identified. Unlike the R-spine, which is composed of side chains, this second spine is completed by the adenine ring of ATP and is referred to as the "catalytic" spine or C-spine. ATP binding thus positions the two lobes so that the catalytic residues are aligned optimally for catalysis. Both spines are anchored to the αF Helix. The catalytic loop is also firmly anchored through hydrophobic residues to the αF Helix.

1.5 Flanking Domains and Tails

Although the core that defines the protein kinase superfamily contains most of the essential catalytic machinery, surprisingly it is not usually sufficient to mediate

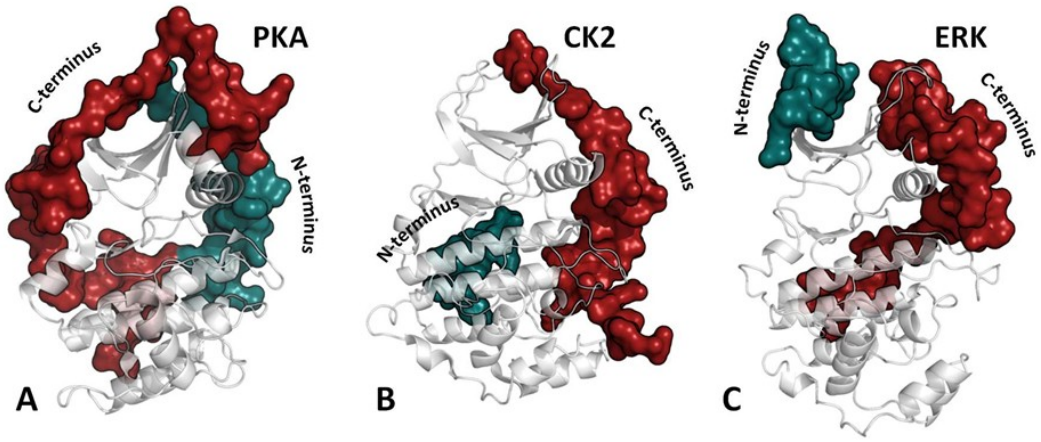

Figure 1.9. Tails and Linkers. Flanking regions wrap around the conserved kinase core in different ways for the various kinases but typically the kinase core alone is not sufficient for optimal activity. These tails provide stability and allosteric mechanisms for regulation. Three EPK examples are shown: protein kinase A (**A**), casein kinase II (**B**) and ERK2 (**C**). Each kinase core is displayed as a ribbon. The N-terminal tails are shown as a teal surface while the C-terminal tails are in red.

optimal catalysis on its own. Instead, it is assembled into a fully active state by interactions with flanking regions or domains that are anchored to the core (**Fig. 1.9**). In the case of PKA there is a short N-tail (39 residues) and C-tail (50 residues) that wrap around both lobes of the core. Without these tails the kinase is neither stable nor active. Mitogen activated protein kinase (MAPK) is similar in that it has N- and C-tails that wrap around the core in different ways but nevertheless achieve the same function of stabilizing the active kinase and contributing to catalysis (Zhang et al., 1994). The non-receptor tyrosine kinases such as Src typically have two N-terminal domains, an SH2 and SH3 domain, and these interact with the core to keep it turned on or off (Wong et al., 2004). The receptor tyrosine kinases are the most challenging because they contain a large extracellular domain that binds typically to a growth factor. Binding of the growth factor to the extracellular domains promotes dimerization and also releases the inhibition of the cytoplasmic kinase domain. In addition to a single trans membrane helix, there is a linker region that joins the trans membrane helix to the kinase core and also a C-tail. The linker and the C-tail are filled with various phosphorylation sites that constitute a regulatory mechanism, and transitioning of these linkers between ordered and disordered states is a critical part of the signaling mechanism.

The highly sophisticated ways in which the tails can contribute to both regulation and catalysis has been studied well in the PKA catalytic subunit (**Fig. 1.9**). At the N-terminus of PKA is the A-helix, a long amphipathic helix which lies outside of the kinase core and is modified by an N-terminal myristyl moiety. The hydrophobic surface of the helix is anchored to the large lobe of the kinase core at the base of the

active site cleft (Herberg et al., 1997). The hydrophilic surface of the helix provides a docking site for another PKA interacting protein called A Kinase Interacting Protein 1 (AKIP1). AKIP1 is involved in trafficking the catalytic subunit to the nucleus (Sastri et al., 2005). A variety of roles have been proposed for N-terminal myristylation including regulation of activity, stability, and localization (Bastidas et al., 2012; Gaffarogullari et al., 2011; Tholey et al., 2001; Yonemoto et al., 1993b).

The AGC Kinase C-Tail - While the N-tail is unique to PKA, the C-tail is highly conserved in the AGC protein kinases and it can be divided into three functionally distinct segments (Kannan et al., 2007a). The first segment (residues 301-318), referred to as the C-lobe tether (CLT) is bound firmly to the large C-lobe of the kinase core. Several conserved motifs are embedded within this segment including a PXXP motif, followed by a highly dynamic active site tether (AST) containing an FDDY motif. Recent studies have shown that the PXXP motif in PKC binds to Hsp90 and Cdc37, and regulates hydrophobic motif phosphorylation and processing of PKC (Gould et al., 2009). The FDDY motif is an integral part of the ATP binding site. The first Phe is part of the adenine binding pocket, and mutation of this Phe results in significant loss of activity (Kennedy et al., 2009; Yang et al., 2009). The second aromatic residue Tyr lies on top of the ribose ring when the enzyme is in a closed conformation. Mutation of Tyr330 also leads to loss of activity in PKA (Batkin et al., 2000). In the absence of bound nucleotide, the AST segment is highly disordered in crystal structures while binding of the nucleotide stabilizes the closed conformation of

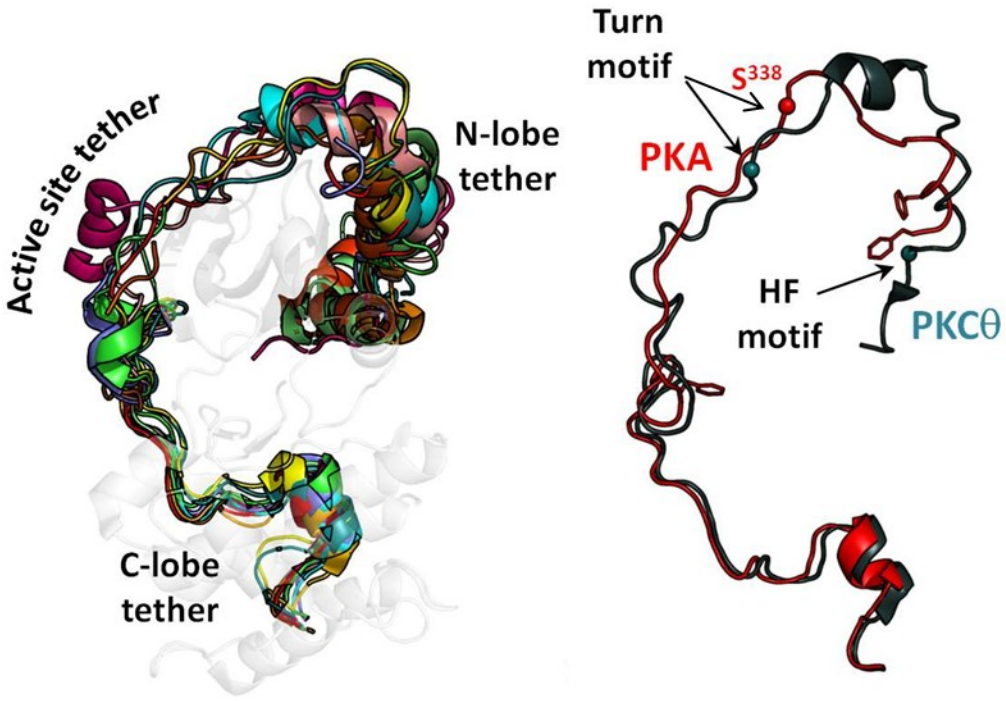

Figure 1.10. Alignment of the AGC kinase C-tails. The three conserved AGC kinase C-tail motifs, the CLT, AST, and NLT are shown on left and the two conserved phosphorylation sites the TM and the HM are shown on right for PKCθ (black) and the offset position of the PKA TM (red). PKA lacks the HM phosphorylation site.

the kinase and orders the AST. The end of the C-tail (residues 336-350) is anchored to the N-lobe in the active enzyme and is referred to as the N-lobe tether (NLT). At the end of the NLT is a hydrophobic motif, and this motif (FXXF) is anchored to the αC-helix in the N-lobe (**Fig. 1.10**) and is essential for enzyme activity (Batkin et al., 2000).

1.6 Regulation of the AGC Kinases by Phosphorylation

In addition to the activation loop, activation of the AGC kinases usually involves the phosphorylation of two highly conserved regulatory motifs in the C-terminal tail; the turn motif (TM) and the hydrophobic motif (HM) (**Fig. 1.10**). Between the AST and the NLT is a phosphorylation site that is referred to as the TM. In PKA this phosphorylation site (Ser338) lies at the apex of a structural turn and the phosphate makes interactions to adjacent residues including four side chain and two main chain hydrogen bonds. In other AGC kinases, the position of the TM is slightly offset compared with PKA and the phosphate makes hydrogen bonding interactions with the glycine-rich loop in the N-lobe. In PKA this interaction is mediated by a Glu (E333) instead of a phosphate. The function of the TM phosphorylation site is not clearly identified, however several functions have been reported including regulation of processing, activity, binding to cytosolic shaperones like Hsp70 and Hsp90 and in some kinases it may act cooperatively with the HM phosphorylation site (Gao and Newton, 2002; Hauge et al., 2007; Ikenoue et al., 2008; Newton, 2003). In PKA the C-tail TM site is phosphorylated by intramolecular autophosphorylation whereas, the activation loop occurs intermolecularly (Iyer et al., 2005b; Keshwani et al., 2012). The

turn motif is phosphorylated cotranslationally on the ribosome and the activation loop is phosphorylated immediately after translation (Keshwani et al., 2012). Similarly, in Akt and S6K, TM phosphorylation is known to precede activation loop phosphorylation and, in the case of Akt, TM phosphorylation occurs cotranslationally (Keshwani et al., 2011; Oh et al., 2010).

With the exception of PKA and PKG, most of the other AGC kinases have an additional phosphorylation site that follows the C-terminal HM. This HM phosphorylation site interacts with a phosphate binding pocket in the N-lobe of the kinase. The HM site is turned over by a specific phosphatase called PHLPP (Gao et al., 2005). This phosphorylation site can regulate the activity and substrate specificity of Akt and the rate of turnover for PKC (Brognard and Newton, 2008). As the AGC kinases are regulated by multiple phosphorylations that involve usually more than one heterologous kinase, understanding the order and mechanism for regulation of the C-tail phosphorylation sites has been challenging.

In PKA, once the TM and activation loop are phosphorylated they are highly resistant to removal by phosphatases (Humphries et al., 2005). This is not true for other AGC kinases, and this allows the C-subunit to be packaged as part of a holoenzyme complex where activation is dependent on the cellular levels of cAMP. These PKA signaling complexes also recruit phosphatases, and in this way the phosphatase is committed to the dephosphorylation of the protein substrate but not to the dephosphorylation of the C-subunit. The only known physiological condition that makes the C-subunit susceptible to dephosphorylation is oxidation of Cys199, adjacent to the activation loop phosphorylation site (Thr197), and this only happens

when the C-subunit is not inhibited by the R-subunit (Humphries et al., 2005; Keshwani et al., 2012). Additionally, in the absence of activation loop phosphorylation, the TM is susceptible to dephosphorylation (Keshwani et al., 2012).

PDK1-Dependent Phosphorylation - Many of the AGC kinases are phosphorylated on their activation loops by the phosphoinositide-dependent protein kinase (PDK1) including Akt, PKC, S6K, SGK, and RSK. This has led some to call it the master regulator of the AGC kinases (Mora et al., 2004). PDK1, also an AGC kinase, is unique among this group of kinases in that is does not contain a standard AGC C-tail. Instead, it contains a C-terminal pleckstrin-homology (PH) domain. The PH-domain binds phosphoinositides which can localize PDK1 to the cell membrane to activate certain membrane bound substrates such as Akt (Bayascas et al., 2008; Belham et al., 1999). PDK1 lacks the homologues AST and NLT and the associated turn motif and hydrophobic motif, elements that are essential for activity in other AGC kinases. However, PDK1 contains all of the features on its kinase core which typically interact with the AGC C-tail. The kinase is active without the C-tail but has increased activity when incubated with a peptide containing the HM from another AGC kinase (Biondi et al., 2001). Based on these results, a mechanism was proposed whereby a hydrophobic pocket in the N-lobe of PDK1, termed the PIF pocket, docks to the C-tail HM of its substrate kinase (Biondi et al., 2002) (**Fig. 1.11**). This interaction brings the substrate kinase in close proximity to PDK1 and allosterically activates PDK1 to phosphorylate the substrate kinase (Biondi et al., 2001). In some cases, activation loop phosphorylation by PDK1 is dependent on the phosphorylation state of the C-tail in

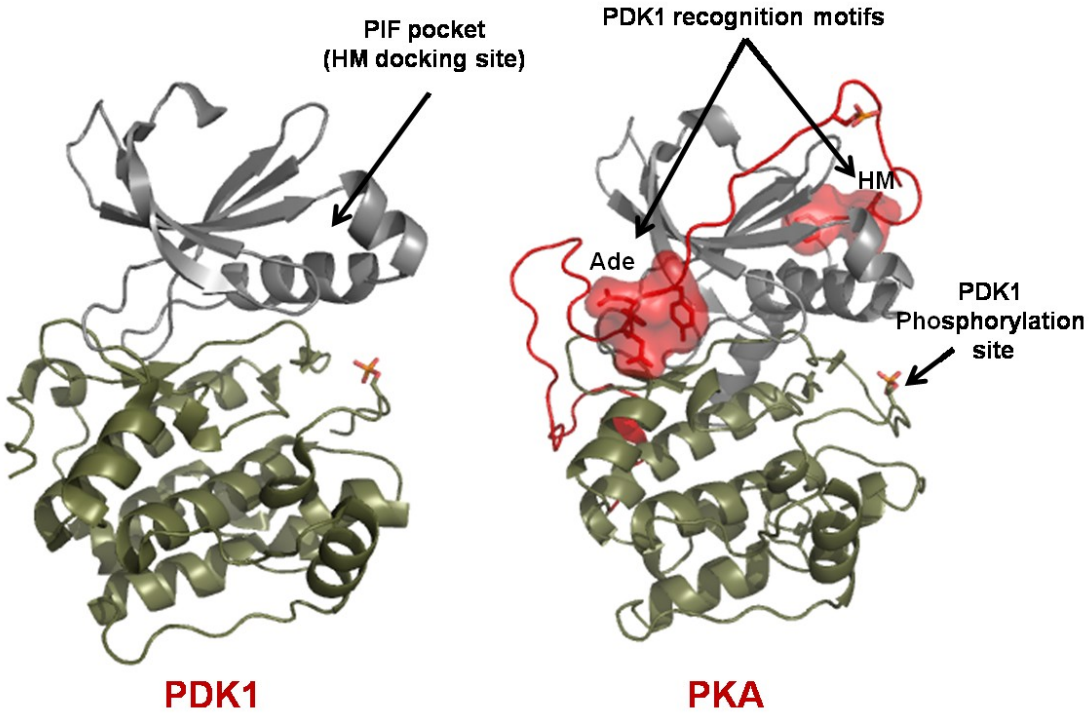

Figure 1.11. The structure of PDK1 and PDK1 interacting motifs. PDK1 (**left**) lacks the conserved AGC C-tail including the AST and the HM shown on PKA (**right**) in red. The current model for PDK1 recognition is that the PIF pocket in PDK1 docks to the HM of the substrate. This interaction allosterically activates PDK1 to phosphorylate the substrate at the indicated site in the activation loop.

the substrate kinase (Collins et al., 2005) and several C-tail motifs, in addition to the HM, have been proposed to be PDK1 docking sites (Dettori et al., 2009; Romano et al., 2009). In addition to the C-tail recognition sequence, Moore et al. previously identified two residues in the activation loop of PKA that are essential for PDK1-dependent phosphorylation (Moore et al., 2002). These residues, Pro207 and Glu208, are located in the activation loop at the P+10 and P+11 positions relative to the phosphorylation site at Thr197. There have not been any follow up studies to identify the molecular basis for the requirement of these two residues.

1.7 Outstanding Questions and Goals of the Thesis.

The focus of the dissertation was on three questions. (**1**) How does dephosphorylation of the C-subunit inactivate the enzyme and are there any generalizations that can be made regarding the activation loop of each kinase? This question has been difficult to answer because of the instability of unphosphorylated C-subunit mutants described above. Additionally, current research shows a great deal of diversity among the unphosphorylated protein kinases, however, several general modes of inactivation have been described. Because there is a great deal of knowledge about the biochemical properties of the PKA catalytic subunit, this is an ideal kinase to study inactivation. (**2**) What is the function of the TM phosphorylation site in PKA? Most studies focusing on the TM have involved *in vitro* characterization of the S338A mutant. This mutant is unstable and therefore, has been difficult to study. (**3**) How does PDK1 recognize and phosphorylate the activation loop of its substrates? Most

studies have focused on an allosteric docking site on PDK1, called the PIF pocket. While this is an important docking site for many PDK1 substrates, direct recognition of the activation loop is currently not well understood.

There are three major goals of the thesis. The first is to obtain a quantitative understanding of the function of activation loop phosphorylation/dephosphorylation on protein kinase A using biophysical, biochemical, and structural methods. In spite of the >1000 protein kinase structures in the protein data bank, there is currently a limited ability to predict the structural and biochemical effects associated with a dephosphorylated activation loop even in closely related protein kinases.

The second, is to elucidate the biological function of turn motif phosphorylation in protein kinase A. While several *in vitro* studies have been carried out in order to determine the function of turn motif phosphorylation in PKA these studies have not clearly demonstrated the physiological importance of this phosphorylation site.

And the third is to determine the role PDK1 plays in the processing of protein kinase A and to gain an understanding of how PDK1 recognizes itself, PKA, and other members of the AGC kinases as substrates. PDK1 is known to phosphorylate numerous AGC kinases and mutations in PDK1 have been associated with colorectal cancer. Defining the requirements for PDK1 substrate recognition will improve our understanding of this pivotal kinase in AGC signal transduction.

Chapter 1, in part, has been accepted for publication as Taylor, S.S., Keshwani, M.M., Steichen, J.M., Kornev, A.P. Evolution of the eukaryotic protein kinases as

dynamic molecular switches. *Philosophical Transactions B*. The dissertation author was a secondary author of this work.

Chapter 2

Global Consequences of Activation Loop Phosphorylation on Protein Kinase A

2.1 Introduction

The protein kinase superfamily is one of the largest in the human genome and one of the most relevant to disease and the protein kinases serve as major On/Off switches for almost every pathway in the cell. However, most protein kinases are themselves also regulated by a strategic phosphate. Kinases are typically expressed in an inactive state and converted into a fully active form by the addition of a phosphate to the activation loop (Nolen et al., 2004). Here we address the global importance of this one activation loop phosphate.

cAMP-dependent protein kinase (PKA) is one of the best understood members of the protein kinase superfamily and has served as a prototype in many ways. It belongs to the AGC group of protein kinases, and in addition to the general features it shares with all protein kinases, it shares many features unique to the AGC group including a conserved C-terminal tail (Kannan et al., 2007a). In PKA, as with many kinases, phosphorylation of a threonine residue in the activation loop (T197) converts the enzyme from an inactive to an active state. The activation loop phosphate on T197 coordinates the active site by bridging the C-helix (H87), the catalytic loop (R165), β9 (K189), and the activation loop (T195) (**Fig. 2.1**). As a general rule, kinases that require phosphorylation of their activation loop contain an arginine preceding the catalytic aspartate (D166 in PKA) (Johnson and Lewis, 2001). Additionally, the DFG motif (residues 184-186) has been shown to be highly dynamic in many kinases and important for activation by coordinating Mg^{2+} at the active site, as well as for stabilizing the C-helix through a hydrophobic spine (Kannan and Neuwald, 2005; Kornev et al., 2006; Levinson et al., 2006; Vogtherr et al., 2006). Lastly, there is a

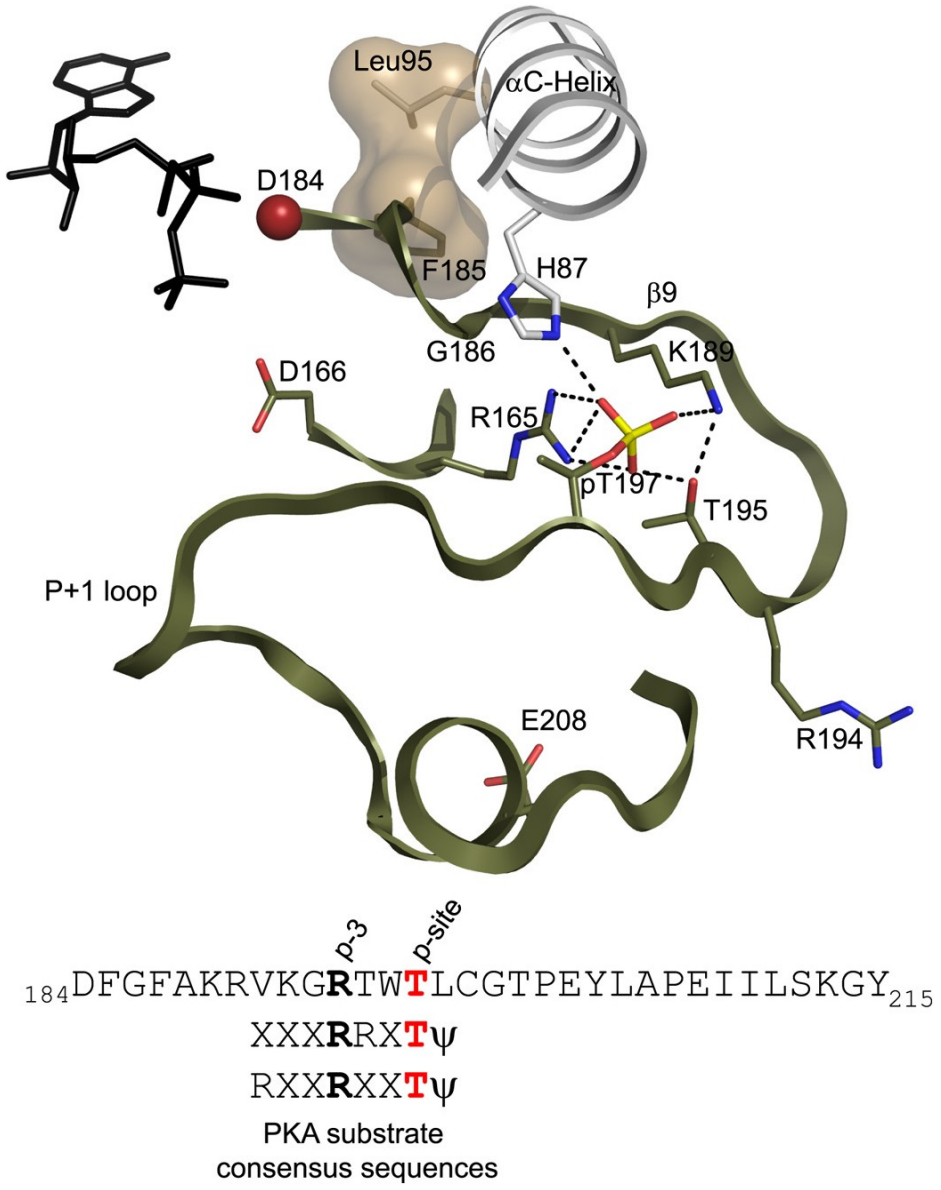

Figure 2.1. Interactions of the activation loop phosphate in the C-subunit and other conserved regions of the activation segment. The activation segment is colored olive with the sequence shown below the structure along with two common consensus sequences of PKA substrates. Phe185 and Leu95 are part of the hydrophobic regulatory spine (Kornev et al., 2006) and are shown as a tan molecular surface. ATP is colored black. The P-3 site and position of R194 are in bold, and the P-site is colored red.

conserved APE motif (residues 206-208) at the C-terminal end of the activation segment. The function of this conserved region has not been well characterized.

Early studies showed qualitatively that T197 phosphorylation was important for binding to Protein Kinase Inhibitor, PKI (Steinberg et al., 1993) and in yeast the C-subunit was shown to be defective in binding the R-subunit when the activation loop was not phosphorylated (Levin and Zoller, 1990). A kinetic study of a T197A mutant demonstrated the significance of having a phosphate on the activation loop (Adams et al., 1995). In a separate study, analysis of a kinase dead mutant of PKA (K72H) showed long range effects on the structure using hydrogen/deuterium exchange coupled with mass spectrometry (H/DMS) (Iyer et al., 2005a). However, the K72H mutation prevented phosphorylation in both the activation loop as well as the turn motif, such that the effects of phosphorylation could not be isolated from the effects of the lysine mutation.

The effects of activation loop phosphorylation in other AGC kinases have also been studied both biochemically (Komander et al., 2005; Liu et al., 2006; Orr and Newton, 1994; Stempka et al., 1997) and structurally (Cheetham et al., 2002; Huang et al., 2003; Komander et al., 2005; Lodowski et al., 2003). These studies demonstrated a surprising amount of variation among very similar kinases. For the conventional protein kinase C isoenzyme, PKCβII, activation loop phosphorylation plays a crucial role in the catalytic activity of the enzyme (Orr and Newton, 1994), while for the novel isoenzyme, PKCδ, phosphorylation does not appear to be important for catalytic activity (Liu et al., 2006; Stempka et al., 1997). There is also structural variation. In the absence of phosphorylation, the C-helix of PDK1 remains in an active

conformation (Komander et al., 2005), while in Akt2, the C-helix is almost completely disordered (Huang et al., 2003). GRK2, on the other hand, does not contain the conserved Ser/Thr on the activation loop and thus, does not require phosphorylation for activity (Lodowski et al., 2003). The majority of these studies have been carried out by mutating the phosphorylation site to an alanine residue. The challenge, is to develop an easily reversible system where one can compare the same protein in its phosphorylated state to its dephosphorylated state.

PKA, like many kinases, is complicated further because there are two phosphorylation sites, T197 on the activation loop and S338 in the turn motif. In bacteria, T197 is autophosphorylated by another C-subunit molecule (*trans* phosphorylation) whereas S338 is autophosphorylated by an intramolecular (*cis*) mechanism following phosphorylation of the activation loop (Iyer et al., 2005b). In mammalian cells, PKA is likely phosphorylated by PDK1 or a PDK1-like enzyme (Cauthron et al., 1998; Cheng et al., 1998). All of the structures of PKA to date correspond to the fully phosphorylated enzyme. In some cases the enzyme is inactive because it is bound to an inhibitor.

To study the functional consequences of a single phosphate on the activation loop of the PKA C-subunit, we replaced an arginine residue in the activation loop with an alanine (R194A). This P-3 arginine is required for PKA substrate recognition (**Fig. 2.1**). R194 does not have any known function but allows PKA to autophosphorylate T197 when expressed at high levels in *E. coli*. By replacing R194 with alanine, T197 is no longer autophosphorylated. The R194A mutant is stable for expression in bacteria and T197 can be readily phosphorylated by PDK1 *in vitro*. Here, we

demonstrate that S338 is still autophosphorylated in the R194A mutant. Thus we are able to purify an inactive form of the C-subunit that can be converted readily into a fully active enzyme by PDK1. This mutant protein provides a good experimental model to precisely quantitate the effects of adding a single phosphate to PKA. By comparing the catalytic efficiency, stability, and interaction with an inhibitor, we found that all the regions of the protein are profoundly affected. These conclusions were confirmed by using H/D exchange to map solvent accessible sites. Both N-lobe (residues 1-126) and active site peptides showed enhanced deuteration. Most striking, however, was the complete exposure of the region surrounding the APE-motif (residues 199-211) at the end of activation loop; this same region is well protected in the fully phosphorylated enzyme. In all cases the properties of the unphosphorylated R194A protein reverted to those of the wild-type protein following phosphorylation by PDK1. This is the first demonstration showing that the addition of a single phosphate can have such a profound and global effect on the structure and function of Protein Kinase A. It also suggests that phosphorylation of the activation loop may be linked in PKA to an "APE-flip" mechanism.

2.2 Experimental Procedures

Materials - The reagents used were the pET15b expression vector (Invitrogen), *E. coli* strains BL21(DE3) (Novagen, Madison, WI), Quick-Change mutagenesis kit (Strategene), horseradish peroxidase-conjugated anti-rabbit IgG (Amersham Biosciences), SuperSignal West Pico chemiluminiscent substrate detection kit (Pierce), oligonucleotides (Sigma). Antibodies against the catalytic

subunit of PKA and the Ser338 phosphorylation site were described previously (Iyer et al., 2005b), while antibodies which specifically recognize the phosphorylated activation loop of protein kinase C (PKC), referred to as α-Thr197-P, were a gift from A. Newton (University of California, San Diego). DNA sequencing was performed with the ABI PRISM 310 genetic analyzer from Perkin Elmer Life Sciences. All other materials were reagent grade from standard commercial sources.

Expression and Purification of the PKA Catalytic Subunit Mutants - $(His)_6$-tagged R194A mutants in pET15b vector (amp^r) were expressed in *Escherichia coli* [BL21 (DE3)]. Mid-exponential cultures of BL21 cells were induced with 0.5 mM IPTG and grown for another 12 hrs at 16°C prior to harvesting at 6000 rpm. Following resuspension in lysis buffer (50 mM KH_2PO_4, 20 mM Tris-HCl, 100 mM NaCl, 5 mM β- ME, pH 8.0), cells were lysed using a microfluidizer (microfluidics) at 18,000 PSI. Cells were clarified by centrifugation at 17,000 rpm at 4°C in a Beckman JA20 rotor for 50 min and the supernatant was incubated with ProBond Resin (Invitrogen) and pre-equilibrated in the same buffer for 1 hr at 4°C. The resin was then spun down at 3000 rpm and the supernatant was removed. Two washes with the lysis buffer were followed by two washes with wash buffer (50 mM KH_2PO_4, 20 mM Tris-HCl, 100 mM or 1 M NaCl, 10 mM imidazole, and 5 mM β-ME, pH 7). An imidazole elution buffer using four different concentrations of imidazole (50, 100, 200 and 500 mM) in wash buffer was used to elute the His-tagged protein. Samples containing the most protein were loaded onto a pre-packed Mono-S 10/10 (GE health) cation exchange column equilibrated in 20 mM KH_2PO_4, 20 mM KCl, and 2.5 mM DTT, pH 7.15, then

eluted with equilibration buffer containing a KCl gradient ranging from 0 to 1 M. To obtain the phosphorylated form of R194A, cells were co-expressed with PDK1 enzyme cloned in PGEX and T197-phosphorylated R194A (pR194A) was purified using the same approach as R194A. R194A was also co-expressed with untagged wild type C-subunit in pRSET^{kan} and purified by the same method.

Urea Unfolding and Fluorescence Measurements - Amberlite MB-150 (Sigma, St. Louis, MO) mixed-bed exchanger was added to 8.0 M urea solution and stirred for 1 h to remove ionic urea degradation products. The urea solution was filtered and frozen at -20°C. Proteins (0.12 mg/mL) were unfolded in various concentrations of urea ranging from (0 – 6 M) for 0.5 h at room temperature and monitored by steady-state fluorescence. Fractional unfolding curves were constructed assuming a two-state model and using $F_U = 1 - [(R - R_U) / (R_F - R_U)]$, where F_U is the fraction of the unfolded protein, R is the fluorescence measurement, and R_F and R_U represent the values of R for the folded and unfolded states, respectively (Pace, 1986). For unfolding monitored by fluorescence, R is the observed ratio of intensity at 356/334 nm with excitation at 295 nm.

Circular Dichroism – Thermal unfolding measured by circular dichroism was carried out as described previously (Iyer et al., 2005a).

Kinetic Assay - Enzymatic activity was measured spectrophotometrically as described previously (Cook et al., 1982). The K_m values for ATP and peptide substrate

were determined using Michaelis-Menten kinetics. 75 nM C-subunit was pre-equilibrated in 50 mM MOPS buffer (pH 7.0) containing 1 mM ATP, 10 mM $MgCl_2$, 1 mM phosphoenolpyruvate, 0.3 mM NADH, lactate dehydrogenase (12 units), and pyruvate kinase (4 units) in a final volume of 100 μL. Reactions were initiated by adding various amounts of Kemptide (LRRASLG). All measurements were made in triplicate. The K_m and V_{max} were determined from a Hanes-Woolf plot.*Synthesis of FLU-IP20* - To form N-terminal fluorescently tagged IP20, 900 μM of IP20 (PKI_{5-24}) and 9 mM of 5-(and-6)-carboxyfluorescein (Molecular Probes) in 100 mM sodium phosphate (pH 7.4) were mixed overnight at 4°C. Labeled IP20 was purified by HPLC with a 20% to 60% acetonitrile gradient containing 0.1% trifluoroacetic acid on a C18 reverse phase column (Vydac). The mass of the labeled peptide was verified by mass spectrometry on a Voyager DE-STR MALDI-TOF (Applied Biosystems).

Characterization of FLU-IP20 binding by fluorescence polarization - Fluorescence polarization experiments were performed at 25 °C in a Costar 96 well solid black microplate (Corning) with a GeniosPRO microplate reader (Tecan). To determine the apparent K_d for FLU-IP20, serial dilutions of PKA or PKA mutants were made in assay buffer containing 25 mM HEPES (pH 7.4), 0.002% Triton-X100, 8 mM $MgCl_2$ and 250 μM or 2 mM ATP. To these solutions was added FLU-IP20 to a final concentration of 1 nM and the binding reaction was incubated for 30 minutes at 25 °C in the dark. Readings were taken after thirty minutes, since no change in polarization was observed after 15 minutes indicating that the binding reaction had reached equilibrium. Samples were excited at 485 nm, and emission in the parallel and

perpendicular directions was detected at 535 nm. The polarization value measured for each sample was based on the average of 10 reads each with a 40 μs integration time. Data sets were fit to a sigmoidal dose-response by nonlinear regression with GraphPad Prism (San Diego, CA).

H/DMS analysis - Deuterium exchange analysis of the catalytic subunit was carried out as described previously (Yang et al., 2005) with the following changes. The wild-type and R194A mutant C-subunits were at 2.5 mg/mL final concentration in the deuterium exchange buffer. Back exchange was estimated to be 20% based on comparison with previously published analysis of the C-subunit (Iyer et al., 2005a; Yang et al., 2005).

2.3 Results

Purification and phosphorylation state of Arg194Ala. To evaluate the importance of the activation loop phosphate, we expressed and purified a mutant form of the PKA catalytic subunit that cannot be autophosphorylated as was described previously (Moore et al., 2002). The consensus sequence for PKA substrates is shown in **Figure 2.1**. Since the P-3 arginine is required for PKA substrate recognition, the R194A mutation makes it defective in autophosphorylation.

The His6-tagged R194A mutant of PKA was expressed in bacteria and purified by Ni-affinity chromatography followed by ion-exchange chromatography. It eluted in three major peaks and all were phosphorylated on Ser338 but no phosphorylation was detected on Thr197. Co-expression with PDK1 resulted in phosphorylation of the

activation loop on Thr197 (**Fig. 2.2)**. When the R194A mutant was co-expressed with untagged wild type C-subunit and purified on Ni-resin the untagged wild type C-subunit came out in the flow through phosphorylated on Thr197 but R19A, eluted with imidazole, was unphosphorylated on Thr197 (**Fig. 2.3**). This demonstrates the requirement of the R194 (P-3 Arg) side chain for PKA substrate recognition. The purified wild type C-subunit is known to be completely phosphorylated on Thr197 and Ser338 (Herberg et al., 1993) and therefore, all proteins were loaded side by side on a gel and probed for Thr197, Ser338, and C-subunit to demonstrate either complete phosphorylation or absence of phosphorylation on Thr197 and Ser338 (**Fig. 2.4**). The K72H (kinase dead) mutant does not autophosphorylate (Iyer et al., 2005a) and is shown as a control.

The addition of phosphate to the activation loop increases the catalytic efficiency of PKA. The kinetic effects of adding phosphate to the PKA activation loop were measured for the first time without mutating the phosphorylation residue T197. In **Table 2.1**, the steady-state kinetics of the unphosphorylated mutant is compared to the wild type C-subunit. In the unphosphorylated state there was a 15- and 7-fold increase in the K_m for kemptide and ATP, respectively, compared to the phosphorylated state. The k_{cat}, however, was not significantly affected by phosphorylation. Following the phosphorylation of R194A by PDK1 the steady state kinetic parameters were nearly identical to the wild-type C-subunit confirming that the arginine mutation itself does not play a role in catalysis.

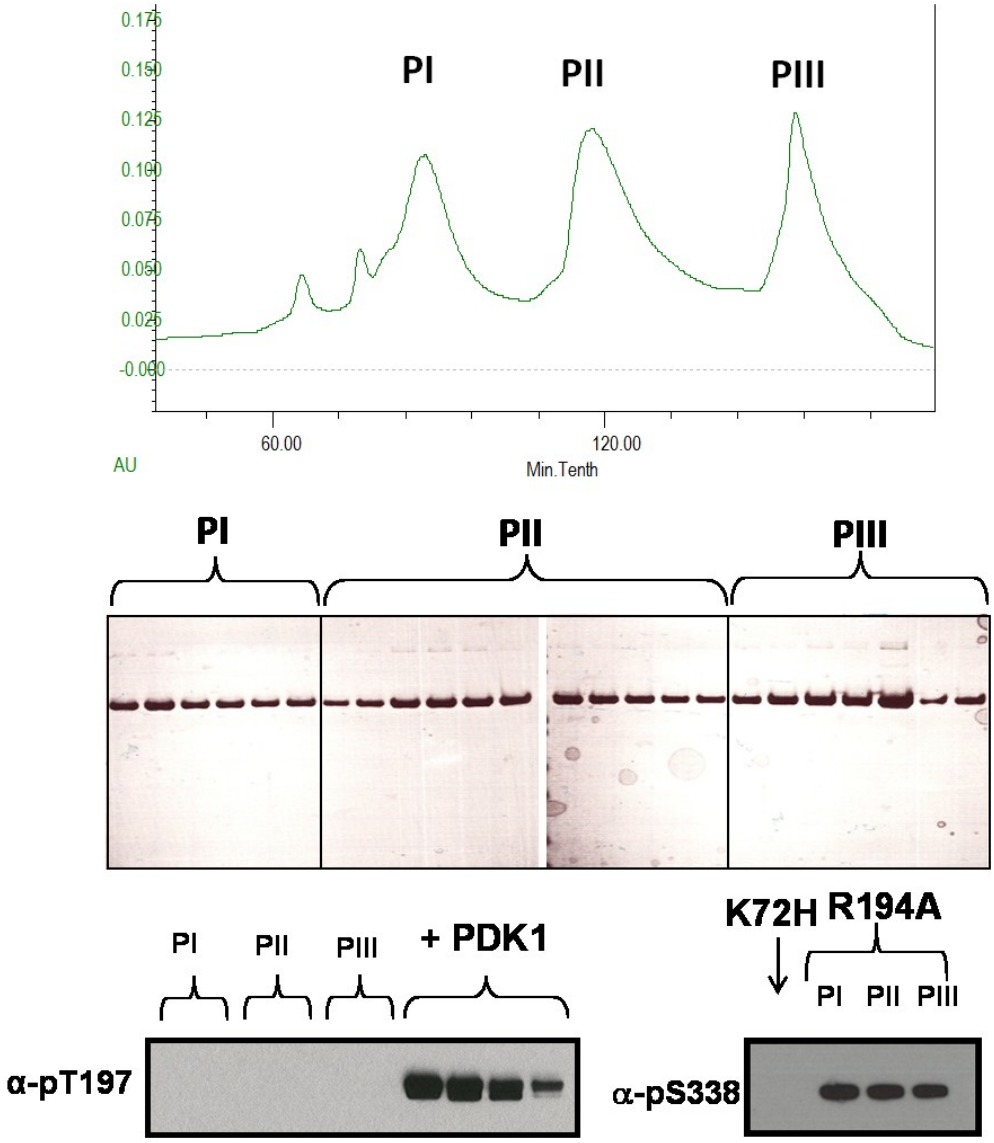

Figure 2.2. Purification and phosphorylation state of R194A. The R194A mutant of PKA eluted in three major peaks from the ion-exchange column (**top**). The purity is shown on an SDS-PAGE gel stained with coomassie blue (**middle**). All three elutions were probed with α-phospho-Thr197, α-phospho-Ser338, and α-C-subunit antibody **(bottom**). Additionally, the phosphorylation state of the R194A mutant coexpressed with PDK1 is shown. The K72H mutant is kinase dead and serves as a negative control.

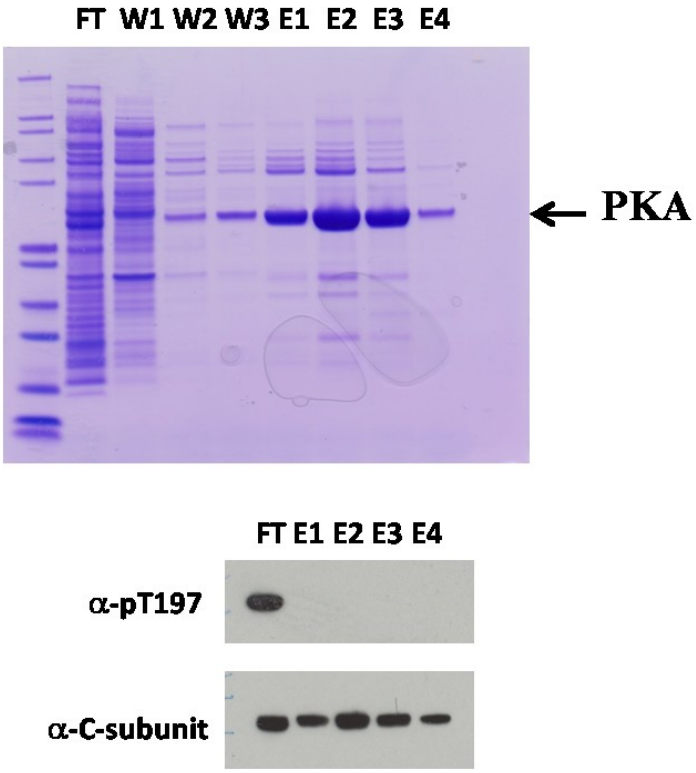

Figure 2.3. Wild type C-subunit does not phosphorylate R194A. The His6-tagged R194A mutant was coexpressed with wild type C-subunit in bacteria and purified on a Ni-resin column (**top**). Each fraction was analyzed by SDS-PAGE and western blotting with α-phospho-Thr197, and α-C-subunit antibody (**bottom**).

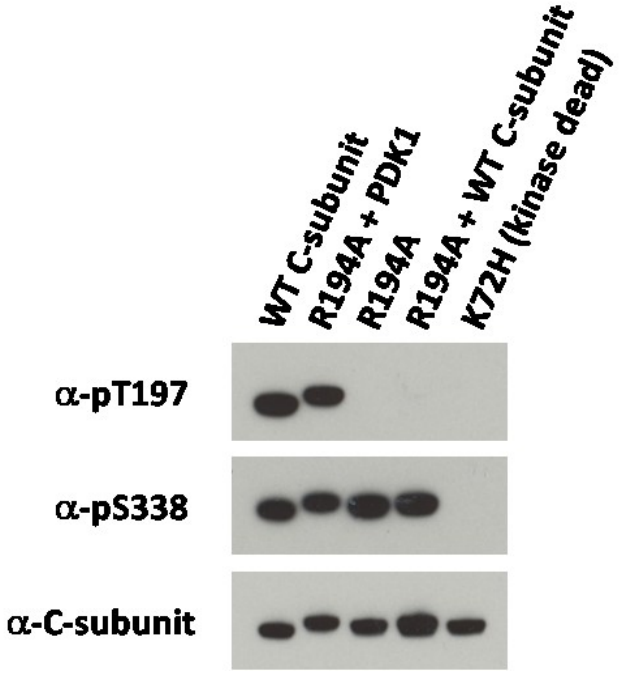

Figure 2.4. Phosphorylation state of R194A mutants. R194A, with and without treatment by PDK1 or wild type C-subunit, were probed with α-phospho-Thr197, α-phospho-Ser338, and α-C-subunit antibody. Wild type C-subunit is a positive control and K72H is a negative control.

Table 2.1. Steady-State Kinetics of R194A. Comparison of steady-state kinetic parameters for WT C-subunit, and pR194A and R194A mutants, measured on kemptide by the method of Cook et al (Cook et al., 1982).

C-subunit	k_{cat} (s^{-1})	K_m (Kemp) (μM)	K_m (ATP) (μM)	k_{cat}/K_m (Kemp)
WT	21 ± 1	26 ± 7	38 ± 5	0.8
pR194A	16 ± 1	27 ± 4	36 ± 6	0.6
R194A	22 ± 3	410 ± 30	275 ± 6	0.05

There is a decreased affinity for the physiological inhibitor PKI without phosphate on the activation loop. To evaluate the effect of activation loop phosphorylation on interaction with an inhibitor of PKA, we utilized the heat stable protein kinase inhibitor (PKI). To measure interactions between the C-subunit and PKI, we labeled a 20 amino acid peptide, corresponding to residues 5-24 of PKI (IP20) with fluorescein and used fluorescence anisotropy to measure its affinity for the different C-subunits. The presence of a phosphate resulted in a 9-fold increase in affinity between the C-subunit and IP20 (**Fig. 2.5**). The EC_{50} was 6.4 and 6.2 nM for the wild-type and pR194A, respectively, and 54 nM for the R194A.

Phosphorylation increases the stability of the catalytic subunit. The unfolding of the C-subunit was measured by monitoring the intrinsic tryptophan fluorescence from 300 – 450 nm (excitation at 295 nm) with increasing urea concentration. There is a ~15 nm shift in λ_{max} when the C-subunit is unfolded in urea (**Fig. 2.6, top**). The wild-type C-subunit had a transition point of 3 M urea compared to 2.8 M for pR194A and 2.4 M for R194A (**Fig. 2.6, bottom**). We also used circular dichroism to evaluate the global conformational state in the presence and absence of ligands. Both Mg/ATP and H89 increased the thermostability of the C-subunit with or without phosphate, however, the unphosphorylated enzyme (R194A) was less stable than the phosphorylated enzymes (WT and pR194A) in each case (**Table 2.2**).

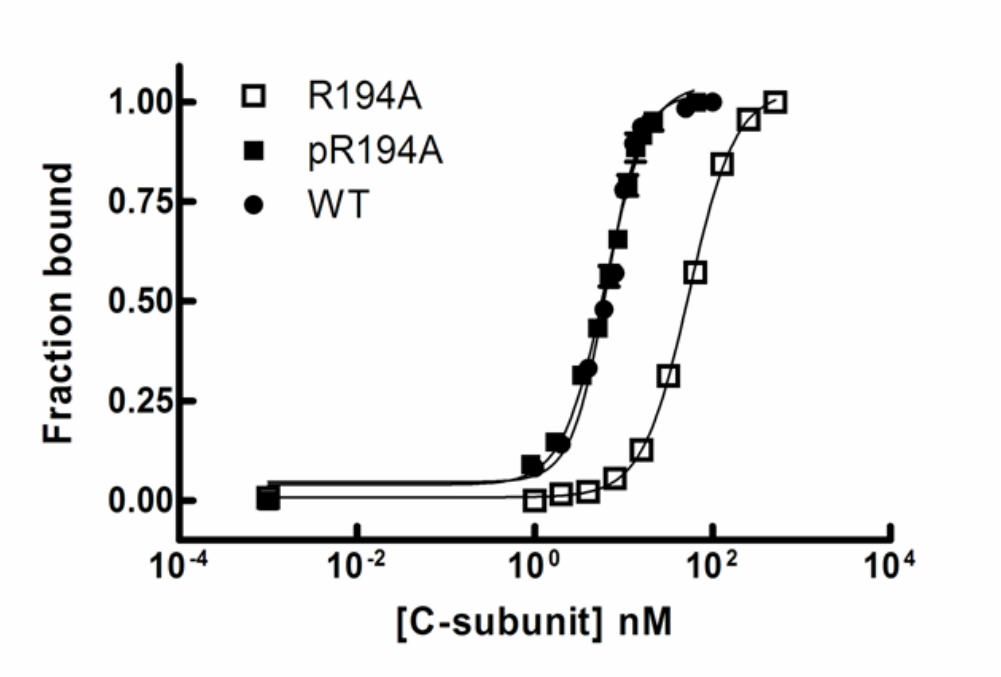

Figure 2.5. Fluorescence polarization of FLU-IP20 binding to the C-subunit. Titration of WT and mutant C-subunits (R194A and pR194A) at fixed concentrations of ATP and fluorescently labeled IP20. Values are mean ± SEM, n=3 for R194A and pR194A and n=2 for WT.

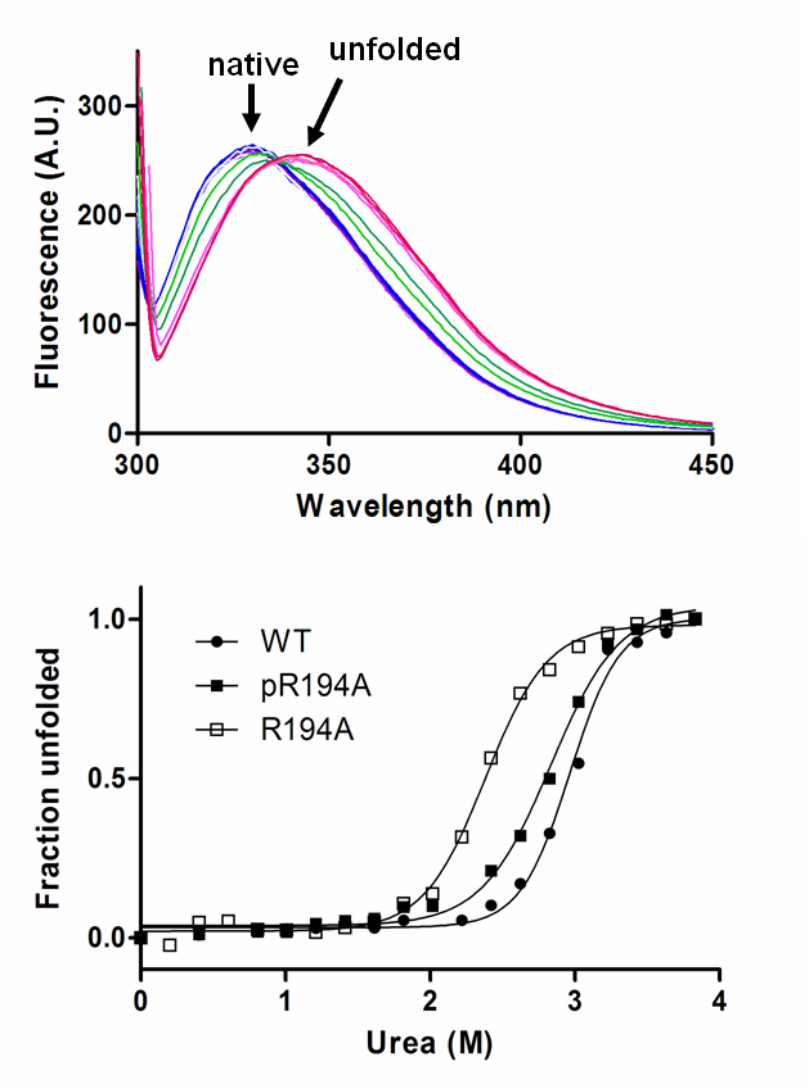

Figure 2.6. Urea-induced unfolding profiles. Tryptophan fluorescence of the Wild type C-subunit is shown at varying concentrations of urea (**top**). Comparison of the urea-denaturation curves for WT, R194A, and pR194A C-subunit (**bottom**). The fraction of protein unfolded is shown as a function of urea concentration monitored by intrinsic tryptophan fluorescence.

Table 2.2. Thermal Denaturation (T_m(˚C)) as an Indicator of Protein Stability measured by CD spectroscopy.

Ligand	Apo	ATP	H-89
WT	46.9 ± 0.1	52.5 ± 0.1	54.2 ± 0.2
pR194A	46.5 ± 0.2	51.3 ± 0.1	53.3 ± 0.5
R194A	41.3 ± 0.1	44.8 ± 0.2	47.1 ± 0.4

Deuterium exchange shows the small lobe of the catalytic subunit is more solvent exposed without T197 phosphorylation. To resolve structural and dynamic changes that occur as a result of T197 phosphorylation we used H/DMS. The results showed that the presence of the phosphate was sensed in the small lobe, in the active site cleft, and in the large lobe (see **Fig. 2.7** for coverage map). Nearly all of the peptides in the small lobe showed an increase in solvent accessibility in the R194A mutant, while the pR194A mutant was nearly identical to WT. The Gly-rich loop (residues 41-54) is a good indicator of the conformational state of the small lobe. Three peptides, including the Gly-rich Loop, identified in all three proteins are mapped onto the PKA structure in its apo conformation (Akamine et al., 2003) in **Figure 2.8**. The solvent accessibility of each peptide was reduced to wild type levels when the mutant protein was phosphorylated by PDK1. In the N-lobe the changes in solvent accessibility are only noticeable over a longer time period (~5 min) indicating that these changes may not play a role in activity, which occurs on the time scale of milliseconds, but may contribute to the overall stability of the enzyme.

The dynamics of the active site are strongly dependent on the phosphorylation state of the activation loop. The DFG motif (residues 184-186) is an indicator of the activation state of the enzyme for many protein kinases (Kannan and Neuwald, 2005; Kornev et al., 2006; Levinson et al., 2006; Vogtherr et al., 2006). The catalytic loop is another critical part of the active site and specifically bridges the activation loop phosphate with the catalytic base. The DFG-peptide (182-186) showed rapid deuterium exchange (<10 seconds) in the unphosphorylated state but exchange

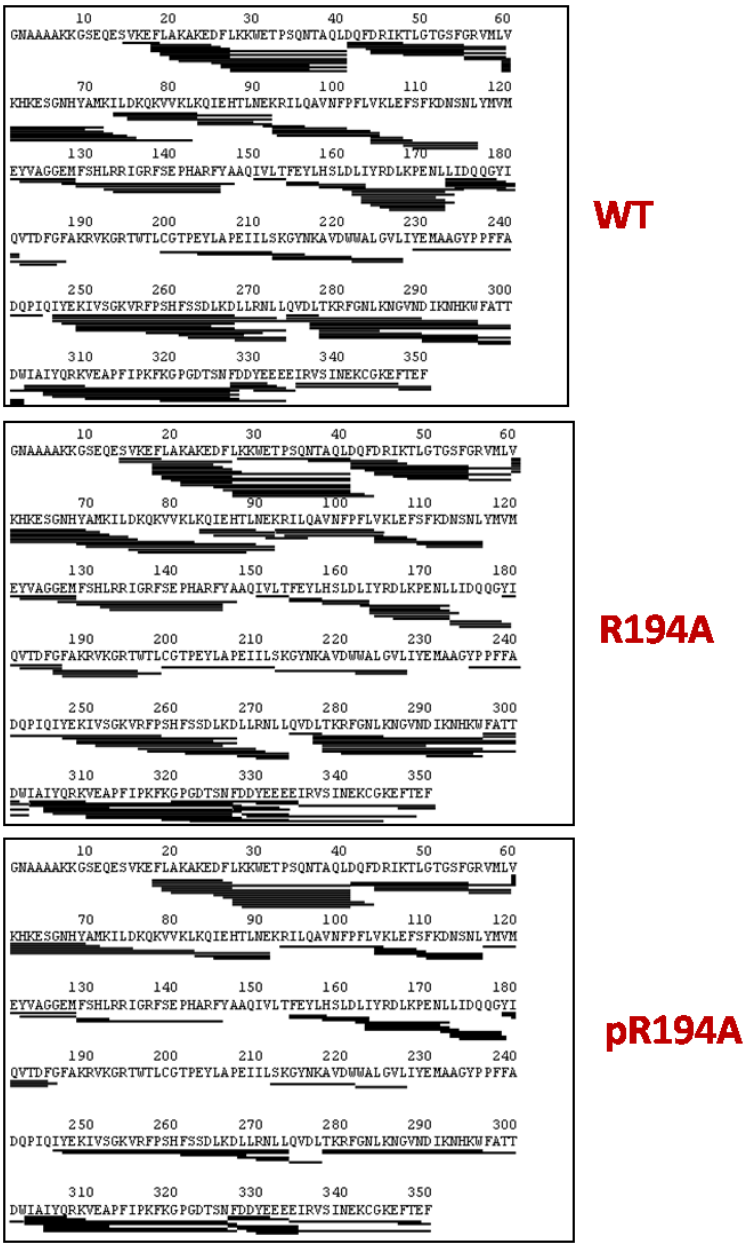

Figure 2.7. **Peptide coverage maps used in H/D exchange analysis**. The peptide coverage maps for wild type, R194A, and pR194A are shown. All peptides shown represent peptides of good quality as judged by previously described criteria (Yang et al., 2005).

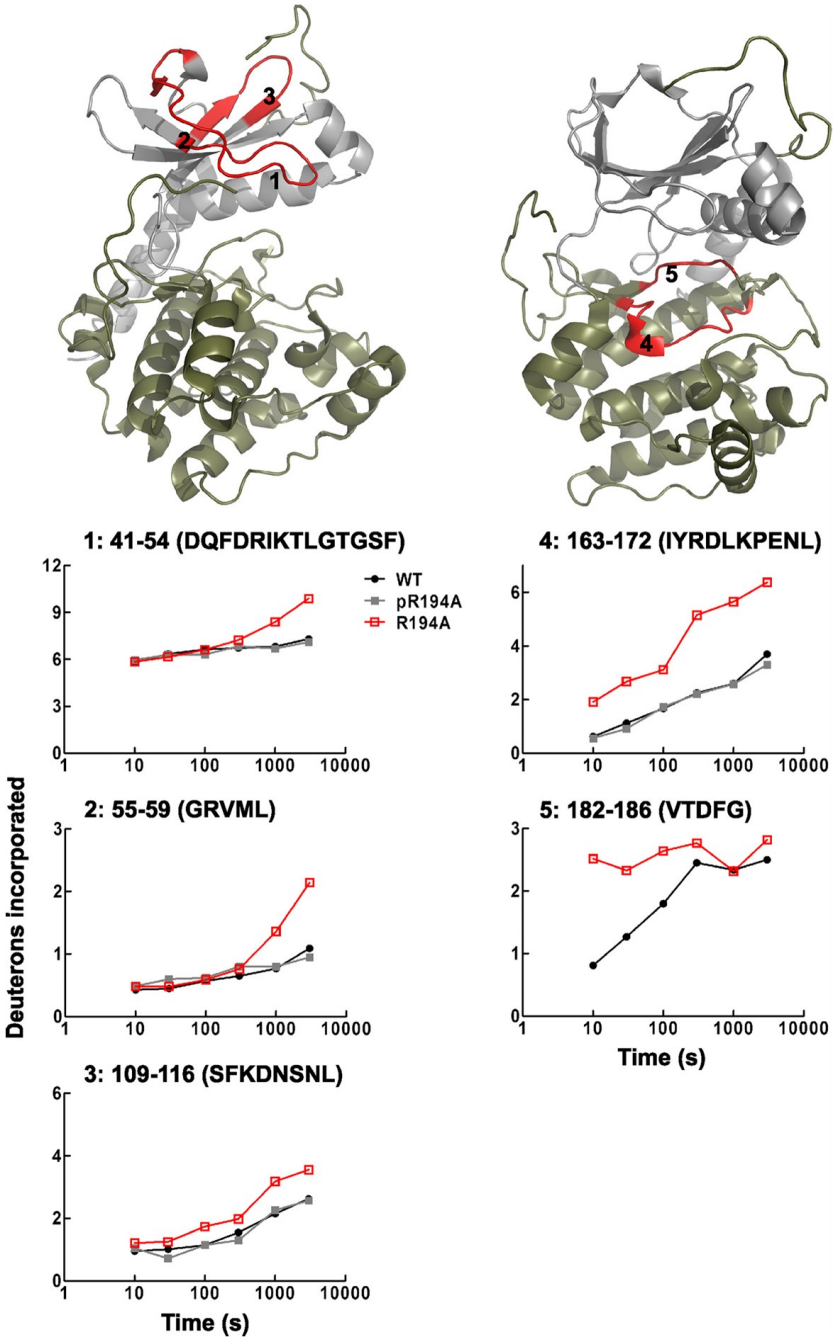

Figure 2.8. H/DMS data for peptides with increased rate of deuterium exchange in the unphosphorylated mutant. Time-course for deuterium exchange in the small lobe with peptides 1(41-54), 2 (55-59), 3 (109-116), and in the active site region, peptides 4 (163-172), and 5 (182-186) shown in red. The scale of the y-axis is the maximum number of exchangeable amides. The large lobe of the C-subunit (residues 127-350) is colored olive and the small lobe (residues 1-126) is colored gray for reference.

was slowed to 5 minutes in the phosphorylated state (**Fig. 2.8**). The catalytic loop peptide (163-172) showed an increase in solvent accessibility, exchanging 5 deuterons in the unphosphorylated state and only 3 deuterons in the phosphorylated state after 50 minutes in deuterium.

Phosphorylation links the activation loop to the αH-αI loop. The largest changes in solvent accessibility occur near the end of the activation segment in the P+1 loop/APE motif (199-211) and the αH-αI loop (278-296) peptides (**Fig. 2.9**), which are linked through a salt-bridge (E208/R280). In the 199-211 peptide, the phosphorylated enzyme is well protected from solvent up to 50 minutes in deuterium while the unphosphorylated enzyme exchanges roughly all of its amide hydrogens after only 5 minutes in deuterium. The 199-211 peptide was obtained only for wild type and R194A. The 278-296 peptide exchanged 4 deuterons more in the unphosphorylated protein than in the phosphorylated protein after 30 seconds in deuterium.

Hydrophobic core - While much of the molecule shows increased solvent accessibility in the unphosphorylated state, there remains a solid helical core that does not exchange deuterons with the solvent (**Fig. 2.10**). The αE and αF helices are buried within the core of the C-subunit while the αC, αH, and αJ helices, although exposed to the solvent, show equally slow rates of deuterium exchange.

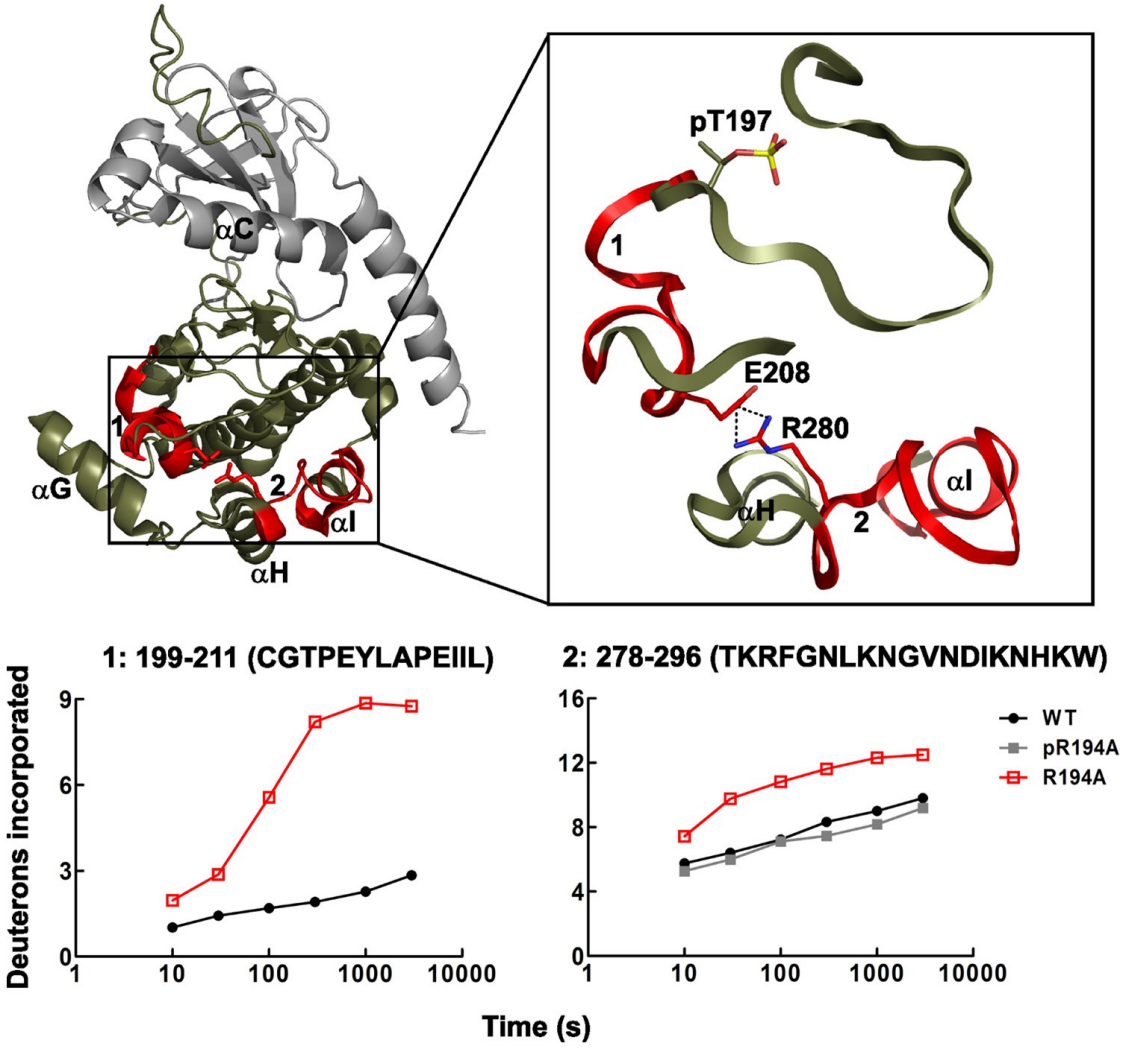

Figure 2.9. Deuterium exchange in the activation segment and the αH-αI loop. Time-course for deuterium exchange in the large lobe with peptides 1 (199-211), and 2 (278-296) colored in red. The scale of the y-axis is the maximum number of exchangeable amides. The large lobe of the C-subunit (residues 127-350) is colored olive and the small lobe (residues 1-126) is colored gray for reference.

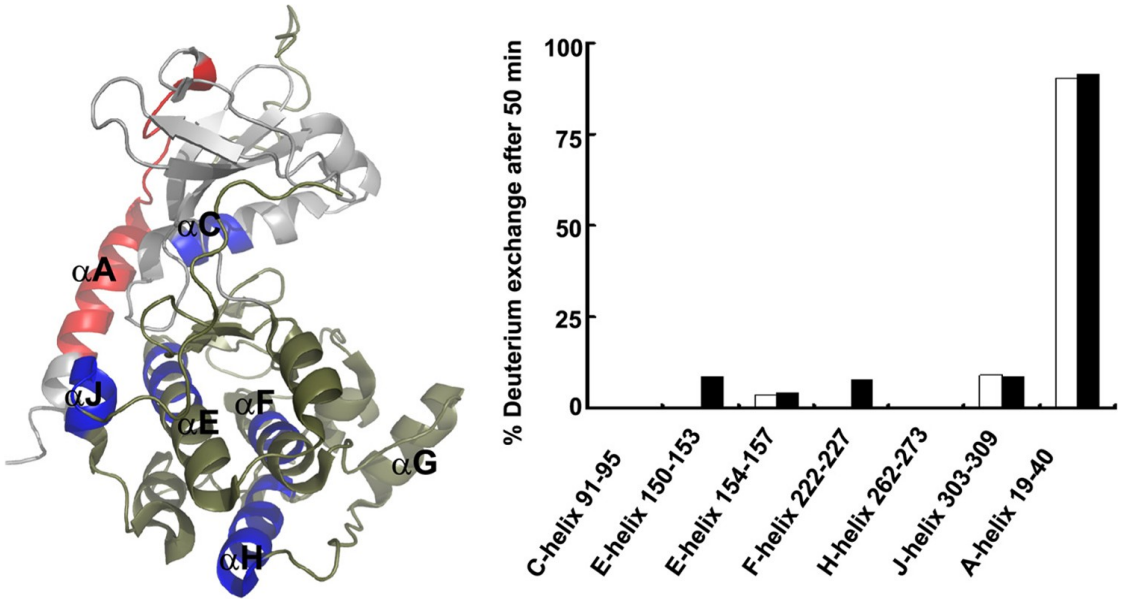

Figure 2.10. Stable helical core of the PKA catalytic subunit. % deuterium exchange after 50 minutes in deuterium in peptides from helices C, E, F, H, and J. WT (white bars) and R194A (black bars). Helical peptides that exchanged less than 10% of their amide hydrogens are mapped onto the structure of the C-subunit and colored blue. The A-Helix is a fast exchanging helix and shown in red. Where bars are not shown, no exchange was observed. The large lobe (residues 127-350) is colored olive and the small lobe (residues 1-126) is colored gray.

2.4 Discussion

Almost every protein kinase is regulated by phosphorylation of its activation loop. The PKA C-subunit is phosphorylated rapidly and constitutively in mammalian cells by a PKA kinase, most likely a PDK1-like kinase (Cauthron et al., 1998; Cheng et al., 1998). The phosphorylated catalytic subunit is then regulated by four R-subunit isoforms that are, in turn, controlled by the second messenger, cAMP. This is in contrast to other kinases such as MAP kinases and protein tyrosine kinases that are controlled by dynamic and transient activation loop phosphorylation and dephosphorylation. Other AGC kinases, such as PKC, are also regulated by second messengers. The activation loop phosphate of PKA is resistant to phosphatases which is, in part, due to its close proximity to a cysteine residue in the activation loop (Humphries et al., 2005).

The effects of activation loop phosphorylation have not been well studied in the AGC kinases without mutating the phosphorylated residue. The results shown here demonstrate for the first time the consequences that result from adding a single phosphate to the activation loop of the PKA catalytic subunit. Previous attempts to study the effects of activation loop phosphorylation have generally been carried out by replacing the phosphorylation site with either an alanine for Ser/Thr protein kinases or a phenylalanine for tyrosine protein kinases. Here, we generated a mutant form of the catalytic subunit that does not autophosphorylate T197, which we were then able to phosphorylate by co-expression with PDK1. This study demonstrates the feasibility of utilizing the R194A mutation as a model system for studying the effects of PKA activation loop phosphorylation. The phosphorylated mutant (pR194A) is similar to the wild-type enzyme in stability, catalytic efficiency, ability to bind IP20, and solvent

accessibility. There was a measurable difference in every property that was tested when comparing the C-subunit in the presence and absence of phosphorylation, including enhanced binding to a physiological inhibitor, increased thermodynamic stability, and ~15-fold increase in catalytic efficiency. Additionally, there were many regions throughout the protein that showed increased solvent accessibility in the unphosphorylated enzyme, most significantly in the P+1 loop/APE region.

In the case of PKA, a mutation of the phosphorylated residue (Thr197) to an alanine had a much more severe effect on the catalytic activity (Adams et al., 1995). The T197A mutant had a catalytic efficiency that was ~500-fold worse than the wild-type C-subunit compared to ~15-fold for the R194A mutant. This indicates that the hydroxyl group of the threonine residue may play a significant role in stabilizing the active site and mutating the phosphorylation site to alanine may not be an appropriate method for studying the effects of activation loop phosphorylation. Thus, our goal was to quantitate the effects of activation loop phosphorylation without mutating the phosphorylation residue. It was also shown previously and qualitatively that activation loop phosphorylation enhances binding to PKI (Steinberg et al., 1993). Here we demonstrate quantitatively that there is ~10-fold increase in affinity between the C-subunit and IP20 when the activation loop is phosphorylated.

Moore et al (Moore et al., 2002), previously found that the E208A mutant in the APE motif blocked PDK1-mediated phosphorylation but did not block autophosphorylation. The structure of PKA in its active state showed that E208 is completely buried, making it difficult to explain how a mutation of E208A could block phosphorylation by another kinase. Additionally, Torkamani et al (Torkamani et

al., 2008) recently identified a conserved ion-pair (E208/R280 in PKA) as a disease "hot spot" in a number of protein kinases. Our H/DMS analysis shows that this APE region (peptide 199-211) is very well protected from solvent in the phosphorylated enzyme, but exchanges all of its amide hydrogens with the solvent in the unphosphorylated state within 5 minutes. Several recently solved crystal structures from diverse protein kinases (including checkpoint kinase 2, Ste20-like kinase, lymphocyte-originated kinase, and Death-associated protein kinase 3) (Lee et al., 2009; Oliver et al., 2007; Oliver et al., 2006; Pike et al., 2008) have revealed that the P+1 loop/APE motif has the capacity to undergo large conformational changes. Our deuterium exchange analysis is the first indication that the P+1 loop/APE motif from an AGC kinase is a highly dynamic region that may undergo large conformational changes in the absence of activation loop phosphorylation. This conformational change may make the activation loop more accessible so that phosphorylation by another kinase, such as PDK1, can occur.

H/DMS has been used previously to analyze the C-subunit of PKA and several mutations were found to increase the solvent accessibility of the αH-αI loop (Iyer et al., 2005a; Yang et al., 2005). Residues 282-286 form a loop that is specific to the AGC kinases (Kannan et al., 2007a). Our data also show that the αH-αI loop becomes more solvent exposed in the unphosphorylated enzyme, and we propose that this is a consequence of the APE conformational change. The only direct interaction between the activation segment and the αH-αI loop is through a salt-bridge formed between E208 in the APE motif and R280 in the αH-αI loop. It is likely that T197 phosphorylation stabilizes this E208/R280 salt-bridge. This ion pair is conserved in all

protein kinases with the exception of the casein kinases. H/DMS has also been used to study two members of the CMGC group of protein kinases, ERK2 and p38 MAP Kinase, in the presence and absence of activation loop phosphorylation (Lee et al., 2005; Sours et al., 2008). Neither protein showed a large change in solvent accessibility in the region around the APE motif (1-2 deuteron difference) and, correspondingly, there was relatively little change in the αH-αI loop peptide. Thus, the solvent accessibility changes in the APE and αH-αI loop regions may be more pronounced in PKA and in other AGC kinases that have a unique and conserved insert in the αH-αI loop.

The deuterium exchange analysis also revealed several helices that do not exchange amide hydrogens with the solvent. The αE and αF helices are buried within the hydrophobic core of the protein, whereas the αC, αH, and αJ helices are at the surface of the enzyme where they are partially exposed to solvent. Nevertheless, many of the backbone amides within these helices appear to form highly stable hydrogen bonds to the backbone carbonyl oxygens which prevents any deuterium exchange from occurring. In contrast, the αA helix exchanges 90% of its amide hydrogens by 50 minutes in deuterium. These data also indicate that the loss of stability in the unphosphorylated mutant is not due to a change in the hydrophobic core of the protein. More likely, it is the dynamic change in the loop regions, in particular the P+1 loop/APE motif and the αH-αI loop, that decreases the stability. The effect on stability was not as severe as that seen with the K72H mutant which, in addition to the lysine mutation, was lacking both T197 and S338 phosphorylation (Iyer et al., 2005a).

In conclusion, we have made a biophysical comparison of two physiological states of the PKA catalytic subunit and have identified several novel properties associated with activation loop phosphorylation. Based on our kinetic analysis, the T197 hydroxyl group may be important for stabilizing the active site in the absence of phosphorylation since it is more active than simply replacing the threonine with alanine. More importantly, while the core of the protein remains stable in the absence of phosphorylation, the loop regions are highly dynamic. Most significantly, the dynamics of the APE motif and αH-αI loop, two regions that are linked by a conserved ion-pair and are known to be associated with many diseases, are strongly dependent on the phosphorylation state of the activation loop.

Chapter 2, in part, was published as Global Consequences of Activation Loop Phosphorylation on Protein Kinase A. Steichen JM, Iyer GH, Li S, Saldanha SA, Deal MS, Woods VL Jr, Taylor SS. *J. Biol. Chem*. 2010 Feb 5; 285(6):3825-32. The dissertation author was the primary investigator and author of this work.

Chapter 3

Structural Basis for the Regulation of Protein Kinase A by Activation Loop Phosphorylation.

3.1 Introduction

The catalytic subunit of the cAMP-dependent protein kinase is a member of the AGC group of protein kinases. It is one of the simplest protein kinases, because it contains a kinase domain with only short N- and C-terminal extensions. Additionally, it can be expressed efficiently in bacteria (Herberg et al., 1993). This has made it an ideal structural and biochemical model for the protein kinase family. One of the most common mechanisms for protein kinase regulation is the phosphorylation of a conserved residue within the activation loop of the kinase. This is generally true in the "RD" class of protein kinases, which includes most protein kinases. In the RD kinases the "RD" arginine from the catalytic loop interacts directly with the phosphate in the activation segment (Johnson et al., 1996). The phosphate on the activation segment makes hydrogen bonding interactions to residues from both lobes of the enzyme which stabilizes the enzyme in an active conformation. In PKA these residues are Lys189 and Thr195 from the activation segment, Arg165 from the catalytic loop, and His87 from the C-helix (**Fig. 3.1**).

At the N-terminus of the activation segment there is a conserved DFG motif, also called the magnesium positioning loop because the aspartate coordinates magnesium at the active site. This region has been found to be a common regulatory motif in protein kinases. The DFG phenylalanine packs into a hydrophobic pocket between one residue from the N-lobe and one residue from the C-lobe thus creating a hydrophobic regulatory (R) spine (Kornev et al., 2006). This packing interaction is referred to as the "DFG-in" conformation. In many kinases, inactivation occurs when this phenylalanine moves out of the hydrophobic pocket disrupting the orientation of

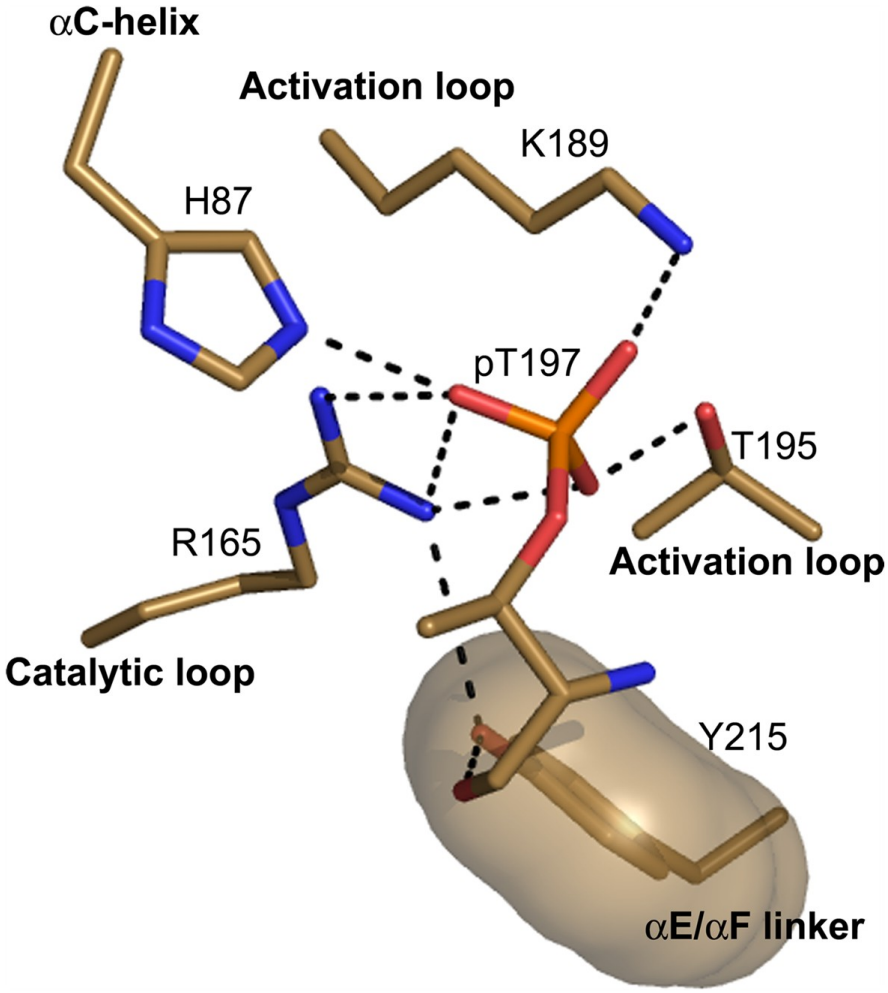

Figure 3.1. The activation loop phosphate stabilizes the active site. The activation loop phosphorylation site ties together numerous regions of the protein through a hydrogen bonding network which includes the activation loop, the catalytic loop, and the αE/αF linker from the C-lobe and the αC-helix from the N-lobe.

the DFG aspartate and in some cases sterically blocking the ATP binding site (Hubbard et al., 1994; Pargellis et al., 2002). These are referred to as "DFG-out" conformations. Due to its proximity to the activation loop phosphorylation site, the DFG phenylalanine is the key regulatory element of the hydrophobic R-spine that bridges the N- and C-lobes of the kinase. In PKA the R-spine consists of two residues from the N-lobe (Leu95 and Leu106) and two residues from the C-lobe (Tyr164 and Phe185). All active protein kinases have the "DFG-in" conformation; however, inactivation does not require the "DFG-out" conformation. In some kinases the spine is broken in other ways such as by rotation of the C-helix (Huse and Kuriyan, 2002; Schulze-Gahmen et al., 1996). In other kinases inactivation occurs without disruption of the spine (Komander et al., 2005). In addition to the R-spine there is a catalytic (C) spine. The C-spine is a non-contiguous hydrophobic ensemble that also traverses both lobes of the enzyme and is completed by the adenine ring of ATP (Kornev and Taylor, 2010).

Numerous protein kinases have been crystallized in the unphosphorylated state. In general, they show a high degree of diversity compared with the enzymes in their phosphorylated state. This may in part be due to the variety of ligands that have been co-crystallized with the kinase domains. The presence of a ligand in the active site may align the N- and C-lobes as well as stabilize the active site. Akt2 is the only AGC kinase that has been crystallized in the unphosphorylated, apo conformation (Huang et al., 2003). It showed a disordered C-helix and the DFG Phe294 occupied the ATP binding site in the "DFG-out" conformation. Other AGC kinases such as PDK1, co-crystallized with ATP, show only subtle structural changes even though the

kinase is catalytically inactive without activation loop phosphorylation (Komander et al., 2005). This indicates that there may be dynamic changes associated with phosphorylation that are masked in the presence of ligand. In some of the more interesting cases the kinases have crystallized as dimers with the activation loops swapped (Lee et al., 2009; Oliver et al., 2007; Oliver et al., 2006; Pike et al., 2008; Sunami et al., 2010). Many of the observed structural changes such as the "DFG-in" to "DFG-out" conformational change as well as the activation loop swapping occur in diverse kinases including both Ser/Thr and Tyr kinases. Therefore many of these changes may be dynamic and generally true for many kinases.

The catalytic subunit of PKA gets constitutively phosphorylated on both the activation loop as well as the turn motif in mammalian cells and when expressed in bacteria it autophosphorylates on both of these sites (Yonemoto et al., 1993a). Several biochemical studies have been carried out on PKA to assess the effects of activation loop phosphorylation. The kinetic effects of mutating the activation loop Thr197, studied previously by solvent viscosity techniques, showed that mutation of the activation loop Thr197 to Ala or Asp primarily reduced the rate of phosphoryl transfer (Adams et al., 1995) and this was found to be generally true for protein kinases (Adams, 2003). It was recently shown that a mutation in the activation loop, Arg194Ala, blocks activation loop phosphorylation due to the disruption of the PKA substrate consensus sequence (Moore et al., 2002; Steichen et al., 2010). This mutant version of the C-subunit (C^{R194A}) can be stably expressed in bacteria and by co-expressing the mutant with PDK1 to obtain activation loop phosphorylation it was determined that the Arg194Ala mutation had little effect on the biochemical properties

of the enzyme. Therefore, the mutant C^{R194A} serves as a good model for studying the biochemical changes associated with activation loop phosphorylation in PKA. The steady-state kinetics of the unphosphorylated C^{R194A} mutant were measured and it was found to have an increased K_m for both ATP as well as kemptide by ~10-fold while the k_{cat} was not affected. In addition to a change in the kinetics of the enzyme it was shown that the enzyme C^{R194A} had decreased affinity for both the regulatory subunit of PKA as well as for the heat stable protein kinase inhibitor PKI (Moore et al., 2002; Steichen et al., 2010). The dynamic structural changes were also studied in C^{R194A} by hydrogen/deuterium exchange coupled to mass spectrometry and the enzyme was found to be much more solvent accessible in the unphosphorylated state, most significantly in regions around the activation loop such as the catalytic loop, the magnesium positioning loop, the P+1 loop, and more distally the αH-αI loop (Steichen et al., 2010). The unphosphorylated enzyme was also more thermolabile.

The C-subunit of PKA has been crystallized in many states including several ATP-analog bound states, inhibitory and regulatory subunit bound states, as well as in its apo state. All structures to date, however, contain phosphate on the activation loop Thr197. In this study we crystallized the apo, unphosphorylated PKA mutant C^{R194A} and solved the structure to 3.0 Å resolution. The two lobes of the enzyme were found to be uncoupled in the unphosphorylated protein compared to all previous PKA structures as measured by an 18˚ rotation of the N-lobe. This could be explained by the disruption of the hydrophobic spine that links the N- and C-lobes of the protein. Additionally, the hydrogen bonding network that integrates the active site was

disrupted in the unphosphorylated enzyme. Finally, this alteration of the active site was correlated with a 20-fold reduction in the rate of phosphoryl transfer.

3.2 Experimental Procedures

Purification and Crystallization – The His6-tagged murine Cα-subunit of PKA containing mutation Arg194Ala (C^{R194A}) in pET15b was expressed in E. coli (BL21 (DE3)) (Steichen et al., 2010). Cultures were grown at 37°C to an OD_{600} of ~0.8 and induced with 0.5 mM Isopropyl β-D-thiogalactopyranoside. The cultures were allowed to grow overnight at 16°C before being harvested. The pellet was resuspended in lysis buffer (50 mM KH_2PO_4, 20 mM Tris-HCl, 100 mM NaCl, 5 mM β-mercaptoethanol, pH 8.0) and lysed using a microfluidizer (microfluidics) at 18,000 p.s.i. The cells were clarified by centrifugation at 17,000 rpm at 4°C for 50 min in a Beckman JA20 rotor, and the supernatant was incubated with ProBond Resin (Invitrogen) for 1 hour at 4°C. The resin was loaded onto a column and washed twice with the lysis buffer and twice with wash buffer (50 mM KH_2PO_4, 20 mM Tris-HCl, 100 mM or 1 M NaCl, 10 mM imidazole, and 5 mM β-ME, pH 7). An imidazole elution buffer using four different concentrations of imidazole (50, 100, 200 and 500 mM) in wash buffer was used to elute the His-tagged protein. Samples containing the most protein were dialyzed overnight into 20 mM KH_2PO_4, 20 mM KCl, and 2.5 mM DTT, pH 6.5 and then loaded onto a pre-packed Mono-S 10/10 (GE health) cation exchange column equilibrated in the same buffer. The protein was eluted with equilibration buffer containing a KCl gradient ranging from 0 to 1 M. In some cases it was necessary to run the protein over the ion-exchange column a second time at pH

7.15 to obtain a high level of purity. The first major peak that eluted was concentrated to ~10-15 mg mL^{-1} and setup for crystallization at 4°C using the hanging drop vapor diffusion method with well solution (100 mM Tris-HCl, 800 mM Naformate, 10% PEG1k, 10% PEG8k, pH 8.5). The largest crystals were obtained from drops that had a protein/mother liquor ratio of 4:1 and appeared after ~2 weeks. The phosphorylation state of the activation loop was confirmed using a polyclonal phospho-Thr197 antibody that was raised in rabbits against the epitope peptide RVKGRTWpTLCGTPEY (Invitrogen).

Data collection and refinement – The crystals were flash cooled in liquid nitrogen with cryoprotectant solution (mother liquor and 15% glycerol). Data was collected on the synchrotron beamline 8.2.2 of the Advanced Light Source, Lawrence Berkeley National Labs (Berkeley, California). The data was integrated using HKL2000 (Otwinowski and Minor, 1997). Molecular replacement was carried out using Phaser (McCoy et al., 2007) with the apoenzyme structure of PKA as a search model (Akamine et al., 2003)(1J3H). The protein crystallized in the $P3_221$ space group and there were two molecules in the asymmetric unit. There was poor density for the small lobe in the initial model and after extensive model building using Coot (Emsley and Cowtan, 2004) it was determined that there was a large change in the relative orientation of the two lobes. After determining the correct orientation of the N- and C-lobes, 1RDQ (the highest resolution structure of PKA with Tyr204Ala mutation)(Yang et al., 2004) was used as a starting model after aligning its N- and C-lobes in the proper orientation. This model was further refined in Coot and refmac5 using

restrained refinement with TLS and setting non-crystallographic symmetry restraints (Murshudov et al., 1997). The TLS groups were defined as group1 (residues 14-126, 333-350) and group2 (residues 127-318). There was a clear break in the density of the activation loop between residues ~189-200 and it was taken to mean that the activation loop is disordered as is seen in many other kinases. However, near the interface of the two molecules in the asymmetric unit there is a stretch of weak density that could potentially belong to the activation loop of either molecule in the asymmetric unit. Attempts were made to model main chain into this density but after further rounds of refinement the density did not improve in this region. The final model contained three water molecules modeled into this density. It is refined to an R_{work}/R_{free} of 25.2/28.6. There were no outliers in the ramachandran plot as determined using MolProbity (Davis et al., 2007). The root-mean-squared deviation (RMSD) between the two molecules in the asymmetric unit is 0.10 Å. The refinement statistics are shown in **table 3.1**. The Fo-Fc map (2.7σ) shown in **Fig. 3.4B** was calculated by deleting the activation loop and running 20 cycles of TLS refinement followed by 20 cycles of restrained refinement.

Rapid Quench Flow Experiments – Pre-steady-state kinetic measurements were made using a KinTek Corp. Model RGF-3 quench flow apparatus following a previously published procedure (Adams JA, Biochemistry, 1996). The apparatus consists of three syringes driven by a stepping motor. Typical experiments were performed by mixing equal volumes of the PKA in one reaction loop and γ-32P-ATP (5000-15000 cpm/pmol) and Kemptide in the second reaction loop all in the presence

Table 3.1. Data Collection and Refinement Statistics for R194A.

PDB ID	4DFY
Data collection	
Space group	$P3_221$
Cell dimensions	
a (Å)	95.745
b (Å)	95.745
c (Å)	173.959
α (°)	90.0
β (°)	90.0
γ (°)	120.0
Molecules per asymmetric unit	2
Unique reflections	18,017 (1,121)
Redundancy	5.3 (4.8)
Resolution range (Å)	50-3.0 (3.11-3.00)[a]
R_{sym} (%)	6.3 (33.2)
$I/\sigma I$	28.1 (2.8)
Completeness (%)	94.9 (59.5)
Refinement	
R_{work}/R_{free} (%)[b]	25.2/28.6
Ramachandran angles (%)[c]	
Favored regions	94.6
Allowed regions	100
r.m.s. deviations	
Bond lengths (Å)	0.012
Bond angles (°)	1.3

[a]Values in parenthesis correspond to the highest resolution shell. [b]5.1% of the data was excluded from the refinement to calculate the R_{free}. [c]Ramachandran plot quality as defined in MolProbity (Davis et al., 2007).

of 100 mM Mops (pH 7.4), 10 mM free Mg2+, 5 mg/mL BSA. The reaction was quenched with 30% acetic acid in the third syringe and the reactions were analyzed using the filter binding assay described above. Control experiments lacking PKA were run to define a background correction. The final concentrations of C-subunit, kemptide, and ATP were 1 μM, 500 μM, and 500 μM, respectively.

3.3 Results

Global changes in the unphosphorylated protein – Three regions in the protein were disordered in the structure: the N-terminus (1-13), the activation loop (189-200), and the C-terminal tail (319-333). The turn motif site Ser338 is phosphorylated and is similar to the wild type enzyme. Using the C-lobe αE and αF helices for alignment, we compared the unphosphorylated enzyme with the wild type apoenzyme in the open conformation (PDB ID 1J3H). There is an additional 18˚ rotation of the N-lobe beta sheet relative to the C-lobe (**Fig. 3.2A and B**). A C-lobe alignment to the wild type enzyme in its closed conformation (PDB ID: 1ATP) shows a total 30˚ rotation of the beta sheet (**Fig. 3.2A**). Individually aligning the N- and C-lobes shows that there are only small changes in the overall structure of each lobe (**Fig. 3.2A and C**). The Cα RMSD between the N- (residues 40-120) and C-lobes (residues 127-290) is 0.456 and 0.644 Å, respectively. Thus, the N- and C-lobes rotate as two ridged bodies in the unphosphorylated enzyme. This rotation is greater than has been observed for other unphosphorylated AGC kinases, however, these protein kinases all have ligands bound to the ATP binding pocket with the exception of Akt2.

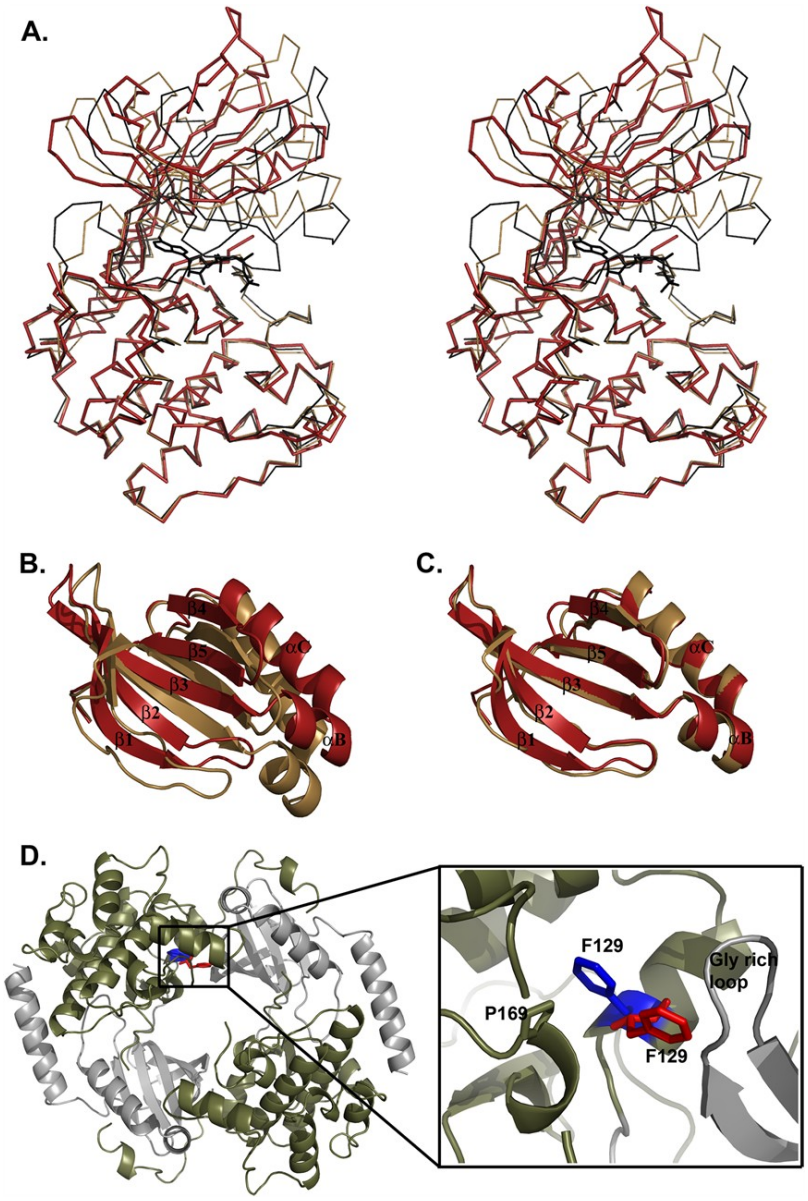

Figure 3.2. Alignment of C^{R194A} with the wild type C-subunit. (**A**) stereo view of the apo wild type C-subunit (1J3H; tan), the closed ternary complex (1ATP; black) with C^{R194A} (red) aligned along the αE and αF helices shows the similarity of the C-lobe and the rotation of the N-lobe. ATP is shown in black. (**B**) The same alignment as shown in (A) between wild type apo and C^{R194A} but showing only the 18˚ rotation of the N-lobe. (**C**) Alignment of the β-sheet in the N-lobe between apo wild type (tan) and C^{R194A} (red). (**D**) shows crystal packing between the two molecules of C^{R194A} in the asymmetric unit. The C-lobe is colored olive and the N-lobe is colored gray. The side chain of Phe129 (shown as blue stick) is rotated away from the glycine rich loop from the other molecule of the asymmetric unit and packs against Pro169. The position of Phe129 in the wild type C-subunit is shown as a red stick.

When comparing the structure to other apo, unphosphorylated protein kinase structures, C^{R194A} shows similar domain twist to p38 kinase but C^{R194A} is in a more open conformation (Wilson et al., 1996).

Disruption of the hydrogen bonding network at the active site – The active site of the unphosphorylated protein is dramatically different from the wild type enzyme. Virtually every catalytic residue in the C-lobe is displaced from the wild type active conformation (**Fig. 3.3**). While many of these changes can be rationalized from the missing phosphate at Thr197 and its subsequent disruption of the hydrogen bonding network that integrates the active site, there is a crystal packing interaction that may be responsible for some of the changes. Phe129 in the αD helix and near the hinge is rotated in the structure relative to its conformation in the wild type protein. This is due to a packing interaction with the glycine rich loop from the other molecule in the asymmetric unit (**Fig. 3.2D**). The new conformation of Phe129 is packing against Pro169 in the catalytic loop. The Cα of Pro169 has shifted ~2 Å compared to the wild type protein. The Cα atoms in the adjacent residues Lys168 and Leu167 are shifted ~3.5 Å and 2.3 Å, respectively (**Fig. 3.3**). Additionally it is important to note that while we are comparing the active site of the unphosphorylated enzyme to the wild type apoenzyme in the open conformation, the conformations of the activation segment as well as the catalytic loop do not depend on substrate binding for the wild type enzyme (**Fig. 3.3A**).

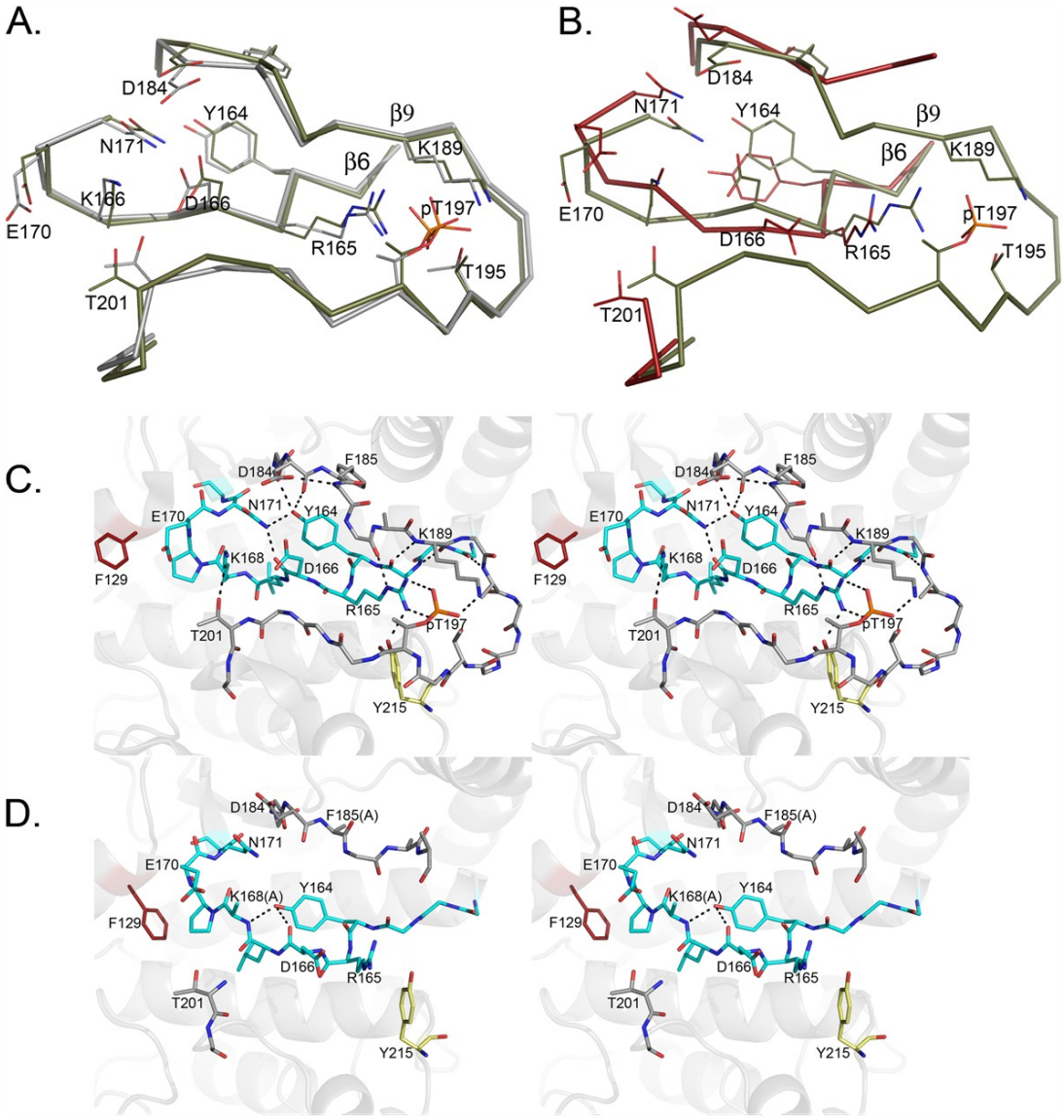

Figure 3.3. There is a loss of hydrogen bonding at the active site of C^{R194A}. (**A**) alignment of wild type apo (1J3H; olive) and ternary complex (1ATP; gray) shows the conformation of the C-lobe portion of the active site is independent of substrate binding. (**B**) alignment of the wild type apoenzyme (olive) with C^{R194A} (red) shows the same view of the active site as in (A). (**C**) stereo view of the active site of wild type apoenzyme showing hydrogen bonds that are present in wild type but absent in C^{R194A}. The catalytic loop is colored teal and the activation loop is colored gray. Phe129 which is rotated in C^{R194A} as a result of crystal packing is shown in red. (**D**) stereo view of the active site of C^{R194A} showing hydrogen bonds that are formed in C^{R194A} but absent in the wild type apoenzyme. Colored as in (C).

The activation segment is disordered from residues ~189-200 in the unphosphorylated enzyme and the main chain starting from the DFG-1 residue Thr183 to Gly186 is moved away from the catalytic loop by ~1 Å. Beyond Gly186 the main chain makes a turn away from the catalytic loop preventing the formation of the β6:β9 sheet. Additionally, there is no electron density for most of the side chains C-terminal to the DFG Asp184 (**Fig. 3.4A and B**). The sum of these changes results in the loss of all hydrogen bonds bridging the activation segment to the catalytic loop (**Fig. 3.3C and D**). The phosphate at Thr197 can make hydrogen bonds to three side chains in the open conformation and four in the closed conformation. Lys189 belongs to β9 and forms a β sheet with β6 directly preceding the catalytic loop. In the wild type enzyme Lys189 makes a hydrogen bond to the phosphate at Thr197 and it is disordered in the unphosphorylated enzyme. Therefore this residue directly links the activation loop to the catalytic loop in the wild type enzyme and may be responsible for the movement of the activation segment away from the catalytic loop in the unphosphorylated protein. Additionally, Arg165 from the catalytic loop makes hydrogen bonding interactions to the activation segment through both the phosphate at Thr197 as well as to the main chain carbonyl oxygen of Phe187 in the wild type protein. In the unphosphorylated enzyme Arg165 has moved away from the activation segment. In the wild type enzyme, the magnesium coordinating residue Asp184 is held in an active conformation by making a hydrogen bond between its side chain oxygen and the main chain nitrogen of Gly186 (**Fig. 3.4C**). In the unphosphorylated protein Asp184 is turned away from Gly186 to a catalytically incompetent conformation similar to that

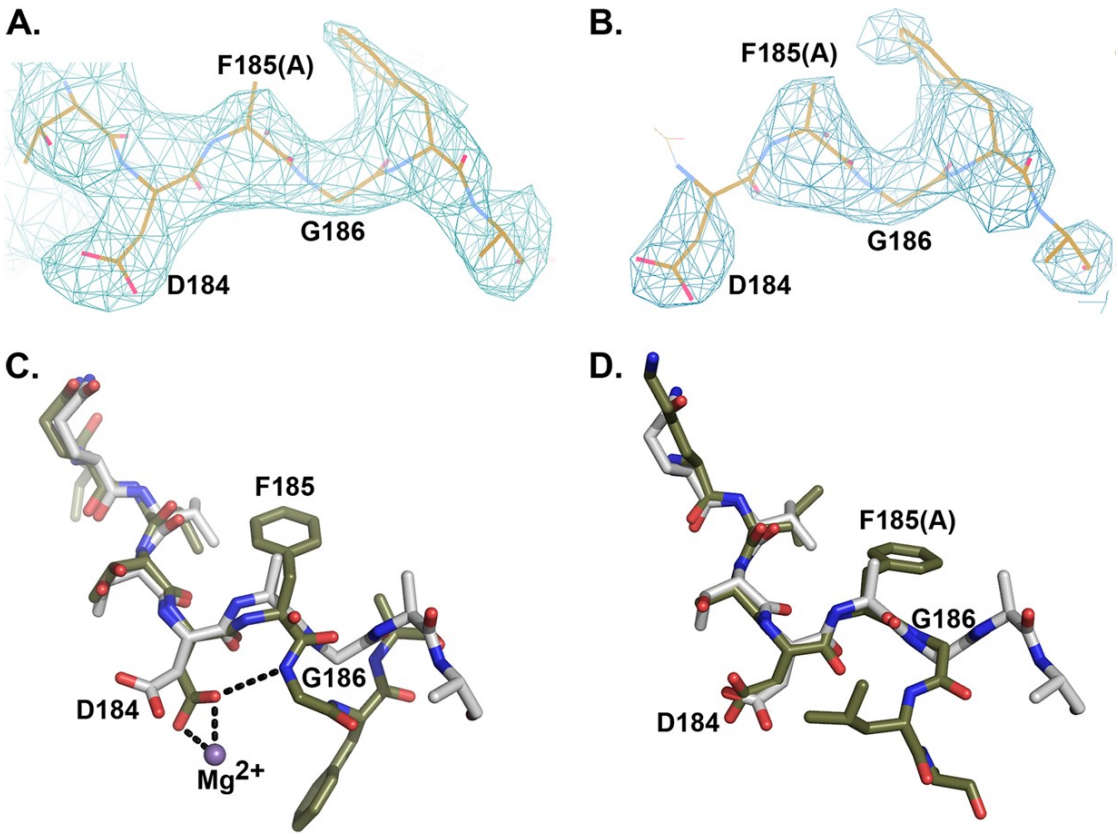

Figure 3.4. The magnesium positioning loop is similar to other inactive kinases. (**A**) the 2Fo-Fc map contoured at 1.0σ for C^{R194A} from the beginning of the activation segment to the disordered region ending at Ala188. (**B**) the same view as in (A) showing the Fo-Fc map at 2.7σ after removing the activation loop from the model as described in "experimental procedures". (**C**) the same region of the activation segment as in (A) aligned to the wild type protein (1ATP; olive) showing the rotation of the magnesium coordinating residue Asp184. The magnesium ion is colored purple. (**D**) alignment of C^{R194A} (gray) to the inactive form of CDK2 (1HCL; olive) shows a similar disruption of the hydrogen bond linking the DFG Asp184 to the Gly186 amide nitrogen.

seen in the inactive CDK2 structure (Schulze-Gahmen et al., 1996) (**Fig. 3.4D**). The shift in the main chain at the C-terminal end of the catalytic loop is likely caused by the crystal packing interaction described above where Phe129 packs against the catalytic loop.

The hydrophobic spine is broken in the unphosphorylated C-subunit – Two hydrophobic spines are a conserved feature of protein kinases in their active conformation (Kornev et al., 2006). The catalytic spine is completed by the adenine ring of ATP whereas the regulatory R-spine is typically assembled as a consequence of phosphorylating the activation loop. The R-spine anchors the N-lobe to the C-lobe and correctly positions the catalytically important Asp184 of the DFG motif. In C^{R194A}, the R-spine is broken and the N-lobe is open as well as rotated substantially more than any other PKA structure (**Fig. 3.5**). The spine residue Phe185 of the DFG motif is disordered in the structure and Ala was modeled in its place (**Fig. 3.4A and B**). In the wild type structure, Phe185 makes hydrophobic packing interactions with both Leu95 from the N-lobe and Tyr164 from the C-lobe. The positions of both Leu95 and Tyr164 are different from wild type C. Leu95 is in a similar conformation to wild type but the rotation of the N-lobe has moved its position away from Phe185 in the C-lobe. In the wild type C-subunit the side chain of Tyr164 in the catalytic loop is within hydrogen bonding distance to the main chain carbonyl oxygens of Asp184, and Thr183, and the side chain nitrogen of Asn171. In C^{R194A} all three of these residues are out of hydrogen bonding distance and the Tyr164 hydroxyl group has moved by ~3Å, losing its hydrophobic packing interaction with Phe185 but forming new hydrogen

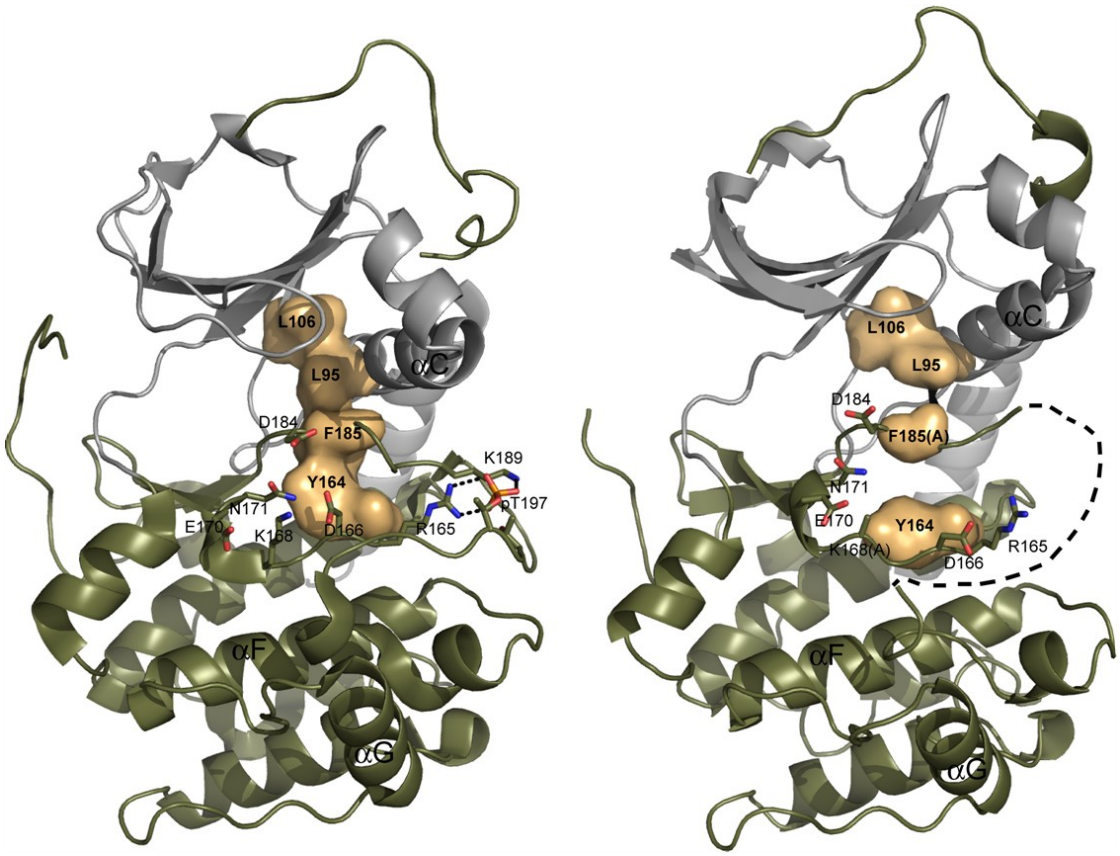

Figure 3.5. Disruption of the hydrophobic spine in C^{R194A}. The hydrophobic spine is shown for the wild type apoenzyme (1J3H; **left**), and C^{R194A} (**right**). The C-lobe is colored olive and the N-lobe is colored gray. The spine is shown as a tan surface and IP20 peptide is colored teal.

bonds with the main chain carbonyl oxygen of Asp166 and main chain nitrogen of Lys168 (**Fig. 3.3D**). Thus, the movement of the activation loop away from the catalytic loop may have the effect of breaking the hydrophobic interaction between Tyr164 and Phe185 causing disorder of the side chain of Phe185 and allowing the rotation of the N-lobe.

Rate of the phosphoryl transfer step in C^{R194A} is diminished – Since the Arg194Ala mutant altered the positions of numerous residues thought to be important for optimal catalytic function, we measured the phosphoryl transfer rate constant using rapid quench flow methods to determine whether there is a direct correlation between these disturbances and serine phosphorylation. The kinetics of the wild type enzyme was previously shown to be biphasic (Grant and Adams, 1996) where the first pre-steady-state exponential phase (burst) represents the rapid phosphoryl group transfer step and the second linear phase represents the rate limiting release of ADP. We confirmed that the wild type enzyme gave a biphasic curve with a burst rate constant of 78 s^{-1} and a linear rate constant of 13 s^{-1}. Unlike the wild type enzyme, no exponential burst phase was observed in C^{R194A} and instead it displayed a linear phase with a rate constant of 3.6 s^{-1} (**Fig. 3.6**). To ensure that the absence of burst phase is not the result of weak substrate binding, pre-steady-state kinetic experiments were repeated using higher Kemptide concentrations (2 mM) (data not shown). Under these conditions no measureable burst phase was detected indicating that the observed changes in the kinetic profiles are likely the result of a 20-fold reduction in the phosphoryl transfer rate constant.

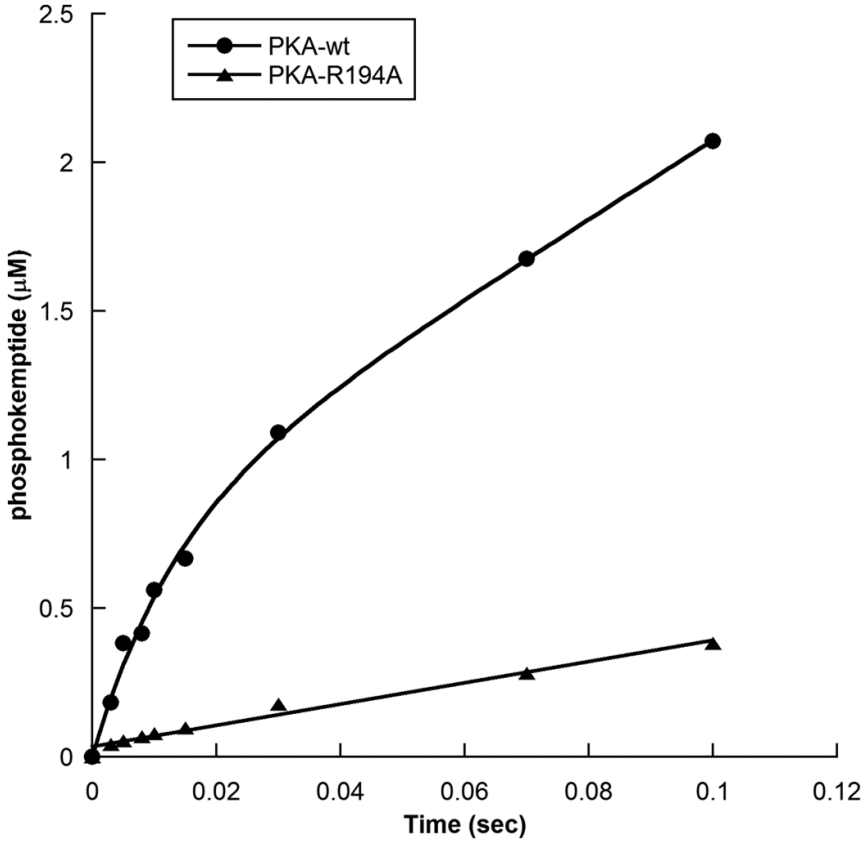

Figure 3.6. Kinetic analysis shows a loss of pre-steady-state burst phase in the unphosphorylated C-subunit. The first 100 ms of the phosphorylation of kemptide by the wild type C-subunit and C^{R194A} were measured using the rapid quench flow methods described in "experimental procedures".

3.4 Discussion

By crystallizing Arg194Ala mutant of the PKA C-subunit we were able to compare the structural consequences of removing this single phosphate from the activation loop without altering the rest of the protein, including Thr197 and the phosphorylated Ser338. Changes were seen in the global conformation, in the hydrogen bonding network at the active site and in the hydrophobic regulatory spine. In addition we used a rapid quench flow assay to define the kinetic consequences of removing the activation loop phosphate.

We previously used hydrogen/deuterium exchange to compare the dynamics of the C^{R194A} mutant to the wild type C-subunit in solution (Steichen et al., 2010). It was found that a peptide containing the DFG motif 182-186 exchanged ~2 amide hydrogens at a faster rate in C^{R194A} compared to the wild type C-subunit and this exchange occurred within 10 seconds, (the first measured time point). The crystal structures show there are two changes to the main chain amides on this peptide when comparing the wild type and C^{R194A} apoenzymes. In the wild type structure, the side chain of Asp184 makes a hydrogen bond to the main chain amide nitrogen of Gly186. In order for the amide hydrogen of Gly186 to exchange with the solvent the hydrogen bond must break. In the structure of C^{R194A}, the side chain of Asp184 is turned away from Gly186 and the backbone amide of Gly186 is free to exchange with the solvent. Additionally, the amide nitrogen of Phe186 is hydrogen bonded to the side chain of Glu91 from the C-helix in the apo wild type structure. Due to the rotation of the N-lobe in C^{R194A} this interaction is also broken. This could explain the increased rate of hydrogen exchange on this peptide in the solution study. The catalytic loop peptide

(residues 163-172) was also shown to exchange at a faster rate in the unphosphorylated enzyme. In this peptide 6-7 amide hydrogens exchanged over the course of 50 min in C^{R194A} compared to 4 amides exchanged in the wild type protein. The resolution of the deuterium exchange study was not high enough to assign specific residues to the increased exchange rates and furthermore, there is a crystal packing contact in this region in the C^{R194A} structure. However, we do see a dramatic loss of hydrogen bonding between side chains of the catalytic loop and the main chain of the activation segment in the C^{R194A} structure that may explain the increased dynamics of the catalytic loop. Additionally, we showed that β6 had a faster rate of hydrogen exchange in C^{R194A} compared to the wild type enzyme. In the wild type C-subunit β6 and β9 form a β-sheet. Lys189 belongs to β9 and its side chain makes a hydrogen bond with the phosphate at Thr197. In the structure of C^{R194A} Lys189 is disordered which explains the increased rate of hydrogen exchange in β6. Several mutants of PKA have been characterized by hydrogen deuterium exchange and were found to be more dynamic in similar regions as the unphosphorylated enzyme. However, when these mutants were co-crystallized with Mg/ATP and IP20 they did not show significant changes compared to the wild type enzyme (Yang et al., 2005; Yang et al., 2004) (Yang et al., 2012). The structure of the apo, unphosphorylated enzyme provides insight into the unstable regions of the protein that would otherwise be masked in the presence of ligand.

In the C^{R194A} structure the disassembled hydrophobic R-spine is not analogous to the "DFG-out" conformation in which the phenylalanine blocks the ATP binding site but is more similar to p38 kinase (PDB ID: 1WFC). In p38 kinase the rotation of

the N-lobe breaks the interactions of Phe169 with Leu75 but its hydrophobic interaction with the C-lobe (His148) remains intact. In PKA, Phe185 has lost hydrophobic interactions from above and below and its side chain is disordered. The main chain does not turn into the ATP binding pocket but rather moves away from the catalytic loop. This has the effect of decoupling the two lobes of the enzyme and hence a greater twist than has been observed in any previous structure of PKA. While the ATP binding site is not sterically blocked, the N-lobe must undergo a 30˚ rotation to form the active or "closed" conformation that is characteristic of the ATP bound ternary complex. Because C^{R194A} is not catalytically dead it must be able to rotate to the wild type closed conformation and therefore, multiple conformations must exist in solution. While this structure is in good agreement with our previous solution data it represents only one conformation which could be stably incorporated into a crystal lattice.

Numerous catalytic residues are displaced in the unphosphorylated C-subunit and this appears to correlate with a large decrease in the rate of phosphoryl transfer as measured by pre-steady-state kinetic methods. The C^{R194A} mutant shows a similar kinetic defect as the C^{T197A} mutant which has the phosphorylation site mutated to an alanine. This mutant was previously analyzed by solvent viscosity techniques (Adams et al., 1995). It showed a more severe kinetic defect compared to the Arg194Ala mutant emphasizing the importance of the threonine hydroxyl group in stabilizing the active site but consistent with C^{R194A} it was primarily defective in the phosphoryl transfer step. It will be interesting to see how the regulation of individual rate

constants can play a role in phosphorylation within the context of macromolecular complexes where a large turnover is not required for a biological response.

The structure we present here represents a novel conformation for a kinase lacking activation loop phosphorylation. Given that protein kinases belong to one of the largest families of enzymes in the human genome it would be of great value to accurately predict the effects of activation loop dephosphorylation on individual protein kinases. PKA is closely related to other AGC kinases whose structures have been solved in their unphosphorylated states and yet there is a great deal of dissimilarity between these structures. Perhaps in some cases the unphosphorylated conformations reflect differences in recognition requirements for the kinases that phosphorylate them. Because unphosphorylated kinases show greater structural diversity compared to the phosphorylated structures, targeting the unphosphorylated enzymes *in vivo* can be used as an alternate approach to designing selective inhibitors and further studies are warranted.

Chapter 3 in its entirety was published in Structural Basis for the Regulation of Protein Kinase A by Activation Loop Phosphorylation. Steichen JM, Kuchinskas M, Keshwani MM, Yang J, Adams JA, Taylor SS. *J. Biol. Chem*. 2012 Apr 27;287(18):14672-80. The dissertation author was the primary investigator and author of this work.

Chapter 4

Turn Motif Phosphorylation Regulates Processing of the Catalytic Subunit of Protein Kinase A

4.1 Introduction

Protein kinase A (PKA) is a member of the AGC family of protein kinases. In cells it forms a tertrameric holoenzyme consisting of two catalytic (C) subunits and two regulatory (R) subunits. The C-subunit is constitutively phosphorylated on two residues, Thr197 in the activation loop and Ser338 on the C-terminal tail which provides maximal activity and stability to the enzyme (Adams, 2003; Batkin et al., 2000; Steichen et al., 2010; Yonemoto et al., 1997). Phosphorylation occurs rapidly (Cauthron et al., 1998) and the enzyme is then regulated by cAMP binding to the R-subunits which releases the active C-subunit. The kinase responsible for the phosphorylation of the PKA activation loop is not yet known, however, some evidence points to PDK1 as the PKA kinase (Moore et al., 2002; Nirula et al., 2006) while other data suggests the PDK1 pathway can be bypassed (Williams et al., 2000).

The C-terminal tail site is known as the turn motif due to its location within a turn in the C-terminal tail of PKA. The turn motif of PKA is not homologous to the turn motif of other AGC kinases which has also been called the zipper/tail site in other kinases due to the fact that it does not reside within a structural turn as in PKA (Hauge et al., 2007). PKA contains a series of glutamates which may serve to mimic the turn/zipper/tail site of other AGC kinases (Hauge et al., 2007). Only the p90 ribosomal S6 kinase has been found to have a phosphate at the site predicted to be homologous to the PKA turn motif (Ballif et al., 2005; Hauge et al., 2007). This Ser338 phosphorylation site is thought to be an autophosphorylation site which occurs via an intramolecular reaction (Iyer et al., 2005b; Pickin et al., 2008). Once phosphorylated, this site is resistant to dephosphorylation by phosphatases (Humphries et al., 2005). It

can however, be dephosphorylated under conditions where the Cys199 in the activation loop is oxidized or modified (Humphries et al., 2005).

The importance of this site has been studied with a number of biophysical approaches. Iyer et al. used a kinase dead mutant co-expressed with PDK1 to obtain the C-subunit containing only activation loop phosphorylation (Iyer et al., 2005a). It was found that this mutant could still bind to the regulatory subunit of PKA with approximately the same affinity as wild type. Mutating Ser338 to Ala resulted in a rapid loss of activity during purification (Yonemoto et al., 1997) while mutations to Glu resulted in decreased kcat. It was also shown previously that Ser338 phosphorylation may regulate the interaction between PKA and Hsp70 (Gao and Newton, 2002). It has been suggested to play a role in recognition by PDK1 (Romano et al., 2009) however Ser338 phosphorylation is not a requirement for PDK1-dependent phosphorylation of PKA *in vitro* (Iyer et al., 2005a). Bossemeyer et al. published the structure of the catalytic subunit purified from porcine heart and the structure contains only the activation loop phosphate. However, the authors stated that they measured 1.8 moles of phosphate per mole of enzyme but only one phosphate was visible in the structure (Bossemeyer et al., 1993). This structure was very similar to other structures of the wild type C-subunit.

The purpose of this study was to identify the function of Ser338 phosphorylation of the PKA C-subunit using structural and biological methods. Here we show that a mutant C^{R336A}, previously shown to be as stable as wild type (Batkin et al., 2000), does not autophosphorylate on the turn motif. This mutation is located at the P-2 site relative to the turn motif and thus blocks the PKA substrate consensus

sequence. We crystallized the unphosphorylated turn motif mutant C^{R336A} in complex with a 20-mer inhibitory peptide IP20 and Mg/AMP-PNP. The structural changes were minimal and localized to the C-terminal tail. However, investigation in mammalian cells revealed a biological role for turn motif phosphorylation in the processing of PKA.

4.2 Experimental Procedures

Purification of the wild type and mutant C-subunits – The wild type murine Cα-subunit was expressed and purified as described previously (Herberg et al., 1993). The Arg336Ala mutation was introduced into the His6-tagged murine Cα-subunit of PKA in pET15b by Quickchange according to the Stratagene protocol and the proteins were expressed in *E. coli* (BL21 (DE3)) (Steichen et al., 2010). Cultures were grown at 37°C to an OD_{600} of ~0.8 and induced with 0.5 mM Isopropyl β-D-thiogalactopyranoside. The cultures were allowed to grow overnight at 16°C before being harvested. The pellet was resuspended in lysis buffer (50 mM KH_2PO_4, 20 mM Tris-HCl, 100 mM NaCl, 5 mM β-mercaptoethanol, pH 8.0) and lysed using a microfluidizer (microfluidics) at 18,000 p.s.i. The cells were clarified by centrifugation at 17,000 rpm at 4°C for 50 min in a Beckman JA20 rotor, and the supernatant was incubated with ProBond Resin (Invitrogen) for 1 hour at 4°C. The resin was loaded onto a column and washed twice with the lysis buffer and twice with wash buffer (50 mM KH_2PO_4, 20 mM Tris-HCl, 100 mM or 1 M NaCl, 10 mM imidazole, and 5 mM β-ME, pH 7). An imidazole elution buffer using concentrations of imidazole ranging from 50 – 500 mM in wash buffer was used to elute the His6-

tagged protein. Samples containing the most protein were dialyzed overnight into 20 mM KH_2PO_4, 20 mM KCl, and 2.5 mM DTT, pH 6.5 and then loaded onto a pre-packed Mono-S 10/10 (GE health) cation exchange column equilibrated in the same buffer. Then the protein was eluted with equilibration buffer containing a KCl gradient ranging from 0 to 1 M. In some cases it was necessary to run the protein over the ion-exchange column a second time at pH 7.15 to obtain a high level of purity. The mutant was very soluble and this procedure yielded similar quantities as is obtained from expression of the wild type C-subunit. The phosphorylation state of the activation loop was confirmed using a polyclonal phospho-Thr197 antibody that was raised in rabbits against the epitope peptide RVKGRTWpTLCGTPEY (Invitrogen). The turn motif phosphorylation state (Ser338) was determined using a polyclonal phospho-Ser338 antibody described previously (Iyer et al., 2005b). The PKA C-subunit antibody was purchased from BD Biosciences.

Crystallization – The C^{R336A} mutant was concentrated to ~10-15 mg mL^{-1} and setup for crystallization at 4°C using the hanging drop vapor diffusion method. The protein crystallized using the same conditions as previous structures of the C-subunit (Wu et al., 2005; Yang et al., 2009). Briefly, the protein was dialyzed into 50 mM Bicine, 150 mM ammonium acetate, pH 8, and 10 mM DTT and mixed with $MgCl_2$, AMP-PNP, and IP20 in a ratio of 1:20:10:10. An equal volume of protein, IP20/Mg/AMP-PNP, and well solution (8-14% MPD, 100 mM Tris-HCl, pH 8, 10 mM DTT) were setup by the hanging drop vapor diffusion method at 4˚C and methanol (11-13%) was added to the well solution before sealing the well.

Data collection and refinement – The crystals were flash cooled in liquid nitrogen with cryoprotectant solution (mother liquor in 15% glycerol). Data was collected on the synchrotron beamline 8.2.2 of the Advanced Light Source, Lawrence Berkeley National Labs (Berkeley, California). The data was integrated using iMOSFLM (Battye et al., 2011). The protein crystallized in the $P2_12_12_1$ space group similar to the wild type structure. Molecular replacement was carried out using Phaser (McCoy et al., 2007) with 1RDQ as a search model. The refinement was done with refmac5 and model building was done in Coot. During the refinement it was apparent that the glycine rich loop was in a more open conformation compared to the wild type structure. When the glycine rich loop was deleted the Fo-Fc map showed density only in the open conformation and it was therefore modeled in the open conformation. However, in the final model the Fo-Fc map shows some electron density in the wild type closed conformation and it is likely that a fraction of the protein is in the wild type conformation. Additionally, 180 images were collected and processed but there was no density for portions of the glycine rich loop. When only 90 images were used for the refinement there was complete density for the glycine rich loop and thus, only 90 images were used for the refinement. The structure was refined to an R_{work}/R_{free} of 18.3/21.7. The refinement statistics are shown in table 4.1.

Steady state kinetics – The kinetics of C^{R336A} and wild type C were carried out essentially as described previously (Steichen et al., 2010) except the buffer was 100 mM HEPES, pH 7.4, 10 mM $MgCl_2$, and 10 mM DTT. To measure the K_m for

Table 4.1. Data Collection and Refinement Statistics for R336A.

Data collection	
Crystal	**C^{R336A}/AMP-PNP/IP20**
PDB ID	4DG3
Space group	$P2_12_12_1$
Cell dimensions	
a (Å)	72.29
b (Å)	76.69
c (Å)	80.31
$\alpha = \beta = \gamma$ (°)	90.0
Molecules per asymmetric unit	1
Unique reflections	37,095 (5,579)
Redundancy	3.9 (3.8)
Resolution range (Å)	38.34-1.8 (1.9-1.8)[a]
R_{sym} (%)	4.5 (47.5)
$I/\sigma I$	15 (3.4)
Completeness (%)	88.9 (92.7)
Refinement	
R_{work}/R_{free} (%)[b]	18.3/21.7
Ramachandran angles (%)[c]	
Favored regions	97.7
Allowed regions	100
r.m.s. deviations	
Bond lengths (Å)	0.007
Bond angles (°)	1.1

[a]Values in parenthesis correspond to the highest resolution shell. [b]5% of the data was excluded from the refinement to calculate the R_{free}. [c]Ramachandran plot quality as defined in MolProbity (Davis et al., 2007).

ATP the concentration of kemptide (LRRASLG) was fixed at 500 μM and ATP was varied from 5 – 320 μM. To measure the K_m for kemptide the concentration of ATP was fixed at 1 mM and kemptide was varied from 5 – 200 μM. The final concentration of enzyme was ~0.003 $mgmL^{-1}$. Data were fit using GraphPad Prism.

Expression of C-subunit mutants in mammalian cells – The Cα subunit of PKA cloned in pCDNA3 with C-terminal HA-tag was transfected in HEK293 cells or cotransfected with myc-tagged PDK1 using lipofectamine 2000 (Invitrogen) according to the manufacturer's protocol. Approximately 20 hours post-transfection cells were harvested by washing once with ice cold PBS and then resuspension in 50 mM Tris, 150 mM NaCl, 2 mM EDTA, and 1% Triton X-100, pH 7.4. Additionally, a protease inhibitor cocktail (Calbiochem) and a phosphatase inhibitor cocktail (Sigma) were added. The cells were lysed by sonication and spun down at 10,000 g for 10 min. The soluble fraction was loaded on SDS-PAGE gels and analyzed by western blotting.

Calyculin A, okadaic acid, and cpt-cAMP treatment of HEK293 cells – Wild type and mutants of the C-subunit were expressed in HEK293 cells as described above and prior to harvesting, cells were treated with 50 nM Calyculin A, 100 nM okadaic acid, or 50 μM 8cpt-cAMP for 30 min.

4.3 Results

Turn motif phosphorylation is required for activation loop phosphorylation in mammalian cells – In order to study the effects of turn motif phosphorylation it was necessary to identify a mutant that does not autophosphorylate. We previously described a mutation in the activation loop Arg194Ala that blocks autophosphorylation of the activation loop but not the turn motif (Moore et al., 2002; Steichen et al., 2010). This is due to the disruption of the PKA substrate consensus sequence at the activation loop phosphorylation site. Similarly there is a P-2 Arg (Arg336) at the turn motif that is essential for autophosphorylation of Ser338. When C^{R336A} is expressed and purified from bacteria the turn motif is not phosphorylated but the activation loop (Thr197) is phosphorylated to the same extent as wild type (**Fig. 4.1**). In contrast, when this mutant was over expressed in HEK293 cells the turn motif was not phosphorylated but the activation loop also showed decreased levels of phosphorylation. Densitometric analysis of the activation loop band showed that C^{R336A} was 35% phosphorylated relative to the wild type protein (**Fig. 4.2**). Short transfection times (6 hours) showed a similar decrease in activation loop phosphorylation (data not shown). Additionally, it was found that CREB, a known substrate of PKA, had a similar reduction in phosphorylation in the cells overexpressing the R336A mutant compared to cells overexpressing the WT C-subunit (**Figs. 4.4 and 4.5, compare lanes 1 and 3 from each gel**). A Ser338Glu phosphomimetic mutation did not rescue activation loop phosphorylation but showed similar levels of activation loop phosphorylation as the Arg336Ala mutant (**Fig. 4.3**).

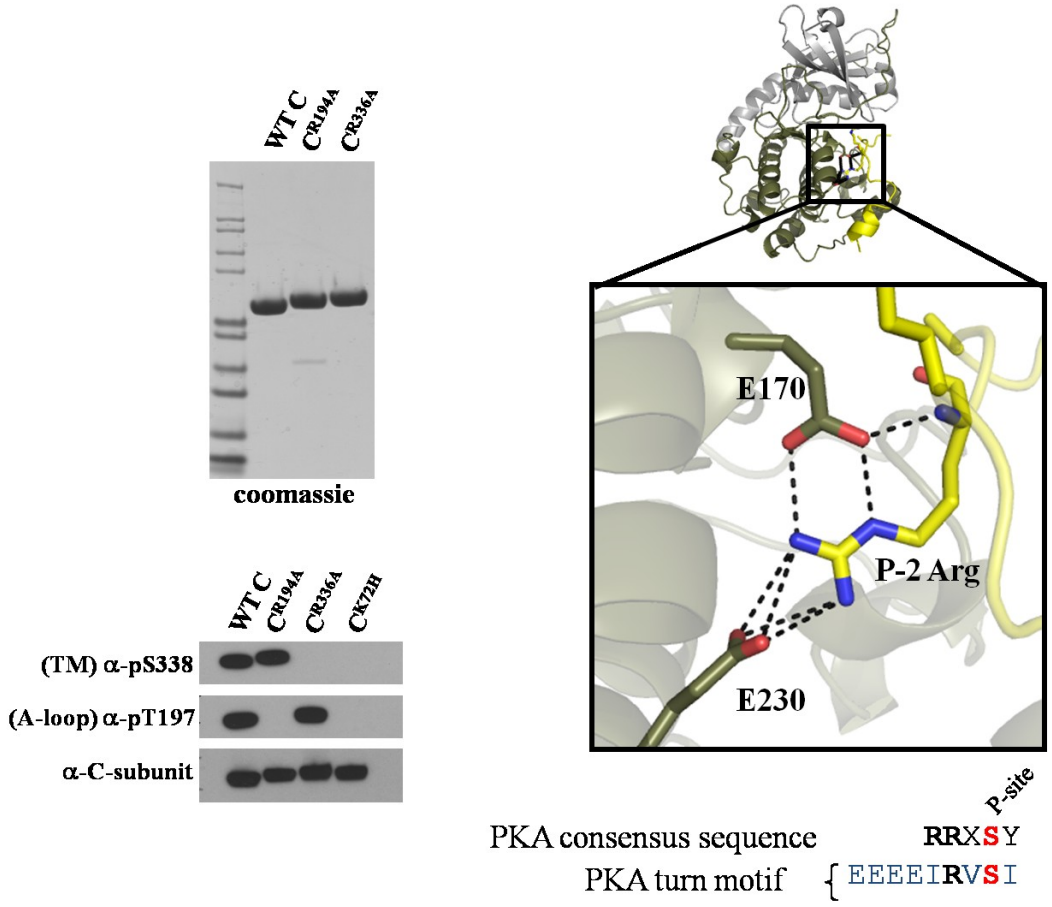

Figure 4.1. **Purification and phosphorylation state of the C^{R336A} mutant expressed in bacteria.** Coomassie gel showing the purified C-subunit proteins after expression in E. coli: untagged wild type, 6xHis tagged C^{R194A}, and C^{R336A} (**Top left**) The purified proteins were probed with α-pThr197, α-pSer338, and α-C-subunit antibodies (**bottom left**). The wild type C-subunit is known to be stoichiometrically phosphorylated on Thr197 and Ser338 (Herberg et al., 1993) and is shown as a positive control. C^{K72H} is catalytically dead and is shown as a negative control. PKA substrates require a P-2 Arg which makes hydrogen bonding interactions to Glu170 and Glu230 (**right**).

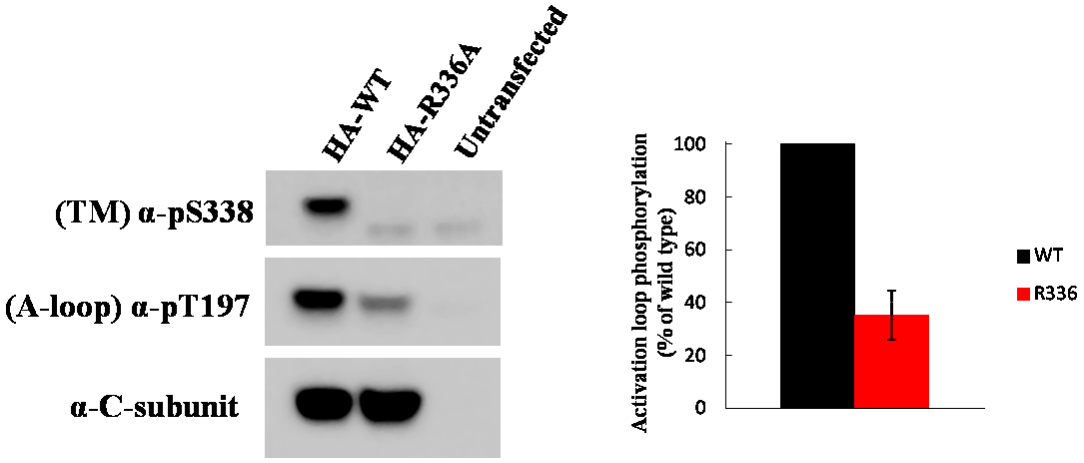

Figure 4.2. **Expression of C^{R336A} in HEK 293 cells shows absence of Ser338 phosphorylation and reduced Thr197 phosphorylation.** The soluble lysates were probed with α-pThr197, α-pSer338, and α-C-subunit antibodies. Quantification of activation loop phosphorylation by densitometry shows C^{R336A} is 35 ± 9% phosphorylated compared to the wild type enzyme. (mean ± SE, n=3).

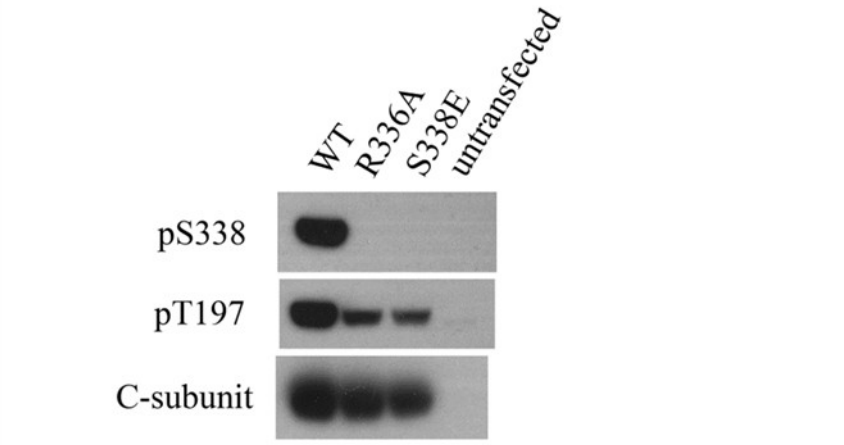

Figure 4.3. **Glutamate phosphomimetic mutation at the turn motif does does not rescue activation loop phosphorylation**. The C^{S338E} mutant was overexpressed in HEK293 cells and the soluble lysates were probed with α-pThr197, α-pSer338, and α-C-subunit antibodies. The phosphorylation state of the activation loop was similar for C^{S338E} and C^{R336A}.

PDK1 but not endogenous PKA can phosphorylate the mutant C^{R336A} – Next we checked the possibility that endogenous inhibitors of PKA could block phosphorylation of the C-subunit activation loop or whether activation of endogenous C-subunit would phosphorylate the C^{R336A} mutant. Treatment of 293 cells with a nonhydrolyzable analog of cAMP (8cpt-cAMP) did not increase the levels of activation loop phosphorylation in the over-expressed mutant C^{R336A}, indicating that the R-subunit does not block activation loop phosphorylation in the C^{R336A} mutant (**Fig. 4.4A**). As a control, 8cpt-cAMP treatment did increase levels of CREB phosphorylation a known PKA substrate.

Next we tested whether PDK1 could phosphorylate the activation loop of C^{R336A}. When myc-tagged PDK1 was coexpressed with C^{R336A} in HEK293 cells and the lysate was blotted for Thr197 phosphorylation, the C^{R336A} mutant was completely phosphorylated, similar to the wild type enzyme (**Fig. 4.4B**).

Decreased levels of activation loop phosphorylation in C^{R336A} is not due to dephosphorylation by phosphatases – To test whether the decrease in activation loop phosphorylation was a result of dephosphorylation by a phosphatase we treated the cells with calyculin A as well as okadaic acid. The results show no change in the amount of activation loop phosphorylation for the R336A mutant in the presence of calyculin A or okadaic acid although CREB phosphorylation was enhanced in the presence of either phosphatase inhibitor (**Fig. 4.5**).

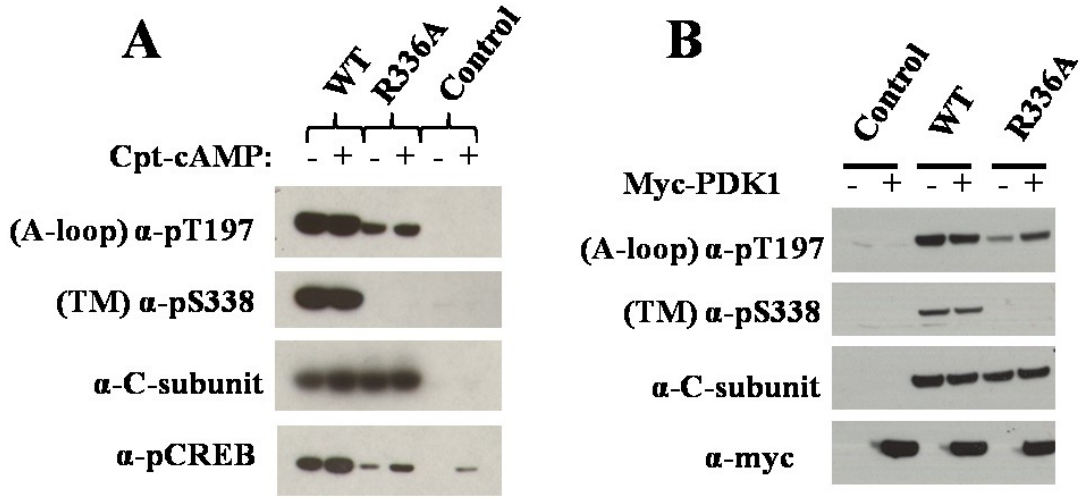

Figure 4.4. **PDK1 but not endogenous PKA phosphorylates the activation loop of C^{R336A}.** (**A**) Wild type C and C^{R336A} were overexpressed in HEK293 cells and treated with 8cpt-cAMP for 30 min. The soluble lysates were probed with α-pThr197, α-pSer338, α-C-subunit, and α-phosphoCREB antibodies. (**B**) CR336A was cotransfected with myc-PDK1 and analyzed by the same method as in (A).

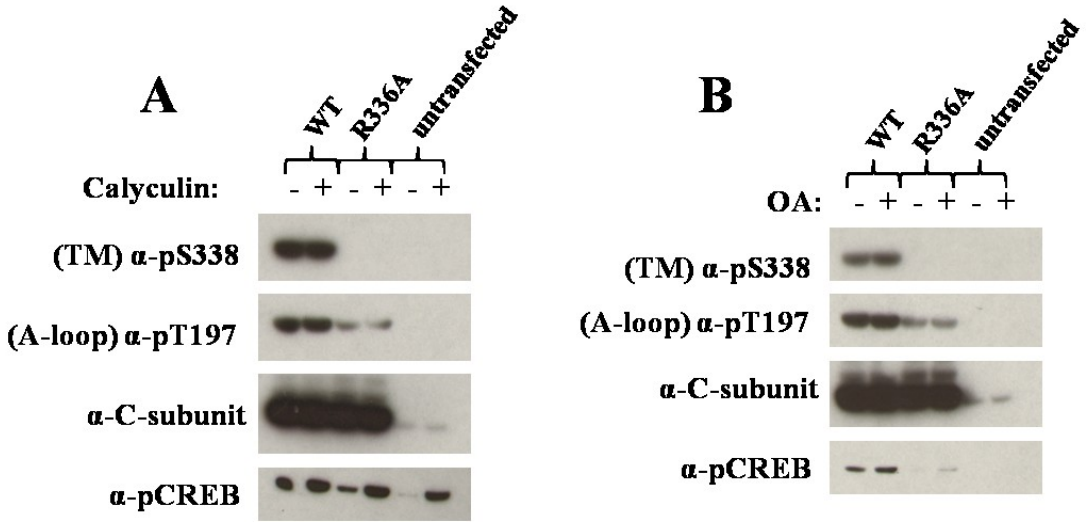

Figure 4.5. **The activation loop of C^{R336A} is not dephosphorylated by phosphatases**. HEK293 cells overexpressing either wild type C or C^{R336A} were treated with phosphatase inhibitors, (**A**) calyculin A or (**B**) okadaic acid for 30 min and the soluble lysates were probed with α-pThr197, α-pSer338, α-C-subunit, and α-phosphoCREB antibodies.

There is a modest decrease in the kcat for C^{R336A} – The steady state kinetics of C^{R336A} were measured using kemptide (LRRASLG) as a substrate. The C^{R336A} mutant showed a slight decrease in k_{cat}, similar to what has been previously shown (Batkin et al., 2000). However, due to a corresponding decrease in K_m the catalytic efficiency (k_{cat}/K_m) was similar to the wild type enzyme (**Table 4.2**).

Structure of the turn motif mutant C^{R336A} – The mutant C^{R336A} crystallized in the presence of Mg/AMP-PNP and IP20 in the $P2_12_12_1$ space group similar to previous structures of the C-subunit (**Table 4.1**). An alignment of C^{R336A} to wild type shows structural changes that are localized to the C-terminal tail adjacent to the turn motif and to the glycine rich loop. The RMSD for C^{R336A} and the wild type C-subunit (1ATP) is 0.403 Å and the B-factors are similar to previous structures of the C-subunit (**Fig. 4.6**). The conformation of the turn motif is not effected by phosphorylation (**Fig. 4.7**). The hydroxyl group of Ser338 is in hydrogen bonding distance to both the amide nitrogen and carbonyl oxygen of Asn340. Unlike C^{R194A} where the absence of phosphate on the activation loop causes disorder of the activation loop, in C^{R336A}, the conformation of the turn motif is maintained by hydrogen bonding of the Ser338 hydroxyl group. The main chain N-terminal to the turn motif is flipped over relative to the wild type enzyme at the site of the R336A mutation and the glycine rich loop was raised slightly compared to the closed conformation.

Table 4.2. Steady-State Kinetics of R336A.

Enzyme	k_{cat} (s^{-1})	K_m Kemp (μM)	K_m ATP (μM)
WT C	17.2 ± 0.6	26 ± 3	33 ± 3
C^{R336A}	13.5 ± 0.5	18 ± 2	33 ± 4

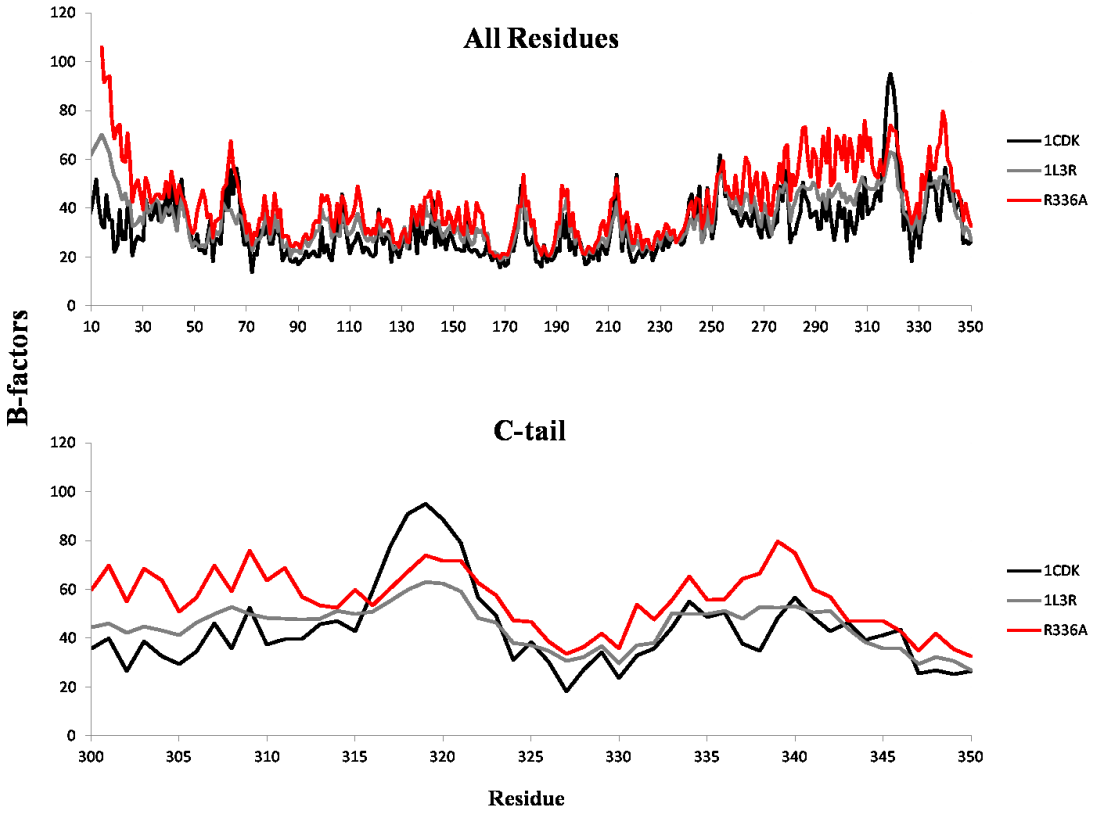

Figure 4.6. **B-factors of the C^{R336A} mutant**. The crystal structure of C^{R336A} shows similar B-factors as the wild type C-subunit PDB IDs: 1CDK and 1L3R. There is a modest increase in the B-factors surrounding the turn motif in C^{R336A}.

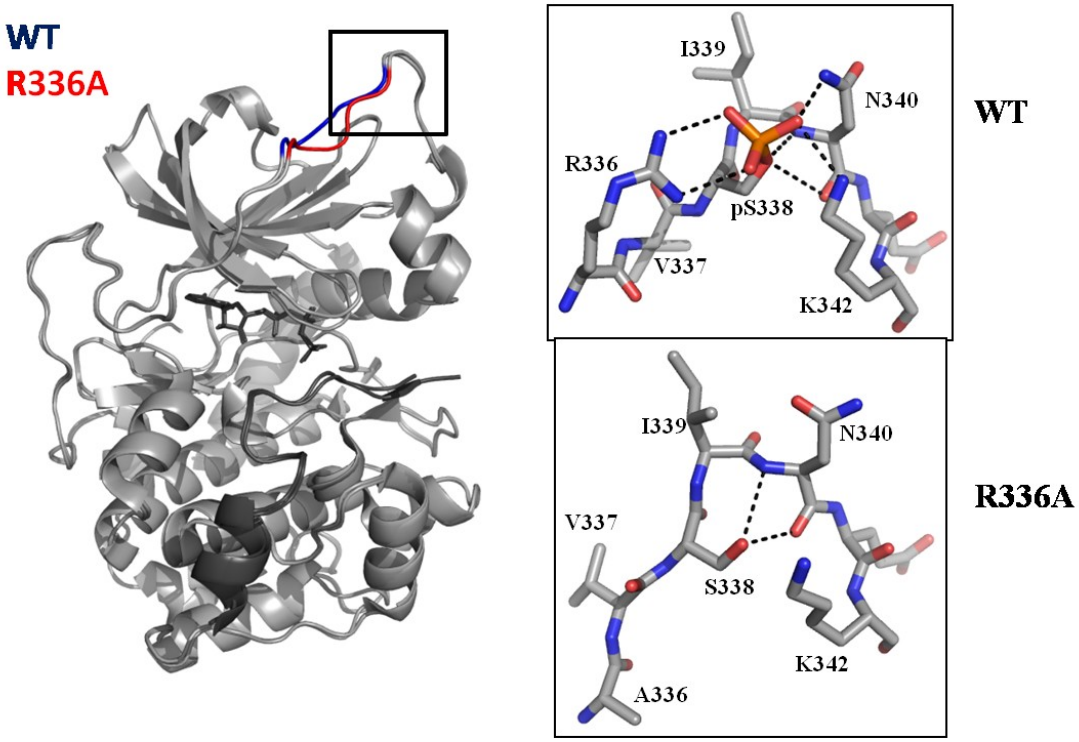

Figure 4.7. **Alignment of C^{R336A} and wild type structures and hydrogen bonding at the turn motif**. Left, the wild type C-terminal tail is shown in blue and C^{R336A} is shown in red. Upper right, shows the maximum number of hydrogen bonds of the turn motif phosphate in the wild type C-subunit as seen in PDB ID: 3OW3 and hydrogen bonds to the Ser338 hydroxyl group of C^{R336A} are shown at bottom right.

4.4 Discussion

In this study we took a structural and biological approach to understand the significance of Ser338 phosphorylation in the PKA catalytic subunit. The structural study showed only minor changes between a mutant (C^{R336A}) which does not autophosphorylate on Ser338 and the phosphorylated wild type enzyme. Over expression of this same mutant in mammalian cells revealed a role for Ser338 phosphorylation in maturation of the C-subunit to its fully active state.

In the wild type structures of PKA, phospho-Ser338 is in hydrogen bonding distance to two main chain atoms of Asn340 and a maximum of four side chain atoms. There is variation among the different structures but in general both main chain atoms are within hydrogen bonding distance to the Ser338 side chain oxygen while the phosphate oxygens interact with the adjacent side chains of Arg336, Asn340, and Lys342. In the C^{R336A} structure both main chain atoms are still in hydrogen bonding distance to the Ser338 hydroxyl group while the adjacent side chains have lost their hydrogen bonds in the absence of phosphate. It was previously shown that Ser338 mutation to Ala severely compromised the stability of the protein and mutation to Asp or Glu only slightly increased the stability compared to Ala (Batkin et al., 2000). It is logical to assume that Asp or Glu, due to the length of their side chains, preferentially make interactions with the side chains of Arg336, Asn340, or Lys342 rather than the main chain atoms of Asn340. Thus, it is evident that the main chain interactions are sufficient for maintaining the turn in the C-tail and these interactions likely provide stability to the protein.

Studies carried out *in vitro* show that the C-subunit can form a disulfide bond between Cys199 in the activation loop and Cys343 in the C-terminal tail in the presence of diamide (Humphries et al., 2005). This disulfide bonded form of the C-subunit is inactive and may resemble the conformation of the enzyme during autophosphorylation of Ser338. Cys343 is at the P+5 position relative to Ser338 and modeling a Cys into a PKA substrate at the P+5 position shows the close proximity to Cys199 (**Fig. 4.8**). While docking of the C-tail to the active site could potentially inhibit the enzyme in a similar manner as in the disulfide bonded state (Cauthron et al., 1998; Humphries et al., 2005), there is no evidence that this conformation is sufficiently stable to inhibit the activity of the enzyme in the absence of a disulfide bond. The R336A mutation could potentially reduce the affinity of the C-tail for the active site due to the disruption of the substrate consensus sequence, To confirm that the R336A mutation was not the primary cause for the alteration in processing we expressed the S338E mutant in cells. This mutant showed a similar decrease in activation loop phosphorylation indicating that mutation of the P-2 Arg is not the cause for the defect in processing of the enzyme.

In many protein kinases, phosphorylation of the activation loop is a dynamic process that is regulated by changing the equilibrium between phosphatase and kinase activity (Chan et al., 2012; Gould et al., 2011). In our study, treatment with phosphatase inhibitors and a cAMP analog show that the altered levels of PKA activation loop phosphorylation are not the result of a dynamic process. The phosphorylation state of the activation loop appears to be stable; either phosphorylated or unphosphorylated, and is determined early in the expression of the protein. Because

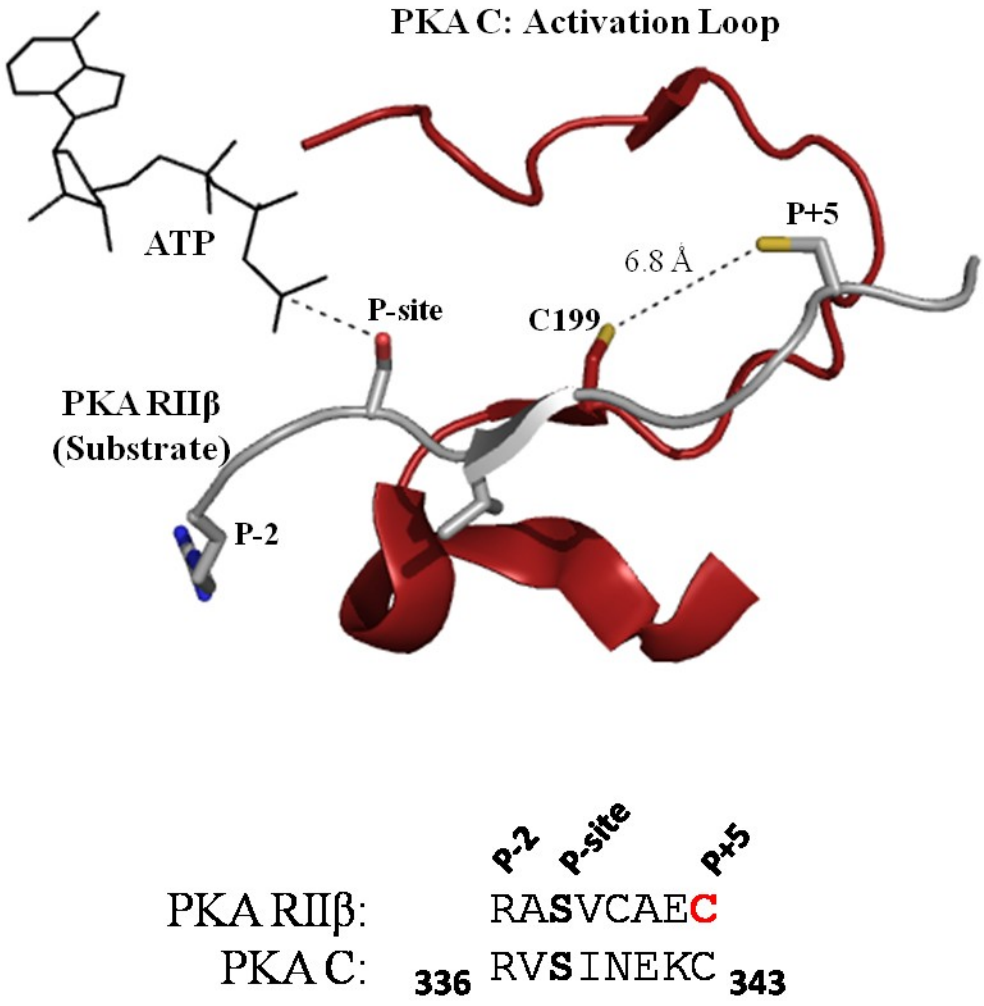

Figure 4.8. Modeling the distance between Cys199 in the activation loop and Cys343 in the C-tail. The crystal structure of PKA RIIβ was used as a reference and the P+5 position was mutated to Cys in pymol. This is predicted to closely resemble the autophosphorylation state for Ser338 in PKA.

phosphorylation of Ser338 occurs intramolecularly, it could be argued that the C-subunit must be expressed in an inactive state in order to block activation loop phosphorylation. Conditions that would cause the expression of catalytically inactive PKA in mammalian cells are not known, however, the results we present here would suggest that activation loop phosphorylation in the absence of PKA activity may have a deleterious effect on cells and evolutionary pressure has provided regulation for processing of the enzyme. Activation loop phosphorylation has been shown to increase the stability of the enzyme and perhaps the lifetime for the C-subunit is shorter in the absence of activation loop phosphorylation. Once phosphorylated on the activation loop, the turn motif phosphorylation is likely to be dispensable for activity and stability of the enzyme based on our *in vitro* data. Nevertheless, this site is resistant to dephosphorylation by phosphatases as long as the activation loop is phosphorylated (Keshwani et al., 2012). The proposed model for processing the PKA C-subunit is shown in **Figure 4.9**.

The identity of the protein kinase responsible for phosphorylation of the PKA activation loop has not yet been elucidated. Potentially there may be multiple kinases that can act redundantly but with different efficiencies. In this study, ~1/3 of the C^{R336A} expressed in mammalian cells is phosphorylated on the activation loop. This may be a result of having two kinases which can phosphorylate PKA, one dependent on the phosphorylation state of Ser338 and the other independent. Alternatively, a single protein kinase may phosphorylate the activation loop at a rate which is dependent on the phosphorylation state of Ser338. The only condition we found that resulted in complete activation loop phosphorylation of the C^{R336A} mutant was

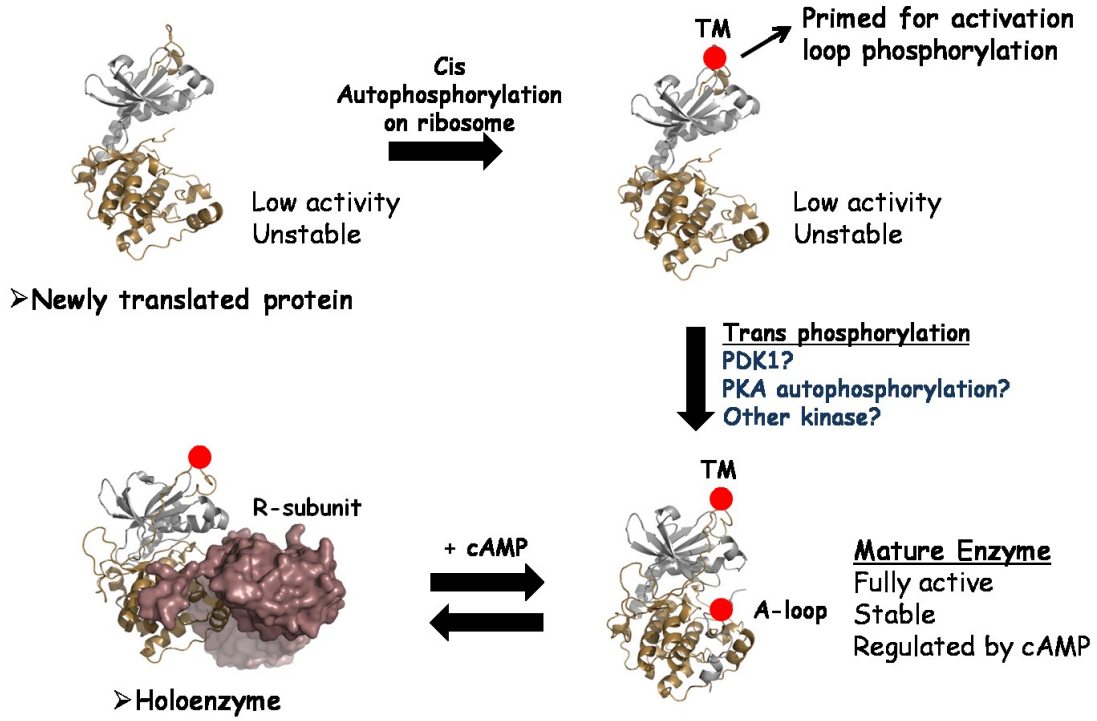

Figure 4.9. Model for processing the catalytic subunit of PKA.

coexpression with PDK1. This suggests that there is not enough endogenous PDK1 to accommodate the overexpressed C^{R336A} mutant. Because wild type PKA does not require coexpression with PDK1 the results of C^{R336A} indicate that the decrease in activation loop phosphorylation is primarily due to a decreased rate of phosphorylation in the absence of Ser338 phosphorylation. Ser338 phosphorylation has not been demonstrated to affect the rate of PDK1-dependent phosphorylation or autophosphorylation of the PKA activation loop *in vitro*. C^{R336A} is completely phosphorylated on the activation loop when expressed in bacteria, and a kinase dead mutant of PKA, which lacks Ser338 phosphorylation, is phosphorylated on the activation loop by PDK1 or PKA *in vitro* (Iyer et al., 2005b; Keshwani et al., 2012). It was previously shown that the R194A mutant of PKA cannot be autophosphorylated but when expressed in mammalian cells it is phosphorylated on the activation loop (Moore et al., 2002; Steichen et al., 2010). This mutation is at the P-3 position relative to the Thr197 phosphorylation site suggesting that the PKA-kinase in cells does not require a P-3 Arg for substrate recognition. In our study, autophosphorylation of the R336A mutant did not occur after treatment with cpt-cAMP indicating that endogenous PKA cannot trans phosphorylate the R336A mutant in mammalian cells. This suggests that individual molecules of PKA may not directly interact in cells or they may contain some modification or binding protein other than the R-subunit that prevents autophosphorylation.

Our results along with previous studies (Batkin et al., 2000; Yonemoto et al., 1997) show that there is a surprisingly large difference between mutating the phosphorylation site Ser338 to Ala compared with blocking autophosphorylation by

mutating the recognition sequence in the C-terminal tail (Arg336Ala). Interestingly, this has been shown to be true for three PKA phosphorylation sites; Ser10, Thr197, and Ser338 (Adams, 2003; Batkin et al., 2000; Steichen et al., 2010; Yonemoto et al., 1997). In the case of the activation loop, mutating Thr197 to Ala resulted in a severe defect in kinetics (~500-fold) whereas mutating the recognition sequence (Arg194Ala) reduced the catalytic efficiency by only ~10-fold (Adams et al., 1995; Steichen et al., 2010). Similarly, mutating the Ser10 phosphorylation site to an Ala resulted in insoluble protein (Yonemoto et al., 1997) whereas the purified wild type enzyme with or without Ser10 phosphorylated is stable and active (Yonemoto et al., 1993a). Similarly, others have found that surface exposed serine residues play an important role in protein solubility (Steinberg, 2012; Trevino et al., 2007, 2008) and they can sometimes stabilize secondary structural elements by forming hydrogen bonding interactions with their own backbone amides (Aubry et al., 1984; Marraud and Aubry, 1984). Mutations of surface exposed Ser, Thr, and Tyr are widely carried out as a method to understand the function of protein phosphorylation and it would be beneficial to further study the contribution of these amino acids to protein solubility. Additionally, mutations blocking the recognition sequence of protein kinase substrates or alternative methods for blocking phosphorylation may serve as better tools for studying the cellular effects of phosphorylation compared to the common method of mutating the phosphorylation site to alanine.

Chapter 5

Defining the Substrate Recognition Requirements of PDK1

5.1 Introduction

Phosphoinositide-dependent protein kinase (PDK1) is a member of the AGC group of protein kinases and is known to phosphorylate the activation loop of numerous other AGC kinases including Akt, PKC, S6K, SGK, and RSK. This has made it an attractive drug target for cancer therapy (Li et al., 2010; Raimondi and Falasca, 2011). It contains a conserved kinase domain as well as a C-terminal pleckstrin-homology (PH) domain. The PH-domain binds phosphoinositides which can localize PDK1 to the cell membrane to activate certain membrane bound substrates such as Akt (Belham et al., 1999). The kinase domain is homologous to other AGC kinases with the exception that it is missing the typical C-terminal tail (C-tail) found in most other AGC kinases. The typical AGC kinase C-tail is composed of several conserved regulatory elements including; a PXXP motif which binds Hsp90 (Gould et al., 2009), an FDDY motif which completes the ATP binding pocket (Batkin et al., 2000; Yang et al., 2009), and two conserved phosphorylation sites termed the turn motif and the hydrophobic motif which may have a variety of regulatory functions (Newton, 2003). Interestingly, while PDK1 lacks a homologous C-tail, it contains all of the elements in the kinase core which are known to interact with the AGC C-tail (Biondi et al., 2002; Frodin et al., 2002; Kannan et al., 2007a). This has led to the proposed model that PDK1 recognizes the C-tail of its substrate kinases in a manner that is homologous to how the C-tail interacts with its own, respective kinase (Balendran et al., 2000; Biondi et al., 2000; Biondi and Nebreda, 2003). In other words, the C-tail of a substrate must dissociate from its own kinase core and dock to the core of PDK1. Thus, in addition to bringing the substrate into close proximity to

PDK1, the C-tail itself may activate PDK1 to phosphorylate the activation loop of its substrate. This was demonstrated when incubating peptides containing the C-terminal HM with PDK1 increased its activity (Biondi et al., 2001).

In addition to the C-tail recognition sequence, Moore et al. previously identified two residues in the activation loop of PKA that are essential for PDK1-dependent phosphorylation (Moore et al., 2002). These residues, Pro207 and Glu208, reside at the C-terminus of the activation loop (P+10 and P+11 relative to Thr197) in a conserved sequence motif Ala-Pro-Glu or APE motif. While the molecular basis for this requirement was not studied any further, Glu208 forms an internal salt bridge with Arg280 in the αH-αI loop. This salt bridge is conserved in nearly all protein kinases and has been found to be mutated in a variety of kinases in several diseases (Torkamani et al., 2008) and its function is not yet known. Bioinformatics analysis of the microbial kinome indicated that distantly related eukaryotic-like kinases in prokaryotes lack the corresponding Glu208-Arg280 pair. Further examination revealed that the activation loop and peripheral structure motifs such as αG, αH, and αI helices, are only present in eukaryotic protein kinases (Kannan et al., 2007b; Taylor and Kornev, 2010). The αG helix has been shown to be a docking site for regulatory or interacting proteins, such as the regulatory subunit for PKA (Kim et al., 2007; Wu et al., 2007), and kinase-associated-phosphatase (KAP) for the cyclin dependent protein kinase CDK2 (Song et al., 2001). This may suggest a role of the Glu208-Arg280 pair in the eukaryotic kinases in substrate binding and in long-range regulation (Kannan et al., 2007b; Taylor and Kornev, 2010).

In this study we attempted to elucidate the role of the Glu208-Arg280 salt bridge in PDK1 recognition. Using mutational analysis we determined that the Glu-Arg salt bridge forms a non-linear recognition motif for PDK1 in members of the AGC protein kinases.

5.2 Experimental Procedures

Materials—Inhibitory peptide IP20 (TTYADFIASGRTGRRNAIHD, residues 5–24 from the heat stable PKA inhibitor PKI) was synthesized on a Milligen peptide synthesizer and purified by high performance liquid chromatography. Pre-packed Mono S 10/10 ion exchange column and Superdex 75 gel filtration column were purchased from GE Healthcare. Other reagents were from Qiagen, Life Technology, and EMD Biosciences. Polycolonal phospho-Thr197 antibody was raised in rabbits against the epitope peptide RVKGRTWpTLCGTPEY (Life Technology). The PDK1 antibody, which recognizes residues 538-556 was purchased from Sigma-Aldrich. The PKA catalytic subunit antibody was purchased from BD Biosciences.

Expression and purification of proteins – The His6-$C^{R194A/E208A}$ and His6-$C^{R194A/R280A}$ proteins were purified through Probond resin (Invitrogen). Briefly, the cell pellet was resuspended in lysis buffer containing 20 mM Tris-HCl, 50 mM KH_2PO_4, pH 7.5, 100 mM NaCl, plus protease inhibitors (5 mM benzamidine, 0.5 mM 4-(2-Aminoethyl) benzenesulfonyl fluoride hydrochloride (AEBSF), 30 μM each of Nα-tosyl-L-phenylalanine chloromethyl ketone (TPCK) and Nα-tosyl-L-lysine

chloromethylketone (TLCK)). The cells were lysed in a microfluidizer at 18,000 psi and spun down by centrifugation at 30,000 g for 45 min at 4˚C. The lysate was incubated with Probond resin for 1 hour at 4˚C. The resin was washed with lysis buffer containing 1 M NaCl followed by 20 mM imidazole. The protein was then eluted with lysis buffer containing 100-300 mM imidazole. Expression of the untagged wild type C-subunit, C^{E208A}, and C^{R280A} were purified essentially as described previously (Herberg et al., 1993). The activation loop (residues 184-220) were cloned into the pGEX vector with GST-fussion and expressed in *E. coli* cells and purified using GST resin. Mutations were introduced into the activation loop construct using quickchange mutagenesis (stratagene). His6-PDK1 was a gift from Dr. Alexandra Newton (University of California, San Diego, CA) and was expressed in bacculovirus-infected *Spodoptera frugiperda* (SF9) cells. The protein was purified on a Profinia protein purification system (Bio-Rad) with a Ni-affinity column and eluted with imidazole buffer.

Urea Unfolding and Fluorescence Measurements - Amberlite MB-150 (Sigma, St. Louis, MO) mixed-bed exchanger was added to 8.0 M urea solution and stirred for 1 h to remove ionic urea degradation products and then filtered. Proteins (0.12 mg/mL) were unfolded in various concentrations of urea ranging from (0 – 4 M) for 0.5 h at room temperature and monitored by steady-state fluorescence. Fractional unfolding curves were constructed assuming a two-state model and using $F_U = 1 - [(R - R_U) / (R_F - R_U)]$, where F_U is the fraction of the unfolded protein, R is the fluorescence measurement, and R_F and R_U represent the values of R for the folded and

unfolded states, respectively. For unfolding monitored by fluorescence, R is the observed ratio of intensity at 356/334 nm with excitation at 295 nm.

Hydrogen/Deuterium exchange analysis.- Preparation of deuterated samples and subsequent DXMS analysis was carried out as previously described (Yang et al., 2005). Briefly, the deuterium exchange reaction was started by combining 5 μL of protein sample (5 mg/mL, or 0.125 mM, mutant or wild type C-subunit) with 15 μL of 20 mM Mops (pH 7.4), 50 mM NaCl, 1 mM DTT in ^{2}H2O (deuteration buffer). After incubation at room temperature for various amount of time, 10, 30, 100, 300, 1000, or 3000 seconds, the reaction was quenched with 30 μL of 0.8% (v/v) formic acid, 1.6 M guanidine-HCl in ^{2}H2O, pH 2.3–2.5 at 0 °C. Samples were frozen on dry ice and stored at -80°C before being thawed and passed through a solid-phase pepsin column followed by a V8 protease column, and eluted with 0.05% trifluoroacetic acid (TFA) at 0.2 ml/minute for two minutes. Proteolytic peptides were collected by a C18 column (Vydac), which was subsequently developed with a linear gradient of 10 ml of 8%–40% (v/v) acetonitrile in 0.05% TFA, at 0.2 ml/minute. Mass spectrometric analysis was carried out with a Finnigan LCQ mass spectrometer as previously described (Yang et al., 2005). Recovered peptide identification and analysis were carried out using in-house software specialized in processing DXMS data (Woods and Hamuro, 2001).

Phosphorylation of His6-C$^{R194A/E208A}$ and His6-C$^{R194A/R280A}$, GST-activation loop, and RSK1 by PDK1- PDK1 phosphorylation of the various PKA mutants and

RSK1 was examined by coexpression of His6-$C^{R194A/E208A}$, His6-$C^{R194A/R280A}$, GST-activation loop, or RSK1 with PDK1 in pGEX vector in *E. coli* BL21(DE3) cells overnight at 16˚C. Cells were lysed by sonication in 50 mM Tris-HCl, 100 mM NaCl, pH 7.0 and the insoluble material was removed by centrifugation at 15,000 g for 30 min. The soluble fraction was subjected to SDS-PAGE, transferred to a nitrocellulose membrane, and blotted for phospho-Thr197, C-subunit, and PDK1. For the *in vitro* assay, 0.1 mg/mL of purified His6-$C^{R194A/E208A}$, His6-$C^{R194A/R280A}$, His6-C^{R194A}, or GST-activation loop proteins were incubated with 0.002 mg/mL purified PDK1 in 50 mM HEPES, pH 7.4, 100 mM NaCl, 10 mM DTT, 10 mM $MgCl_2$, 1 mM ATP, at room temperature for 90 min and aliquots were removed at the indicated times. The reaction was quenched in SDS-sample buffer, and probed for phospho-Thr197 by western blot analysis.

Expression of AGC kinases in mammalian cells – The Cα subunit of PKA cloned in pCDNA3 with C-terminal HA-tag was transfected in HEK293 cells using lipofectamine 2000 (Invitrogen) according to the manufacturer's protocol. Approximately 20 hours post-transfection cells were harvested by washing once with ice cold PBS and then resuspension in 50 mM Tris, 150 mM NaCl, 2 mM EDTA, and 1% Triton X-100, pH 7.4. Additionally, a protease inhibitor cocktail (Calbiochem) and a phosphatase inhibitor cocktail (Sigma) were added. The cells were lysed by sonication and spun down at 10,000 g for 10 min. The soluble fraction was loaded on SDS-PAGE gels and analyzed by western blotting. Similar experiments were carried out with HA-tagged RSK1 N-terminal kinase domain and PKCα and probed with

RSK1 p221 antibody or PKC pT500 antibody. For co-transfection experiments full-length myc-tagged PDK1 was used and lysates were immunoblotted with PDK1 antibody.

Peptide Array – Peptides were synthesized with a MultiPep Flexible Parallel Peptide Synthesizer (Intavis Bioanalytical Instruments, Germany). They are covalently linked to a cellulose membrane at the C-terminus and in some cases peptides contained phospho-serine or phospho-threonine residues. The membranes were soaked in 100% ethanol for 5 minutes and then washed with water prior to use. The membrane was then blocked with 5% milk in TTBS for 20 minutes and then overlayed with 1μM PDK1 in 5% milk and TTBS overnight at 4˚C with rocking. Four washes of five minutes each were then carried out with TTBS at room temp. The array was then overlayed with a PDK1 antibody, which recognizes residues 538-556 (Sigma-Aldrich), overnight at 4˚C. The membrane was again washed four times with TTBS and overlayed with α-mouse antibody for 1 hour at room temp and then washed four times with TTBS. SuperSignal West Pico Chemiluminescent Substrate for detection of HRP (Thermo Scientific) was used for signal detection.

5.3 Results

The Glu208Ala/Arg280Ala mutants are properly folded and active – We wanted to establish whether the E208-R280 salt bridge was essential for proper folding of the C-subunit and whether or not this could explain disruption of PDK1-dependent phosphorylation of the C-subunit. These two residues are completely buried

at the core of the protein (**Fig. 5.1A and B**). Expression of both E208A and R280A in bacteria showed that both mutants were capable of autophosphorylation at Thr197 (**Fig. 5.1C**). Additionally, X-ray crystal structures of both of these mutants were solved in complex with IP20 and Mg/ATP at 1.9 Å and 1.7 Å for E208A and R280A, respectively. The PDB IDs for these two structures are 3QAM (E208A) and 3QAL (R280A). The overall folds of the proteins are very similar to the wild type protein (**Fig. 5.2**). Both mutants are phosphorylated on Thr197 and Ser338. The Arg280 and Glu208 side chains are replaced by water molecules in the mutants. These results indicate that the Glu208-Arg280 salt bridge is not essential for correct folding of the C-subunit and unfolding is not the cause for disruption of PDK1 recognition.

Decreased Stability of C^{R280A} and C^{E208A} – In the absence of ligands, such as MgATP and IP20, both C^{R280A} and C^{E208A} exhibited increased H/D exchange rates mainly in the large lobe of the protein. The large lobe is comprised of a stable hydrophobic core centered by the αE and αF helices; most loop regions outside the core showed increased H/D exchange rates (**Fig. 5.3A**). Due to the increased dynamics throughout the loop regions of the protein we reasoned that the Glu208Ala and Arg280Ala mutations would decrease the stability of the protein. Additionally, if the Glu208 or Arg280 side chains are the primary defects for the increased dynamics we would predict that the decreased stability would be different for each mutation. By contrast, if the change in dynamics is due to the salt bridge then we would predict that the decrease in stability would be the same for both mutants. To assess the effect of

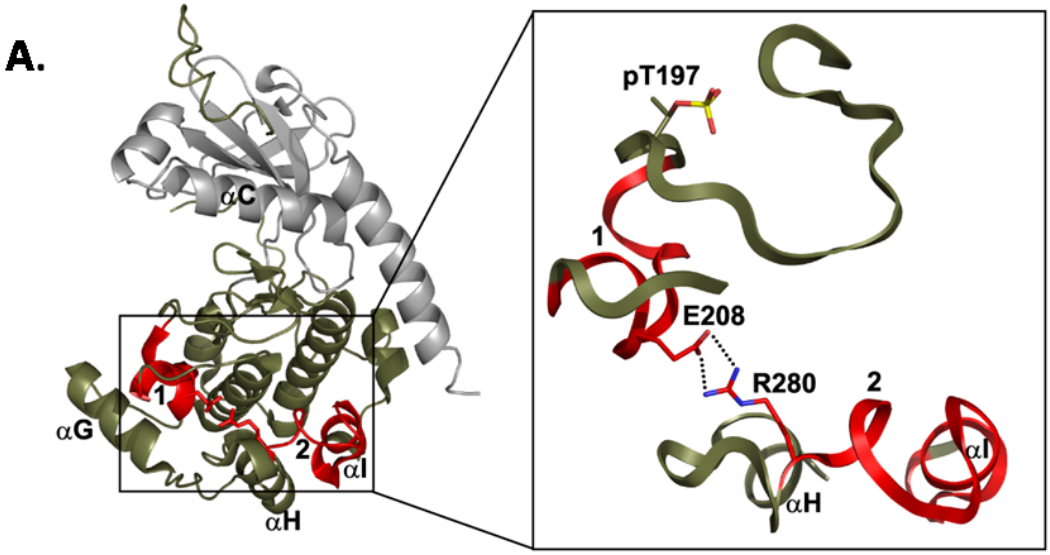

B.

Residue	ASA (Å²)
E208	4
E248	119
E331	134
R280	0
R194	166
R256	182

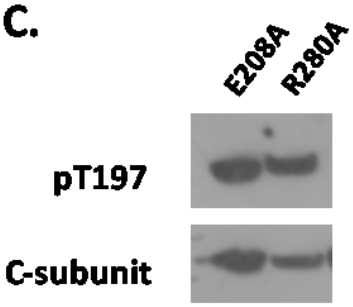

Figure 5.1. Glu208 and Arg280 form a buried salt bridge in the hydrophobic core of the protein. (**A**) Position of the Glu208:Arg280 salt bridge in the structure of PKA C-subunit. Crystal structure of C-subunit (PDB ID 1L3R) is rendered in cartoon presentation. The Glu208 and Arg280 are rendered as sticks, and colored by atom types (O: red, N: blue, C: grey). Hydrogen bonds are shown as dashed lines. The small lobe of the kinase is in light grey and large lobe in olive-green. Functional loops such as Activation Segment (Asp184-Thr197), Substrate Binding Loop (Leu198-Leu205) and the αH-αI loop are colored in red, ADP is rendered in thin stick and color in red. (**B**) The solvent accessible surface area of Glu208 and Arg280 compared to other surface exposed Glu and Arg residues. (**C**) The soluble fraction of an E. coli lysate expressing E208A and R280A probed with αC and α-pT197 show that both mutants autophosphorylate on Thr197.

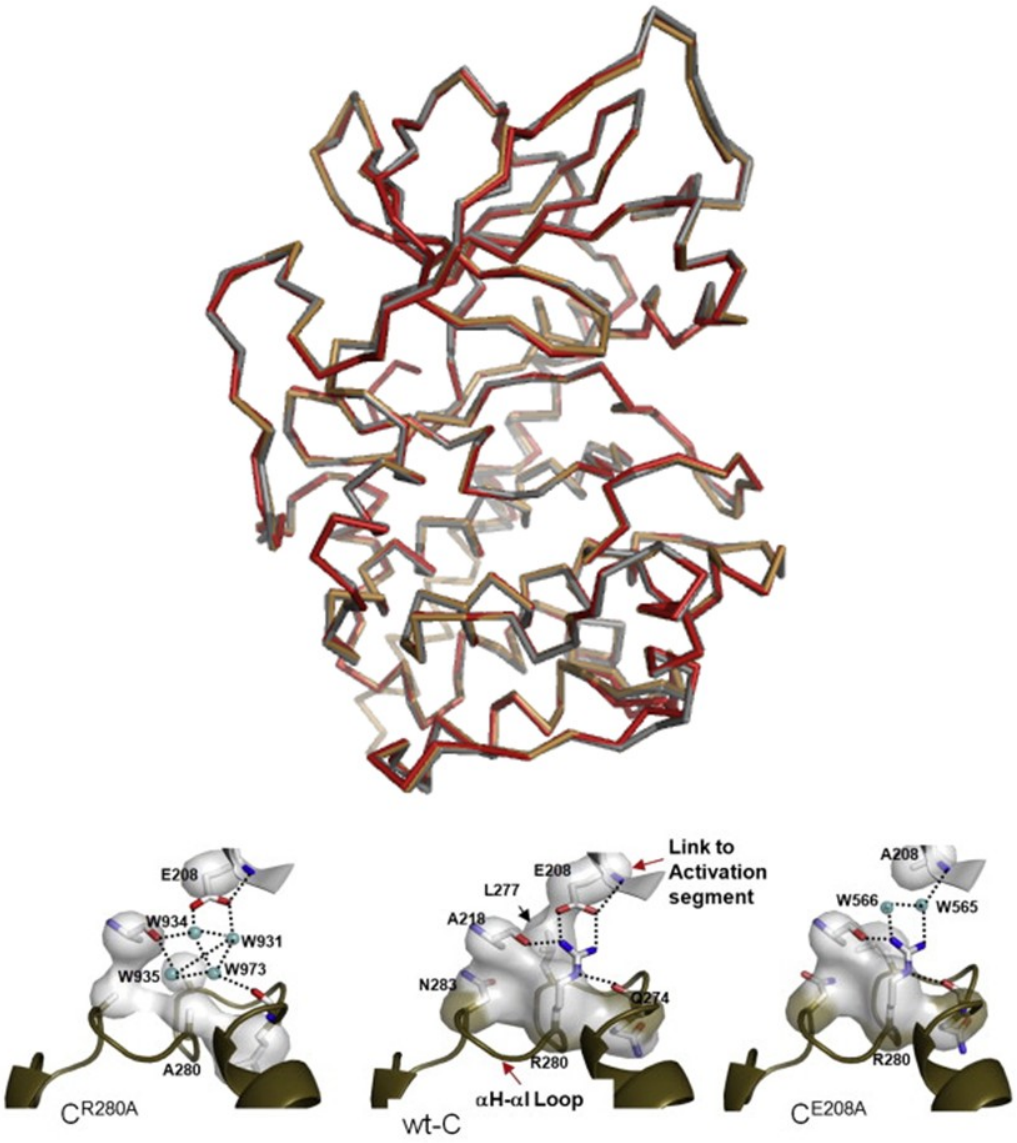

Figure 5.2. X-ray crystal structures of E208A and R280A. The structure of E208A and R280A aligned to the wild type enzyme shows similar overall fold (**top**) with water molecules taking the place of the Glu208 and Arg280 side chains (**bottom**).

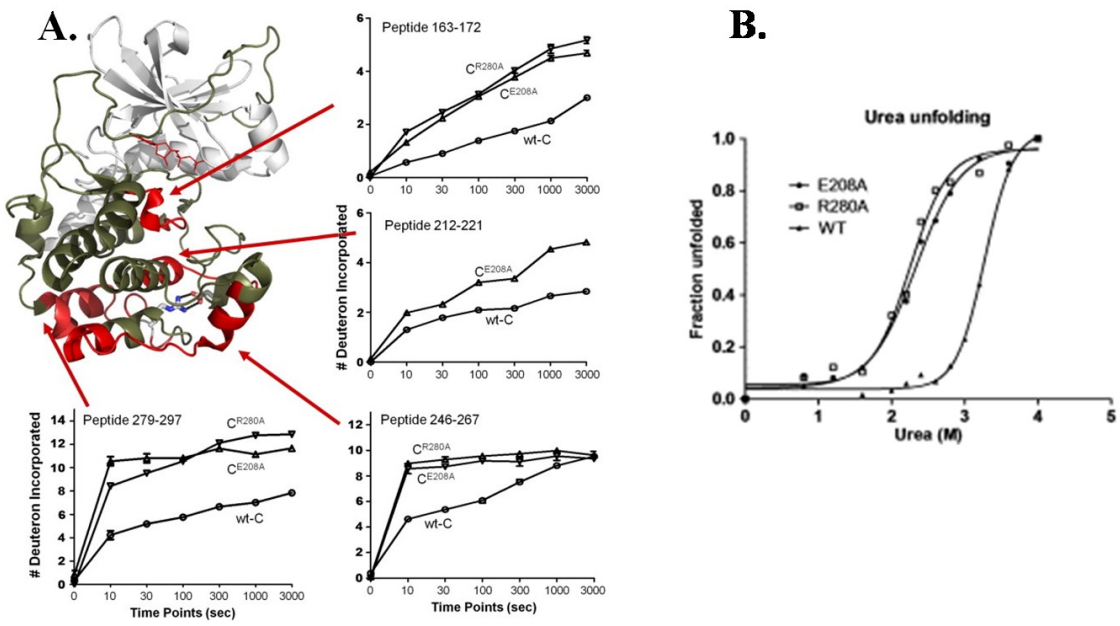

Figure 5.3. Stability and dynamics of the E208A and R280A mutants. (**A**) H/D exchange analysis of wild type C, C^{E208A} and C^{R280A} mutants show that several loops from the C-lobe are more solvent accessible in the mutants. (**B**) Comparison of the urea-denaturation curves for wild type C, C^{E208A}, and C^{R280A}. The fraction of protein unfolded is shown as a function of urea concentration as measured by intrinsic tryptophan fluorescence.

each mutation on the destabilization of the protein, we examined the protein unfolding in the presence of urea, and monitored the fraction of the unfolded protein through internal fluorescent signal. As shown in **Figure 5.3B**, the concentration of urea required to unfold 50% of the protein for C^{R280A} and C^{E208A} were both 2.2 M, compared to 3.2 M required for the wild type protein indicating that destabilization is a result of the salt bridge and not the individual side chains.

The Glu208 side chain does not form a linear recognition sequence for PDK1 – We next tested whether or not the side chain of Glu208 was essential for recognition by PDK1. The activation loop of PKA (residues 184-220) was cloned with a GST-fussion tag and co-expressed in bacteria with PDK1. This showed that PDK1 could phosphorylate the activation loop peptide at Thr197 (**Fig. 5.4A**). Next, a series of mutations were generated in the GST-activation loop construct including E208A and a deletion of the APE motif (residues 184-205). Additionally, the T197A mutant was created as a negative control and Y204A was used as a positive control (Moore et al., 2002). As illustrated in **Figure 5.4A,** PDK1 was able to phosphorylate all versions of the activation loop with the exception of T197A. In a smililar experiment the GST-activation loop was purified from *E. coli* and incubated with PDK1 purified from SF9 cells. This reaction was carried out as a time course in order to gain an estimate of the kinetics of the reaction. PDK1 phosphorylated the wild type and E208A activation loop at approximately the same rate indicating that the Glu208 side chain is not an essential recognition motif for PDK1 (**Fig. 5.4B**).

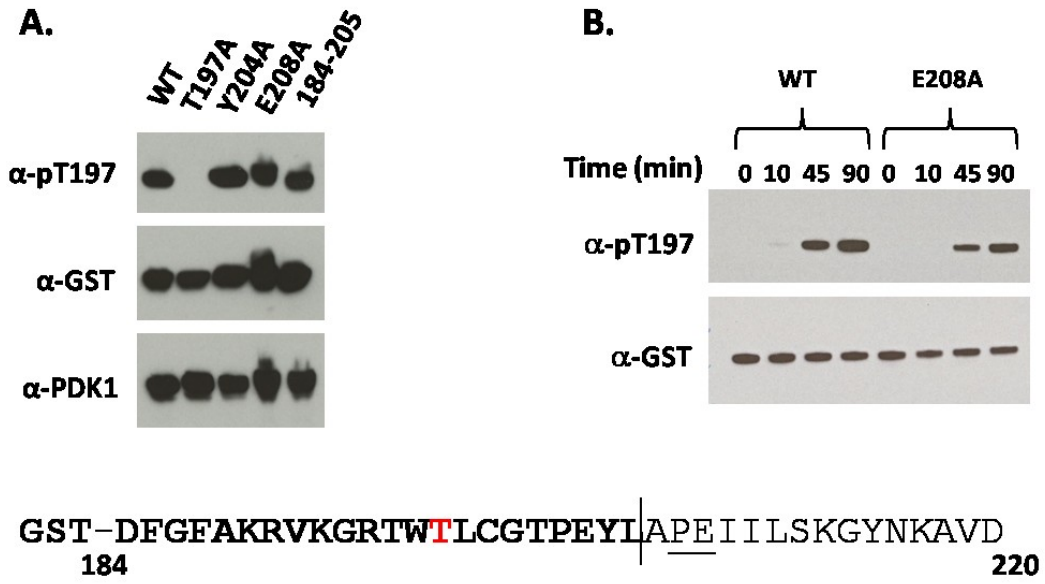

Figure 5.4. The Glu208 side chain is not essential for PDK1 recognition. (**A**) The PKA activation loop peptide with E208A or deletion of the APE motif is phosphorylated by PDK1 when coexpressed in bacteria. The Y204A and T197A mutations are positive and negative controls, respectively. (**B**) The purified activation loop peptide with E208A mutation is phosphorylated by PDK1 at approximately the same rate as the wild type activation loop. The sequence of the activation loop is shown below with the phosphorylation site Thr197 in red and the two residues known to block PDK1-dependent phosphorylation in the full length protein, Pro207 and Glu208, are underlined.

Both Glu208Ala and Arg280Ala block PDK1-dependent phosphorylation of Thr197 in the full-length C-subunit – Having established that the Glu208 side chain was not important for PDK1 recognition we wanted to know if the buried Glu208-Arg280 salt bridge was involved in recognition. Because both E208A and R280A mutants autophosphorylate when expressed in bacteria it was necessary to generate an additional mutation to block autophosphorylation of the activation loop. This was accomplished by introducing the R194A mutation into the C-subunit which blocks autophosphorylation by disrupting the PKA substrate consensus sequence (Moore et al., 2002). We generated two double mutants $C^{R194A/R280A}$ and $C^{R194A/E208A}$ to study the effects of the ion-pair mutation on phosphorylation by PDK1. The mutants were then co-expressed in bacteria under similar conditions to those used for the GST-activation loop experiment in order to directly compare the results. The double mutants $C^{R194A/R280A}$ or $C^{R194A/E208A}$ did not autophosphorylate in the absence of PDK1 and co-expression with PDK1 did not result in phosphorylation at Thr197 (**Fig. 5.5A**). In contrast, the R194A single mutant was phosphorylated at Thr197 when co-expressed with PDK1. As with the GST-activation loop experiments the same reaction was carried out with the purified proteins. As shown in **Figure 5.5B**, purified PDK1 can phosphorylate purified C^{R194A}, but not the $C^{R194A/E208A}$ or $C^{R194A/R280A}$ proteins.

The Glu-Arg salt bridge is essential for PDK1-dependent phosphorylation of other AGC kinases - PDK1 phosphorylates the activation loop of numerous AGC kinases and we wanted to know if this Glu-Arg salt bridge was a requirement for other PDK1 substrates. In HEK293 cells, the overexpressed E208A PKA mutant is not

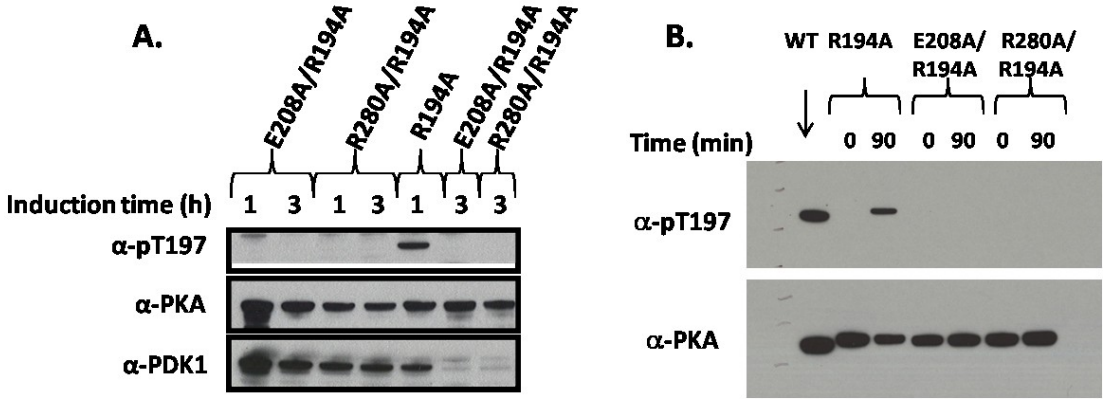

Figure 5.5. The Glu208-Arg280 salt bridge is a requirement for PDK1-dependent phosphorylation of PKA. (**A**) The indicated C-subunit mutants were induced at 37˚C for 1 or 3 hr, either alone or with PDK1, in *E. coli*, and the soluble fraction of the cell lysates were immunoblotted for phospho-Thr197 phosphorylation, C-subunit, and PDK1. (**B**) Purified PDK1 was incubated with purified mutants His6-C^{R194A}, His6-$C^{R194A/E208A}$, and His6-$C^{R194A/R280A}$ and Mg/ATP for 90 min at room temperature and immunoblotted for phospho-Thr197 phosphorylation and C-subunit. Untagged wild type C-subunit was loaded as an antibody control.

phosphorylated on Thr197 and co-transfection with PDK1 does not increase Thr197 phosphorylation (**Fig. 5.6, left**). Similarly when PKCα carrying the equivalent Glu to Ala mutation was expressed in HEK293 cells it showed reduced activation loop phosphorylation compared to the wild type (**Fig. 5.6, middle**). When the N-terminal kinase domain of RSK1 was expressed in HEK293 cells it was phosphorylated on the activation loop. However, when the R280A mutation was introduced into RSK1, activation loop phosphorylation was blocked (**Fig. 5.6, right**). PDK1 is known to autophosphorylate its own activation loop, and therefore, we tested whether the Glu-Arg salt bridge was required for PDK1 autophosphorylation. Two GST-PDK1 constructs were generated where the Glu-Arg salt bridge was mutated (the equivalent of PKA E208R and R280A). These mutants were then co-expressed in *E. coli* with RSK1. Wild type PDK1 showed autophosphorylation at S241 but autophosphorylation was dramatically reduced in the PDK1 mutants. Additionally, wild type PDK1 but not the E208R or R280A mutants could phosphorylate RSK1 at S221 in the activation loop (**Fig. 5.7, left**). A similar experiment was carried out with PKA where the PDK1 mutants E208R and R280a were co-expressed with the C-subunit autophosphorylation-deficient mutant R194A. While wild type PDK1 phosphorylated PKA R194A on the activation loop, neither of the PDK1 salt bridge mutants were able to phosphorylate PKA (**Fig. 5.7, right**).

PDK1 interaction with AGC kinase C-terminal tails – In order to test the interaction of PDK1 with other AGC kinases in a relatively high-throughput manner, we utilized peptide arrays. Peptides of varying lengths corresponding to the C-terminal

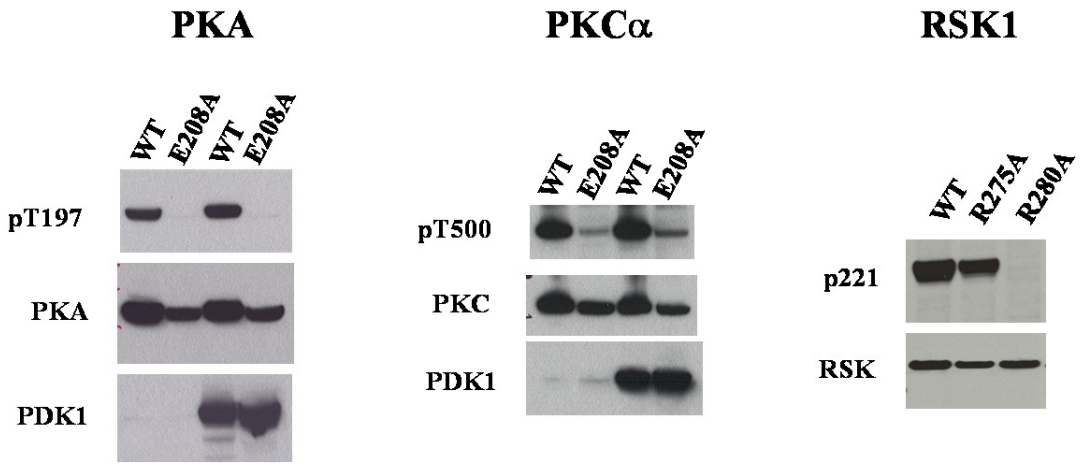

Figure 5.6. The Glu-Arg salt bridge is essential for activation loop phosphorylation of PDK1 substrates in mammalian cells. The HA-tagged PKA C-subunit (**Left**) with E208A mutation and PKCα (**Middle**) with the equivalent Glu to Ala mutation, were overexpressed in HEK293 cells with or without co-transfection of PDK1. The soluble fraction of the lysate was blotted for PKA, PKA pT197, PDK1, PKC, and PKC pT500. The HA-RSK1 NTK (**Right**) with the equivalent mutation of PKA C^{R280A} was transfected in HEK293 cells and the total cell lysate was blotted with α-HA, and α-RSK p221. RSK1(R275A) and wild type RSK1 were used as controls.

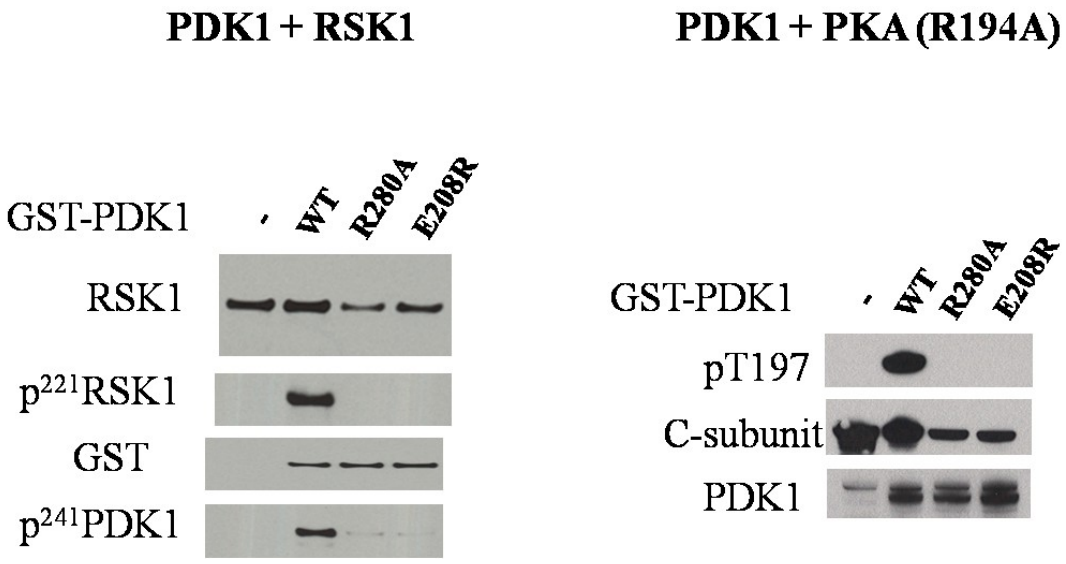

Figure 5.7. Mutation of the Glu-Arg salt bridge in PDK1 blocks autophosphorylation, RSK1 phosphorylation and PKA C^{R194A} phosphorylation. GST-tagged PDK1 carrying the equivalent mutations of PKA E208R and R280A was co-expressed in *E. coli* with RSK1 (**Left**) or PKA C^{R194A} (**Right**). The cells were lysed and the soluble fraction was blotted with α-RSK, α-RSK p221, α-GST, αPDK1 p241 for the experiment on the left and α-C-subunit, α-pT197, and αPDK1 on the right.

tail of several AGC kinases were covalently linked at the C-terminus to cellulose membranes and overlayed with purified PDK1. In an initial screen using the purified kinase domain of PDK1, the strongest interacting peptides appeared to be the C-tails of PKCθ and ROCK1 (**Fig. 5.8**). An ala scan of the PKCθ C-tail showed that the hydrophobic motif was essential for the interaction with PDK1. Interestingly, both PKCθ and ROCK1 showed a requirement for residues C-terminal to the hydrophobic motif with the ROCK1 peptide requiring seven residues beyond the hydrophobic motif and the PKCθ peptide requiring four residues in order to interact with PDK1 (**Figs. 5.9 and 5.10**).

Next we tested the effects of turn motif and hydrophobic motif phosphorylation on the interaction with PDK1. An array containing the C-tails of all isoforms of PKC, S6K, and RSK was synthesized with or without phospho-hydrophobic motif and phospho-turn motif. The results showed that the phosphorylation state of the turn motif had no effect on the interaction with PDK1 whereas, phosphorylation of the hydrophobic motif was inhibitory to three isoforms of PKC (ε, η, θ) and all isoforms of RSK (**Fig. 5.11**). Interestingly, all of these proteins contain a basic residue (Arg or Lys) at the P-3 position relative to the phosphorylation site (F<u>R</u>XF**S**) whereas the non-interacting proteins, including the other PKC isoforms do not contain the P-3 basic residue (**Fig. 5.12**). By contrast, S6K showed the opposite trend where only peptides phosphorylated on the hydrophobic motif interacted with PDK1, although the interaction was weaker compared to PKC and RSK.

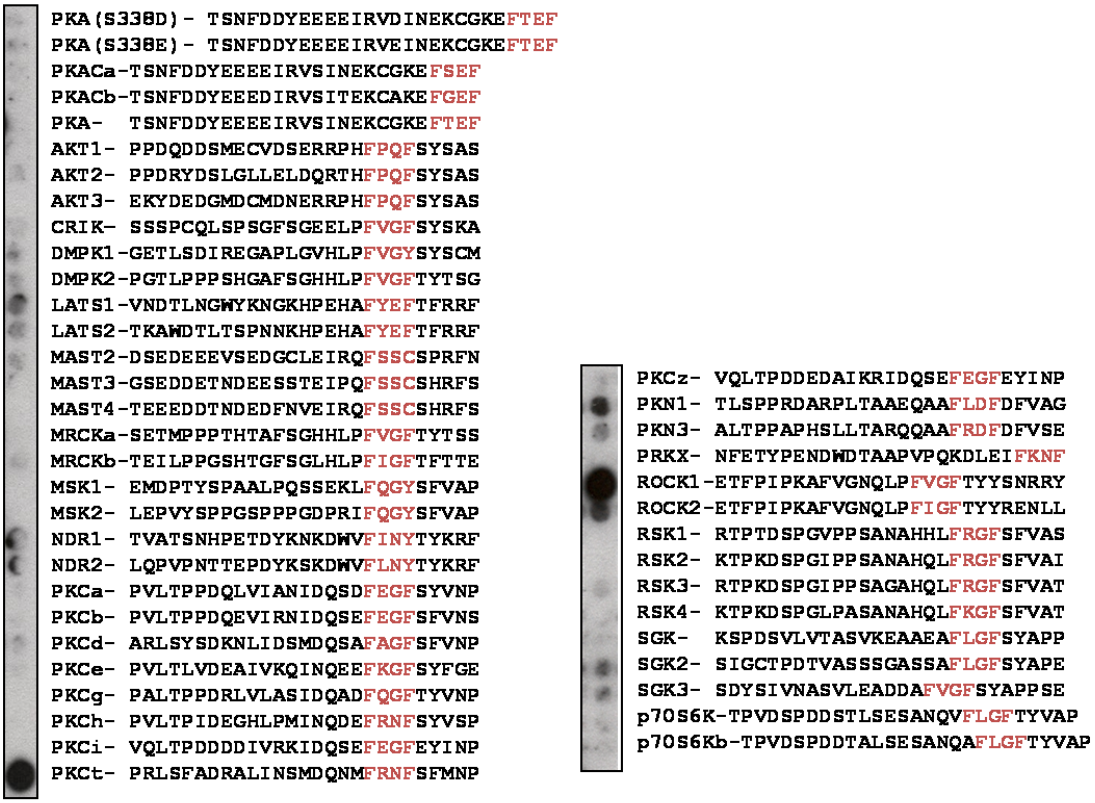

Figure 5.8. Peptide array analysis of PDK1 binding to AGC kinase C-tails. An array containing 43 AGC kinase C-tails was overlayed with the purified 6xHis-PDK1 kinase domain and blotted with α-6xHis antibody.

Figure 5.9. The hydrophobic motif is essential for PDK1 binding to the PKCθ C-tail peptide. A peptide array containing PKCθ C-tail peptides mutated by deletion (**left**) or Ala scanning (**right**) was overlayed with full length PDK1 and blotted with α-PDK1 antibody.

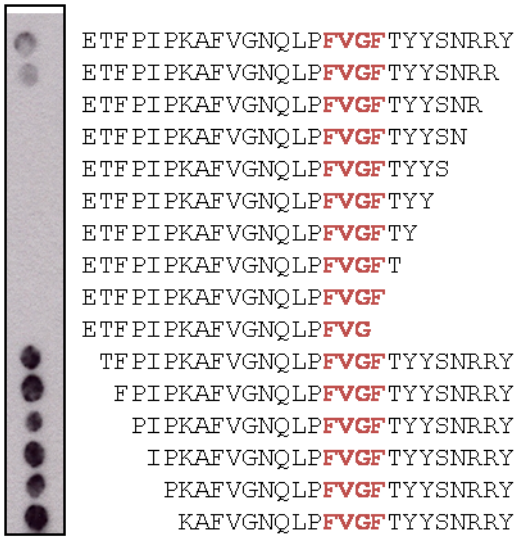

Figure 5.10. Residues C-terminal to the hydrophobic motif of ROCK1 are essential for interaction with PDK1. A ROCK1 peptide array was synthesized containing the C-tail with either N- or C-terminal deletions. Full length PDK1 was overlayed and the array was blotted with α-PDK1 antibody.

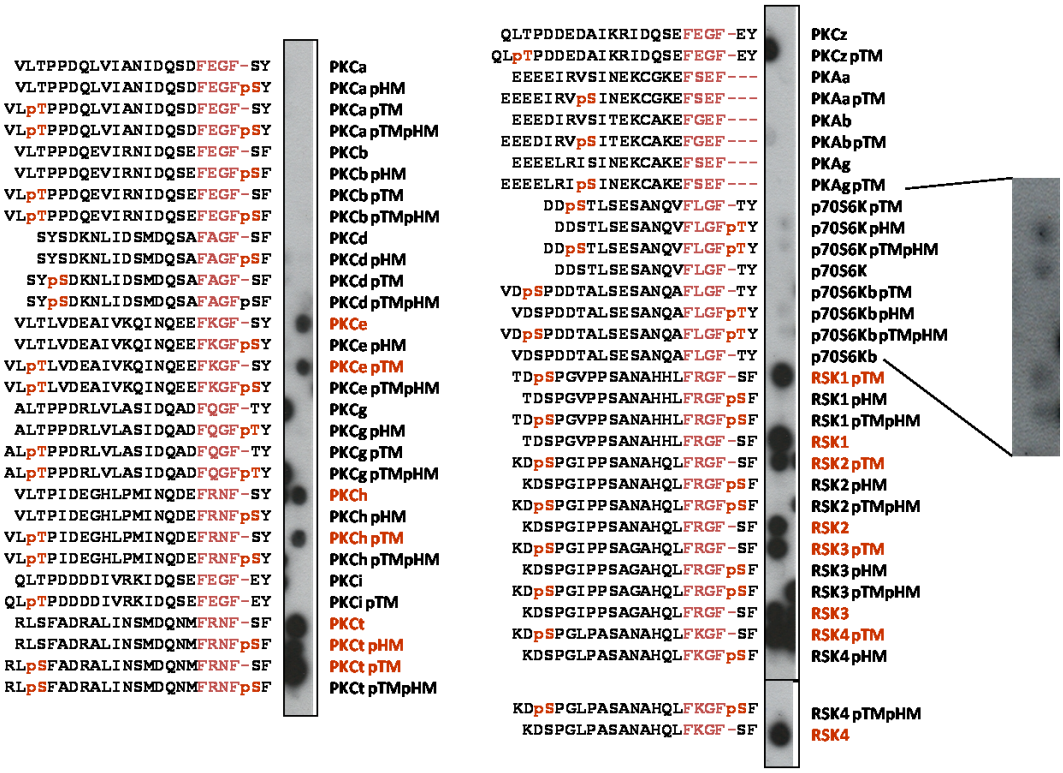

Figure 5.11. Phospho-array reveals dependence of PDK1 on the phosphorylation state of AGC kinase C-tails. A peptide array containing the C-tails of all isoforms of PKC, S6K, and RSK either with or without TM and HM phosphorylation was overlayed with PDK1 and probed with α-PDK1 antibody. Inset shows a close up view of the S6K peptides with altered contrast to make visualization easier.

pHM blocks binding	P-3 (pHM)
	FXXFS/T
	FRXFS/T
PKCe	Lys
PKCh	Arg
PKCt	Arg
RSK1	Arg
RSK2	Arg
RSK3	Arg
RSK4	Arg

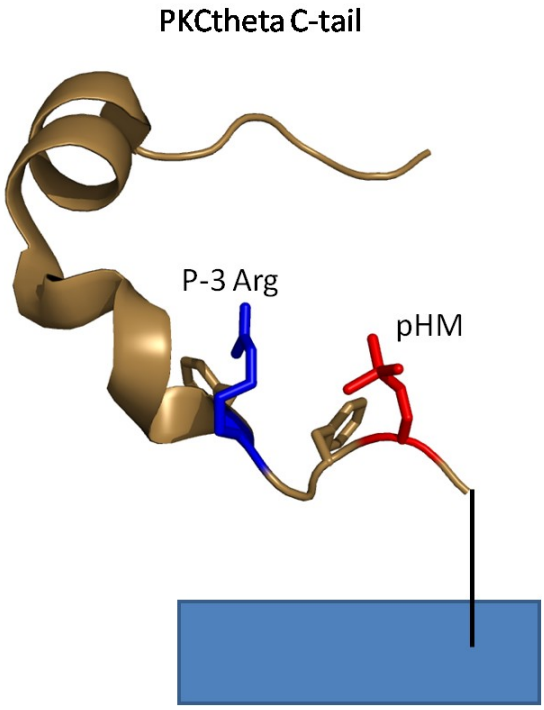

Figure 5.12. Hydrophobic motif phosphorylation is correlated with a P-3 Arg in regulating PDK1 binding. The kinases that did not bind to PDK1 in the presence of a phosphorylated HM and the conserved residue at the P-3 position in these kinases are shown. The structure of the PKCθ C-tail is shown with the P-3 Arg in blue and the phosphorylated HM in red.

The hydrophobic motif is not essential for PDK1-dependent phosphorylation of PKA - Numerous Ala mutations were made in the C-tail of PKA, including all residues of the hydrophobic motif (F347 to F350), in combination with the Arg194Ala mutation to block autophosphorylation. The double mutants were co-expressed with PDK1 in bacteria. All mutants were phosphorylated to the same extent as the Arg194Ala single mutant indicating that the hydrophobic motif is not essential for phosphorylation of PKA at Thr197 by PDK1 (**Fig. 5.13**).

5.4 Discussion

PDK1 phosphorylates the activation loop of numerous AGC kinases including PKC, Akt, S6K, and RSK. It is thought to recognize distinct structural elements on its protein kinase substrates. The hydrophobic motif on the C-tail of the substrate kinase contains the sequence FXXFXS/T and this motif docks to the C-helix of its own kinase and presumably docks to the equivalent sight on PDK1. The Ser/Thr of the FXXFS/T is also a phosphorylation site and phosphorylation of this residue enhances the interaction with PDK1 (Biondi et al., 2001). The hydrophobic motif was proposed to be a high affinity binding sight as well as an activator of PDK1. This interaction is being studied extensively for its potential as a drug binding site that is distinct from the ATP binding pocket and can thus provide a greater degree of specificity. The second structural element that interacts with PDK1 is the activation loop which is the site where PDK1 phosphorylation occurs. However, there are far fewer studies exploring PDK1 recognition of the activation loop site. Previous studies showed that a

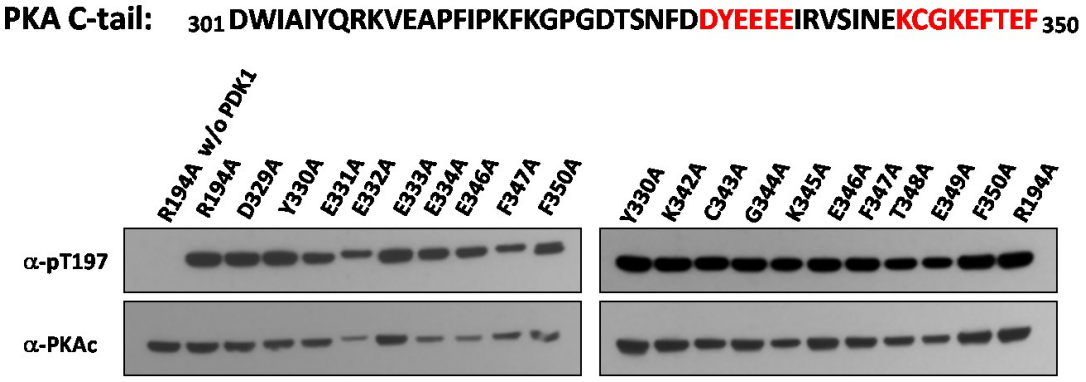

Figure 5.13. The C-terminal tail residues are not a requirement for phosphorylation of the PKA activation loop by PDK1. C-subunit double mutants containing the R194A mutation to block autophosphorylation as well as the indicated C-tail mutations were coexpressed in *E. coli* with PDK1 and the soluble lysate was blotted for α-C-subunit and α-pT197.

conserved glutamate in the activation loop of the substrate kinase is essential for PDK1-dependent phosphorylation. Interestingly, we find that the side chain of this glutamate is not a requirement for PDK1 recognition as determined by mutational analysis of the PKA activation loop peptide fused to GST. Mutation of E208A in this peptide had no effect on PDK1-dependent phosphorylation of Thr197. However, in the full-length protein, E208A completely blocked phosphorylation of PKA by PDK1. Instead, we found that the formation of a conserved salt bridge between E208:R280 is essential for PDK1 substrates. The E208A and R280A mutants were both able to autophosphorylate when expressed in bacteria, indicating that this salt bridge does not disrupt the folding of the protein, which was confirmed by X-ray crystal structures of these two mutants. Both structures were highly similar to the wild type enzyme. Additionally, this result shows that the E208:R280 salt bridge is not a requirement for activation loop phosphorylation by all kinases but may be unique to PDK1.

Several models can be proposed for why the internal salt bridge disrupts PDK1 phosphorylation. H/D exchange analysis of the E208A and R280A mutants reveals that the loop regions of the mutants are more flexible relative to the wild type enzyme which indicates there may be a change in dynamics at the activation loop in the absence of the salt bridge. Unfortunately the activation loop peptide was not obtained in the mass spectrometry analysis. Also, both of these mutants were already phosphorylated at the activation loop in the H/D exchange experiments and the dynamics of the enzyme may not reflect the actual dynamics in the unphosphorylated state. However, mutation of the salt bridge clearly alters the dynamics throughout the large lobe of the enzyme and this may play an important factor in recognition by

PDK1. Importantly, the altered dynamics were nearly identical for the E208A and R280A mutants indicating that it is an effect of breaking the salt bridge and not an effect caused simply by mutating the individual glutamate or arginine side chains. Similarly, the decrease in stability was equivalent for both E208A and R280A as measured by urea unfolding experiments.

An alternative model can be proposed based on the observation of several protein kinase crystal structures including the structure of the unphosphorylated S6K, a known substrate of PDK1. In this structure the highly conserved E208:R280 pair within one molecule swaps with the same pair in an adjacent molecule either in a naturally-occurring dimer or in a crystal packing induced dimer (Lee et al., 2009; Oliver et al., 2007; Pike et al., 2008; Sunami et al., 2010) and **Figure 5.14**. This observation provides an interesting hypothesis that when one kinase acts on another kinase, the switch/swapping of the conserved E208:R280 pair might serve as a mechanism for interaction. Thus, in the case of the PDK1-PKA interaction, the E208 of PKA would interact with the R280 of PDK1 and R280 of PKA would interact with E208 of PDK1 (**Fig. 5.15**). This model is consistent with our data showing that mutating the salt bridge in either PDK1 or its substrate kinase blocks phosphorylation.

Here we demonstrated that PKA can serve as a model to understand some aspects of PDK1 recognition. We found that RSK1 and PKCα also required the internal salt bridge for PDK1-dependent phosphorylation in mammalian cells. Additionally, the internal salt bridge was required for PDK1 to recognize itself as a substrate. Based on previous studies showing that mutations of the glutamate and arginine salt bridge are prevalent disease-associated mutations (**Table 5.1**) we propose

that this may be a common mechanism for recognition of the protein kinase activation loop.

While the E208:R280 salt bridge interaction appears to be similar for most PDK1 substrates, the C-tail interaction seems to be highly variable among the different substrates. In PKA phosphorylation of the hydrophobic motif is not essential for PDK1-dependent phosphorylation of the activation loop (Iyer et al., 2005a) but the hydrophobic motif is essential for PDK1-dependent phosphorylation of some other AGC kinases (Collins et al., 2005). In order to test the PDK1 interaction with the C-tails of its substrates in a high throughput manner we utilized peptide arrays. This demonstrated a large variation among the C-tails of various AGC kinases. We found that phosphorylation of the hydrophobic motif can inhibit interaction with PDK1 in contrast to previous studies. All peptides that were inhibited by phosphorylation contained a P-3 basic residue. This residue could potentially interact with and neutralize the charge of the phosphate which could affect the interaction with PDK1. However, this interaction was not tested on full length protein where the C-tail makes numerous interactions with the core of the kinase. A further analysis of the full length AGC kinases will be required in order to fully define the recognition requirement at the C-tail hydrophobic motif site.

Chapter 5, in part, was published as A conserved Glu-Arg salt bridge connects co-evolved motifs that define the eukaryotic protein kinase fold. Yang, J., Wu, J., Steichen, J.M., Kornev, A., Deal, M.S., Li, S., Sankaran, B., Woods, V.L. Jr, and Taylor, S.S. *J. Mol. Biol*. 2012. Jan 27: 415(4):666-679. The dissertation author was a secondary investigator and author of this work.

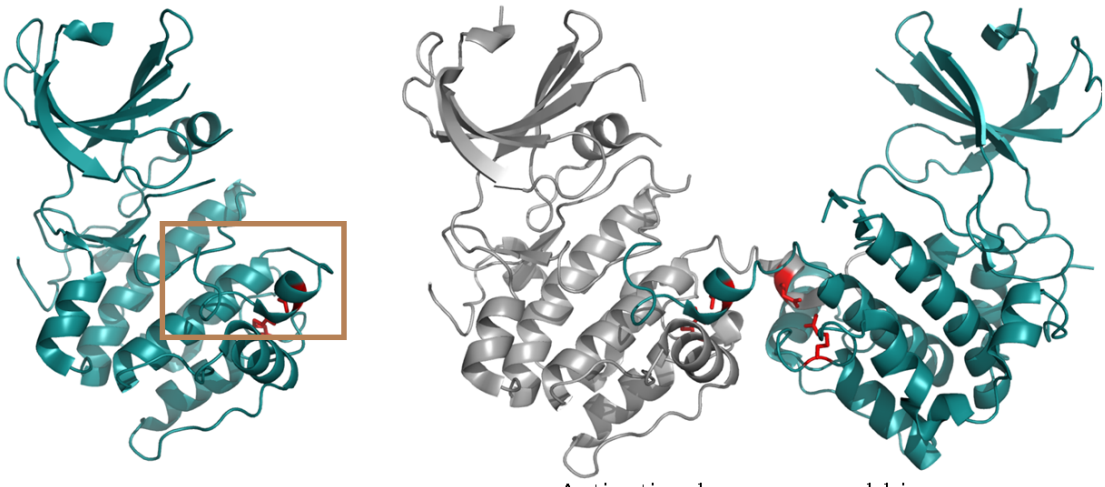

Figure 5.14. The crystal structure of PDK1 substrate S6K shows an activation loop swapped dimer. Two recently reported crystal structures of unphosphorylated S6K (PDB IDs: Left, 3A61 and Right, 3A60) are shown (Sunami et al., 2010). The structure on the right shows a dimer in which the Glu-Arg salt bridge has exchanged between symmetry mates. A list of other activation loop swapped kinases is given below, all of which display the Glu-Arg salt bridge switch.

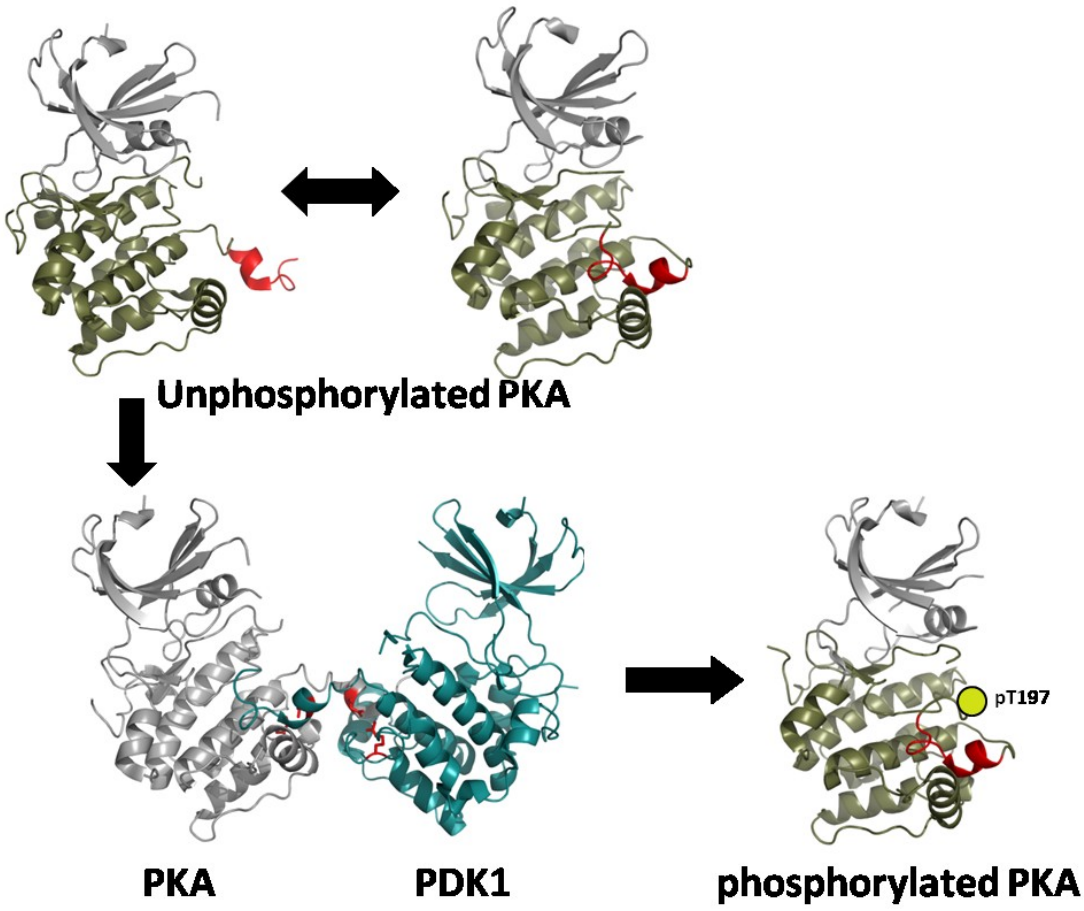

Figure 5.15. Model for PDK1 substrate recognition. Unphosphorylated PDK1 substrates contain a dynamic activation loop (red) which can flip in and out. PDK1 recognizes the out conformation and swaps the Glu-Arg salt bridge with its substrate. After phosphorylation, activation loop is stable in the in conformation. The activation loop out conformation is represented by the S6K crystal structure (PDB ID: 3A60).

Table 5.1. List of Protein Kinases in which Mutations of the Glu-Arg Salt Bridge have been Associated with Disease. Previously reported in (Torkamani et al., 2008).

Glutamate 208	**Disease**
ALK1 (E-K)	Haemorrhagic telangiectasia 2
BMPR2 (E-G)	Pulmonary hypertension, primary
BTK (E-D,K)	Agammaglobulinaemia
INSR (E-D,K)	Leprechanism
JAK3 (E-K)	Immunodeficiency, severe combined
KIT (E-K)	Childhood-onset sporadic mastocytosis
PINK1 (E-G)	Parkinson disease, early-onset
RET (E-K)	Hirschsprung disease
Arginine 280	
ALK1 (R-L)	Haemorrhagic telaniectasia 2
ANPb (R-W)	Acromesomelic dysplasia, Maroteaux type
BMPR2 (R-W,Q)	Pulmonary hypertension, primary
BTK (R-C)	Agammaglobulinaemia
LKB1 (R-K,S)	Peutz-Jeghers syndrome
RHOK (R-H)	Retinitis pigmentosa
TGFbR2 (R-C,H)	Loeys-dietz syndrome

Chapter 6

Conclusions

While PKA is typically regulated by cAMP binding to the regulatory subunits in cells, like in many AGC kinases, the two phosphorylation sites at the activation loop (Thr197) and the turn motif (Ser338) play a key role in processing the catalytic subunit to a fully active state. Despite PKA being the first kinase to be crystallized and more than 100 additional high resolution structures being solved over the years, all of these structures correspond to the phosphorylated enzyme. Understanding the structure of the unphosphorylated kinases can provide information about the inactivation process of PKA and other kinases which can be used for better drug design. The primary goal of this dissertation was to investigate the regulation of PKA by phosphorylation at the activation loop and turn motif and to define the molecular details of how these phosphates can alter the biochemical and structural properties of the enzyme.

Activation Loop Phosphorylation

One of the challenges in studying the effect of phosphates was the instability of the protein resulting from the mutations introduced in the phosphorylation site. This problem was addressed by introducing a mutation in PKA that blocks the auto-recognition sequence. To study the effects of activation loop phosphorylation we generated a P-3 arginine to alanine (R194A) mutation. This Arg in PKA does not have any apparent function but allows PKA to autophosphorylate at the activation loop. The R194A mutant expressed at high levels in *E. coli*, no longer autophosphorylated at the activation loop, but still autophosphorylated on the hydrophobic motif. Additionally, this mutant protein could be efficiently phosphorylated at the activation loop by

PDK1, the kinase that likely phosphorylates PKA in mammalian cells. Thus, we were able to generate the inactive form of the C-subunit that could be converted into the active enzyme by PDK1. This strategy, developed in the beginning of my thesis work, provided the basis for a wide array of experiments during the course of my study not only in understanding the role of activation loop phosphorylation, but also the hydrophobic motif phosphorylation site, Ser338.

Only one AGC kinase, Akt, has previously been crystallized in the unphosphorylated apo state. It showed a disordered αC-helix, and a DFG-out conformation with the activation loop blocking the active site. Thus, it was not possible to determine if this was common to all AGC kinases or specific to Akt. In this study we solved the X-ray crystal structure of the unphosphorylated PKA C-subunit which allowed us for the first time to compare the structures of two AGC kinases in their unphosphorylated apo states. The structure revealed a different mechanism of inactivation for PKA, where the two lobes of the enzyme are decoupled, and destabilization of the active site occurs as judged by the loss of numerous hydrogen bonds. Thus, from this study it is clear that the effects of activation loop dephosphorylation can be different even for closely related AGC kinases. While this indicates that it will be difficult to predict the structures of unphosphorylated protein kinases it also supports the possibility of selectively targeting and distinguishing between closely related kinases with drugs that are designed to inhibit the unphosphorylated states of the enzymes. The hydrogen/deuterium exchange analysis showed an increase in dynamics at the active site, consistent with the loss of hydrogen bonding observed in the crystal structure. Similarly, kinetic studies showed that while

activation loop phosphorylation causes an increase in activity in PKA, it is not essential for activity as in many other protein kinases. Together the results of these studies described in Chapters 2 and 3 indicate that dephosphorylation of the activation loop can have a wide range of affects on the kinetic activity of different kinases which reflects the variability of their structures, and this offers opportunities for the design of selective inhibitors.

Turn Motif Phosphorylation

The TM of PKA is unusual in that its location within the C-tail is offset relative to the TM of other AGC kinases. This makes it questionable as to whether or not its function is analogous to the TM of other AGC kinases. To understand the role of this phosphate on the structure and function of the enzyme, we used a similar strategy and mutated the P-2 arginine to alanine (R336A) that completely blocked the TM phosphorylation in *E. coli* and in mammalian cells. Structural analysis of the unphosphorylated enzyme did not show a substantial difference from the wild type enzyme. However, studies in mammalian cells revealed that the phosphorylation on the TM might have a key role in regulating activation loop phosphorylation and thus, processing of PKA. While the precise mechanism of how this phosphorylation site effects processing has not yet been established we were able to show that phosphorylation of Ser338 is an important precursor step for obtaining complete activation loop phosphorylation in mammalian cells. Prior to this study the biological function of the TM phosphorylation site in PKA was completely unknown. Unlike most other AGC kinases, the TM in PKA cannot be dephosphorylated by

phosphatases. PKA achieves its mature state rapidly in cells and is then regulated by cAMP. Only the oxidized form of the C-subunit can be dephosphorylated by phosphatases but this has not yet been shown to occur in cells. Therefore, in Chapter 4 we have shown that while PKA's TM is offset relative to other AGC kinases in sequence and structure, perhaps to protect it from dephosphorylation, its function as a processing step is preserved.

How does PDK1 recognize its substrates?

PDK1 phosphorylates the activation loop of at least 23 AGC kinases. However, the mechanism by which PDK1 recognizes its substrates has not yet been established. While it is typical for protein kinases to phosphorylate a linear recognition sequence, such as RRXS in PKA, PDK1 does not recognize a linear sequence to select substrates. Instead it relies on several recognition motifs derived from different regions of the protein kinase substrate. In Chapter 5, we described the results of our analysis from different PDK1 substrate kinases and showed a novel interaction that is dependent on an internal salt bridge in the substrate that joins the activation loop to the αH-αI loop at the opposite face of the enzyme. This salt bridge may stabilize a conformation of the activation loop that accommodates PDK1 or mediate an exchange of the PDK1 activation loop with the substrate activation loop. This activation loop exchange has been observed in crystal structures of numerous protein kinase homodimers. The mechanism of PDK1 recognition was conserved in all of the PDK1 substrates that were tested.

Strategy for Studying Protein Phosphorylation

One of the most surprising results from the study was the finding that mutating a surface exposed serine or threonine can have a large effect on the solubility of a protein. Mutating a surface serine or threonine is the most common method for studying the effects of protein phosphorylation but very few studies have been carried out to assess the roles that serine or threonine can play in protein stability and solubility. Our studies showed that in PKA, mutating any of the phosphorylation sites to alanine has a dramatic effect on protein stability. This thesis has outlined a new method for studying the effects of protein phosphorylation by mutating the kinase recognition sequence within the substrate. This strategy could potentially be used to study the effects of phosphorylation on any protein so long as the kinase recognition sequence is known. While mutating the recognition sequence may occasionally lead to erroneous results when the residues forming the recognition sequence have additional roles, this strategy could still be used in combination with the more traditional method of mutating the phosphorylation site directly. Together these two methods could substantially increase the reliability when determining the effects of phosphorylation on protein kinase substrates.

In summary, the structures and biochemical studies of the unphosphorylated C-subunit in this work provide insights into a molecular mechanism of PKA processing that had not previously been described.

6.1 Future Work

Determining the rules for protein kinase inactivation

Protein kinases show a high degree of structural diversity in their unphosphorylated states compared to the phosphorylated states. This provides the opportunity to improve drug selectivity by targeting the unphosphorylated kinases. However, it is currently not possible to predict the structure of the unphosphorylated proteins as accurately as prediction of the phosphorylated states of the kinases. Thus, it would be extremely valuable to be able to accurately predict the confirmation of the kinases in their unphosphorylated/inactive states. It will require computational methods as well as experimental techniques to elucidate the rules that regulate the conformation of unphosphorylated/inactive kinases. Additionally, the R194A mutant of PKA could be crystallized in the presence of various drugs/ligands to provide further information about its complete range of inactive conformations. For example the class of compounds derived from imatinib bind to the DFG-out conformation and can therefore be used to determine which kinases display the DFG-out conformation in solution. The unphosphorylated C-subunit of PKA has only been studied/crystallized in the apo state and thus the full range of inactive conformations are not known for this protein.

Which protein kinase phosphorylates the PKA activation loop?

One of the outstanding questions regarding the PKA catalytic subunit is which protein kinase phosphorylates Thr197 of the activation loop in mammalian cells. This

question has been extremely difficult to address because PKA activation loop phosphorylation occurs rapidly after translation and it is resistant to dephosphorylation by phosphatases. Therefore, the use of kinase inhibitors proved to be difficult as often the inhibitors must be present throughout the life of the protein at concentrations that are often lethal to cells. One of the strategies to address this in future studies would be the use of a high throughput siRNA library targeting AGC kinases and analyzing the PKA activation loop phosphorylation. Understanding the upstream kinase of PKA will also provide mechanistic insights into how the turn motif phosphorylation effects the activation loop phosphorylation.

Understanding the complete mechanism by which PDK1 recognizes its substrates

PDK1 relies on multiple protein kinase motifs as a method for recognition of the activation loop phosphorylation. Previous studies have shown the importance of docking to the hydrophobic pocket on PDK1 as a method for activation. In this study it was shown that a buried salt bridge also plays a crucial role in PDK1 substrate recognition. Because PDK1 has been extensively studied as a drug target, elucidating the complete mechanism would be extremely valuable. Ideally, a crystal structure of PDK1 in complex with one of its substrates would provide the most detailed understanding of its mechanism. In addition, based on previously characterized disease mutations and crystal structures there is a possibility that recognition through the conserved Glu-Arg salt bridge is common among the protein kinases. Thus, future projects could focus on other kinases which are likely to use a similar mechanism as PDK1. Here I provide a list of those potential kinases. The kinases fall into two

categories; those which have been crystallized in an activation loop swapped conformation and those whose Glu-Arg salt bridge mutations have been implicated in disease. Protein kinases with swapped activation loop in crystal structures: CHK2, DAPK3, SLK, LOK, STK10, OSR1. Protein kinases in which either Glu or Arg (E208 or R280 in PKA) is mutated in disease: ALK1, BMPR2, BTK, INSR, JAK3, KIT, PINK1, RET, ANPb, LKB1, RHOK, TGFbR2.

References

Adams, J.A. (2003). Activation loop phosphorylation and catalysis in protein kinases: is there functional evidence for the autoinhibitor model? Biochemistry *42*, 601-607.

Adams, J.A., McGlone, M.L., Gibson, R., and Taylor, S.S. (1995). Phosphorylation modulates catalytic function and regulation in the cAMP-dependent protein kinase. Biochemistry *34*, 2447-2454.

Akamine, P., Madhusudan, Wu, J., Xuong, N.H., Ten Eyck, L.F., and Taylor, S.S. (2003). Dynamic features of cAMP-dependent protein kinase revealed by apoenzyme crystal structure. J Mol Biol *327*, 159-171.

Aubry, A., Ghermani, N., and Marraud, M. (1984). Backbone side chain interactions in peptides. I. Crystal structures of model dipeptides with the Pro-Ser sequence. Int J Pept Protein Res *23*, 113-122.

Balendran, A., Biondi, R.M., Cheung, P.C., Casamayor, A., Deak, M., and Alessi, D.R. (2000). A 3-phosphoinositide-dependent protein kinase-1 (PDK1) docking site is required for the phosphorylation of protein kinase Czeta (PKCzeta) and PKC-related kinase 2 by PDK1. J Biol Chem *275*, 20806-20813.

Ballif, B.A., Roux, P.P., Gerber, S.A., MacKeigan, J.P., Blenis, J., and Gygi, S.P. (2005). Quantitative phosphorylation profiling of the ERK/p90 ribosomal S6 kinase-signaling cassette and its targets, the tuberous sclerosis tumor suppressors. Proc Natl Acad Sci U S A *102*, 667-672.

Bastidas, A.C., Deal, M.S., Steichen, J.M., Keshwani, M.M., Guo, Y., and Taylor, S.S. (2012). Role of N-Terminal Myristylation in the Structure and Regulation of cAMP-Dependent Protein Kinase. J Mol Biol.

Batkin, M., Schvartz, I., and Shaltiel, S. (2000). Snapping of the carboxyl terminal tail of the catalytic subunit of PKA onto its core: characterization of the sites by mutagenesis. Biochemistry *39*, 5366-5373.

Battye, T.G., Kontogiannis, L., Johnson, O., Powell, H.R., and Leslie, A.G. (2011). iMOSFLM: a new graphical interface for diffraction-image processing with MOSFLM. Acta Crystallogr D Biol Crystallogr *67*, 271-281.

Bayascas, J.R., Wullschleger, S., Sakamoto, K., Garcia-Martinez, J.M., Clacher, C., Komander, D., van Aalten, D.M., Boini, K.M., Lang, F., Lipina, C.*, et al.* (2008). Mutation of the PDK1 PH domain inhibits protein kinase B/Akt, leading to small size and insulin resistance. Mol Cell Biol *28*, 3258-3272.

Beene, D.L., and Scott, J.D. (2007). A-kinase anchoring proteins take shape. Curr Opin Cell Biol *19*, 192-198.

Belham, C., Wu, S., and Avruch, J. (1999). Intracellular signalling: PDK1--a kinase at the hub of things. Curr Biol *9*, R93-96.

Biondi, R.M., Cheung, P.C., Casamayor, A., Deak, M., Currie, R.A., and Alessi, D.R. (2000). Identification of a pocket in the PDK1 kinase domain that interacts with PIF and the C-terminal residues of PKA. EMBO J *19*, 979-988.

Biondi, R.M., Kieloch, A., Currie, R.A., Deak, M., and Alessi, D.R. (2001). The PIF-binding pocket in PDK1 is essential for activation of S6K and SGK, but not PKB. EMBO J *20*, 4380-4390.

Biondi, R.M., Komander, D., Thomas, C.C., Lizcano, J.M., Deak, M., Alessi, D.R., and van Aalten, D.M. (2002). High resolution crystal structure of the human PDK1 catalytic domain defines the regulatory phosphopeptide docking site. EMBO J *21*, 4219-4228.

Biondi, R.M., and Nebreda, A.R. (2003). Signalling specificity of Ser/Thr protein kinases through docking-site-mediated interactions. Biochem J *372*, 1-13.

Boettcher, A.J., Wu, J., Kim, C., Yang, J., Bruystens, J., Cheung, N., Pennypacker, J.K., Blumenthal, D.A., Kornev, A.P., and Taylor, S.S. (2011). Realizing the allosteric potential of the tetrameric protein kinase A RIalpha holoenzyme. Structure *19*, 265-276.

Bossemeyer, D., Engh, R.A., Kinzel, V., Ponstingl, H., and Huber, R. (1993). Phosphotransferase and substrate binding mechanism of the cAMP-dependent protein kinase catalytic subunit from porcine heart as deduced from the 2.0 A structure of the complex with Mn2+ adenylyl imidodiphosphate and inhibitor peptide PKI(5-24). EMBO J *12*, 849-859.

Brognard, J., and Newton, A.C. (2008). PHLiPPing the switch on Akt and protein kinase C signaling. Trends Endocrinol Metab *19*, 223-230.

Cauthron, R.D., Carter, K.B., Liauw, S., and Steinberg, R.A. (1998). Physiological phosphorylation of protein kinase A at Thr-197 is by a protein kinase A kinase. Mol Cell Biol *18*, 1416-1423.

Chan, T.O., Pascal, J.M., Armen, R.S., and Rodeck, U. (2012). Autoregulation of kinase dephosphorylation by ATP binding in AGC protein kinases. Cell Cycle *11*, 475-478.

Cheetham, G.M., Knegtel, R.M., Coll, J.T., Renwick, S.B., Swenson, L., Weber, P., Lippke, J.A., and Austen, D.A. (2002). Crystal structure of aurora-2, an oncogenic serine/threonine kinase. J Biol Chem *277*, 42419-42422.

Cheng, X., Ma, Y., Moore, M., Hemmings, B.A., and Taylor, S.S. (1998). Phosphorylation and activation of cAMP-dependent protein kinase by phosphoinositide-dependent protein kinase. Proc Natl Acad Sci U S A *95*, 9849-9854.

Cohen, P. (2002). Protein kinases--the major drug targets of the twenty-first century? Nat Rev Drug Discov *1*, 309-315.

Collins, B.J., Deak, M., Murray-Tait, V., Storey, K.G., and Alessi, D.R. (2005). In vivo role of the phosphate groove of PDK1 defined by knockin mutation. J Cell Sci *118*, 5023-5034.

Cook, P.F., Neville, M.E., Jr., Vrana, K.E., Hartl, F.T., and Roskoski, R., Jr. (1982). Adenosine cyclic 3',5'-monophosphate dependent protein kinase: kinetic mechanism for the bovine skeletal muscle catalytic subunit. Biochemistry *21*, 5794-5799.

Davis, I.W., Leaver-Fay, A., Chen, V.B., Block, J.N., Kapral, G.J., Wang, X., Murray, L.W., Arendall, W.B., 3rd, Snoeyink, J., Richardson, J.S.*, et al.* (2007). MolProbity: all-atom contacts and structure validation for proteins and nucleic acids. Nucleic Acids Res *35*, W375-383.

Dettori, R., Sonzogni, S., Meyer, L., Lopez-Garcia, L.A., Morrice, N.A., Zeuzem, S., Engel, M., Piiper, A., Neimanis, S., Frodin, M.*, et al.* (2009). Regulation of the interaction between protein kinase C-related protein kinase 2 (PRK2) and its upstream kinase, 3-phosphoinositide-dependent protein kinase 1 (PDK1). J Biol Chem *284*, 30318-30327.

Dhanasekaran, N., and Premkumar Reddy, E. (1998). Signaling by dual specificity kinases. Oncogene *17*, 1447-1455.

Emsley, P., and Cowtan, K. (2004). Coot: model-building tools for molecular graphics. Acta Crystallogr D Biol Crystallogr *60*, 2126-2132.

Fantozzi, D.A., Harootunian, A.T., Wen, W., Taylor, S.S., Feramisco, J.R., Tsien, R.Y., and Meinkoth, J.L. (1994). Thermostable inhibitor of cAMP-dependent protein kinase enhances the rate of export of the kinase catalytic subunit from the nucleus. J Biol Chem *269*, 2676-2686.

Fischer, E.H., and Krebs, E.G. (1955). Conversion of phosphorylase b to phosphorylase a in muscle extracts. J Biol Chem *216*, 121-132.

Frodin, M., Antal, T.L., Dummler, B.A., Jensen, C.J., Deak, M., Gammeltoft, S., and Biondi, R.M. (2002). A phosphoserine/threonine-binding pocket in AGC kinases and PDK1 mediates activation by hydrophobic motif phosphorylation. EMBO J *21*, 5396-5407.

Gaffarogullari, E.C., Masterson, L.R., Metcalfe, E.E., Traaseth, N.J., Balatri, E., Musa, M.M., Mullen, D., Distefano, M.D., and Veglia, G. (2011). A myristoyl/phosphoserine switch controls cAMP-dependent protein kinase association to membranes. J Mol Biol *411*, 823-836.

Gao, T., Furnari, F., and Newton, A.C. (2005). PHLPP: a phosphatase that directly dephosphorylates Akt, promotes apoptosis, and suppresses tumor growth. Mol Cell *18*, 13-24.

Gao, T., and Newton, A.C. (2002). The turn motif is a phosphorylation switch that regulates the binding of Hsp70 to protein kinase C. J Biol Chem *277*, 31585-31592.

Gould, C.M., Antal, C.E., Reyes, G., Kunkel, M.T., Adams, R.A., Ziyar, A., Riveros, T., and Newton, A.C. (2011). Active site inhibitors protect protein kinase C from dephosphorylation and stabilize its mature form. J Biol Chem *286*, 28922-28930.

Gould, C.M., Kannan, N., Taylor, S.S., and Newton, A.C. (2009). The chaperones Hsp90 and Cdc37 mediate the maturation and stabilization of protein kinase C through a conserved PXXP motif in the C-terminal tail. J Biol Chem *284*, 4921-4935.

Grant, B.D., and Adams, J.A. (1996). Pre-steady-state kinetic analysis of cAMP-dependent protein kinase using rapid quench flow techniques. Biochemistry *35*, 2022-2029.

Gschwind, A., Fischer, O.M., and Ullrich, A. (2004). The discovery of receptor tyrosine kinases: targets for cancer therapy. Nat Rev Cancer *4*, 361-370.

Hanks, S.K., and Hunter, T. (1995). Protein kinases 6. The eukaryotic protein kinase superfamily: kinase (catalytic) domain structure and classification. FASEB J *9*, 576-596.

Hauge, C., Antal, T.L., Hirschberg, D., Doehn, U., Thorup, K., Idrissova, L., Hansen, K., Jensen, O.N., Jorgensen, T.J., Biondi, R.M.*, et al.* (2007). Mechanism for activation of the growth factor-activated AGC kinases by turn motif phosphorylation. EMBO J *26*, 2251-2261.

Heller, W.T., Vigil, D., Brown, S., Blumenthal, D.K., Taylor, S.S., and Trewhella, J. (2004). C subunits binding to the protein kinase A RI alpha dimer induce a large conformational change. J Biol Chem *279*, 19084-19090.

Herberg, F.W., Bell, S.M., and Taylor, S.S. (1993). Expression of the catalytic subunit of cAMP-dependent protein kinase in Escherichia coli: multiple isozymes reflect different phosphorylation states. Protein Eng *6*, 771-777.

Herberg, F.W., Zimmermann, B., McGlone, M., and Taylor, S.S. (1997). Importance of the A-helix of the catalytic subunit of cAMP-dependent protein kinase for stability and for orienting subdomains at the cleft interface. Protein Sci *6*, 569-579.

Huang, X., Begley, M., Morgenstern, K.A., Gu, Y., Rose, P., Zhao, H., and Zhu, X. (2003). Crystal structure of an inactive Akt2 kinase domain. Structure *11*, 21-30.

Hubbard, S.R., Wei, L., Ellis, L., and Hendrickson, W.A. (1994). Crystal structure of the tyrosine kinase domain of the human insulin receptor. Nature *372*, 746-754.

Humphries, K.M., Deal, M.S., and Taylor, S.S. (2005). Enhanced dephosphorylation of cAMP-dependent protein kinase by oxidation and thiol modification. J Biol Chem *280*, 2750-2758.

Hunter, T. (2000). Signaling--2000 and beyond. Cell *100*, 113-127.

Huse, M., and Kuriyan, J. (2002). The conformational plasticity of protein kinases. Cell *109*, 275-282.

Ikenoue, T., Inoki, K., Yang, Q., Zhou, X., and Guan, K.L. (2008). Essential function of TORC2 in PKC and Akt turn motif phosphorylation, maturation and signalling. EMBO J *27*, 1919-1931.

Iyer, G.H., Garrod, S., Woods, V.L., Jr., and Taylor, S.S. (2005a). Catalytic independent functions of a protein kinase as revealed by a kinase-dead mutant: study of the Lys72His mutant of cAMP-dependent kinase. J Mol Biol *351*, 1110-1122.

Iyer, G.H., Moore, M.J., and Taylor, S.S. (2005b). Consequences of lysine 72 mutation on the phosphorylation and activation state of cAMP-dependent kinase. J Biol Chem *280*, 8800-8807.

Johnson, L.N. (2009). Protein kinase inhibitors: contributions from structure to clinical compounds. Q Rev Biophys *42*, 1-40.

Johnson, L.N., and Lewis, R.J. (2001). Structural basis for control by phosphorylation. Chem Rev *101*, 2209-2242.

Johnson, L.N., Noble, M.E., and Owen, D.J. (1996). Active and inactive protein kinases: structural basis for regulation. Cell *85*, 149-158.

Kannan, N., Haste, N., Taylor, S.S., and Neuwald, A.F. (2007a). The hallmark of AGC kinase functional divergence is its C-terminal tail, a cis-acting regulatory module. Proc Natl Acad Sci U S A *104*, 1272-1277.

Kannan, N., and Neuwald, A.F. (2005). Did protein kinase regulatory mechanisms evolve through elaboration of a simple structural component? J Mol Biol *351*, 956-972.

Kannan, N., Taylor, S.S., Zhai, Y., Venter, J.C., and Manning, G. (2007b). Structural and functional diversity of the microbial kinome. PLoS Biol *5*, e17.

Kennedy, E.J., Yang, J., Pillus, L., Taylor, S.S., and Ghosh, G. (2009). Identifying critical non-catalytic residues that modulate protein kinase A activity. PLoS One *4*, e4746.

Keshwani, M.M., Klammt, C., von Daake, S., Ma, Y., Kornev, A.P., Choe, S., Insel, P.A., and Taylor, S.S. (2012). Cotranslational cis-phosphorylation of the COOH-terminal tail is a key priming step in the maturation of cAMP-dependent protein kinase. Proc Natl Acad Sci U S A *109*, E1221-1229.

Keshwani, M.M., von Daake, S., Newton, A.C., Harris, T.K., and Taylor, S.S. (2011). Hydrophobic motif phosphorylation is not required for activation loop phosphorylation of p70 ribosomal protein S6 kinase 1 (S6K1). J Biol Chem *286*, 23552-23558.

Kim, C., Cheng, C.Y., Saldanha, S.A., and Taylor, S.S. (2007). PKA-I holoenzyme structure reveals a mechanism for cAMP-dependent activation. Cell *130*, 1032-1043.

Kim, C., Xuong, N.H., and Taylor, S.S. (2005). Crystal structure of a complex between the catalytic and regulatory (RIalpha) subunits of PKA. Science *307*, 690-696.

Knighton, D.R., Zheng, J.H., Ten Eyck, L.F., Ashford, V.A., Xuong, N.H., Taylor, S.S., and Sowadski, J.M. (1991a). Crystal structure of the catalytic subunit of cyclic adenosine monophosphate-dependent protein kinase. Science *253*, 407-414.

Knighton, D.R., Zheng, J.H., Ten Eyck, L.F., Xuong, N.H., Taylor, S.S., and Sowadski, J.M. (1991b). Structure of a peptide inhibitor bound to the catalytic subunit of cyclic adenosine monophosphate-dependent protein kinase. Science *253*, 414-420.

Komander, D., Kular, G., Deak, M., Alessi, D.R., and van Aalten, D.M. (2005). Role of T-loop phosphorylation in PDK1 activation, stability, and substrate binding. J Biol Chem *280*, 18797-18802.

Kornev, A.P., Haste, N.M., Taylor, S.S., and Eyck, L.F. (2006). Surface comparison of active and inactive protein kinases identifies a conserved activation mechanism. Proc Natl Acad Sci U S A *103*, 17783-17788.

Kornev, A.P., and Taylor, S.S. (2010). Defining the conserved internal architecture of a protein kinase. Biochim Biophys Acta *1804*, 440-444.

Lee, S.J., Cobb, M.H., and Goldsmith, E.J. (2009). Crystal structure of domain-swapped STE20 OSR1 kinase domain. Protein Sci *18*, 304-313.

Lee, T., Hoofnagle, A.N., Resing, K.A., and Ahn, N.G. (2005). Hydrogen exchange solvent protection by an ATP analogue reveals conformational changes in ERK2 upon activation. J Mol Biol *353*, 600-612.

Levin, L.R., and Zoller, M.J. (1990). Association of catalytic and regulatory subunits of cyclic AMP-dependent protein kinase requires a negatively charged side group at a conserved threonine. Mol Cell Biol *10*, 1066-1075.

Levinson, N.M., Kuchment, O., Shen, K., Young, M.A., Koldobskiy, M., Karplus, M., Cole, P.A., and Kuriyan, J. (2006). A Src-like inactive conformation in the abl tyrosine kinase domain. PLoS Biol *4*, e144.

Li, Y., Yang, K.J., and Park, J. (2010). Multiple implications of 3-phosphoinositide-dependent protein kinase 1 in human cancer. World J Biol Chem *1*, 239-247.

Liu, Y., Belkina, N.V., Graham, C., and Shaw, S. (2006). Independence of protein kinase C-delta activity from activation loop phosphorylation: structural basis and altered functions in cells. J Biol Chem *281*, 12102-12111.

Lodowski, D.T., Pitcher, J.A., Capel, W.D., Lefkowitz, R.J., and Tesmer, J.J. (2003). Keeping G proteins at bay: a complex between G protein-coupled receptor kinase 2 and Gbetagamma. Science *300*, 1256-1262.

Manning, G., Whyte, D.B., Martinez, R., Hunter, T., and Sudarsanam, S. (2002). The protein kinase complement of the human genome. Science *298*, 1912-1934.

Marraud, M., and Aubry, A. (1984). Backbone side chain interactions in peptides. II. Solution study of serine-containing model dipeptides. Int J Pept Protein Res *23*, 123-133.

McCoy, A.J., Grosse-Kunstleve, R.W., Adams, P.D., Winn, M.D., Storoni, L.C., and Read, R.J. (2007). Phaser crystallographic software. J Appl Crystallogr *40*, 658-674.

Moore, M.J., Kanter, J.R., Jones, K.C., and Taylor, S.S. (2002). Phosphorylation of the catalytic subunit of protein kinase A. Autophosphorylation versus phosphorylation by phosphoinositide-dependent kinase-1. J Biol Chem *277*, 47878-47884.

Mora, A., Komander, D., van Aalten, D.M., and Alessi, D.R. (2004). PDK1, the master regulator of AGC kinase signal transduction. Semin Cell Dev Biol *15*, 161-170.

Murshudov, G.N., Vagin, A.A., and Dodson, E.J. (1997). Refinement of macromolecular structures by the maximum-likelihood method. Acta Crystallogr D Biol Crystallogr *53*, 240-255.

Newton, A.C. (2003). Regulation of the ABC kinases by phosphorylation: protein kinase C as a paradigm. Biochem J *370*, 361-371.

Nirula, A., Ho, M., Phee, H., Roose, J., and Weiss, A. (2006). Phosphoinositide-dependent kinase 1 targets protein kinase A in a pathway that regulates interleukin 4. J Exp Med *203*, 1733-1744.

Nolen, B., Taylor, S., and Ghosh, G. (2004). Regulation of protein kinases; controlling activity through activation segment conformation. Mol Cell *15*, 661-675.

Oh, W.J., Wu, C.C., Kim, S.J., Facchinetti, V., Julien, L.A., Finlan, M., Roux, P.P., Su, B., and Jacinto, E. (2010). mTORC2 can associate with ribosomes to promote cotranslational phosphorylation and stability of nascent Akt polypeptide. EMBO J *29*, 3939-3951.

Oliver, A.W., Knapp, S., and Pearl, L.H. (2007). Activation segment exchange: a common mechanism of kinase autophosphorylation? Trends Biochem Sci *32*, 351-356.

Oliver, A.W., Paul, A., Boxall, K.J., Barrie, S.E., Aherne, G.W., Garrett, M.D., Mittnacht, S., and Pearl, L.H. (2006). Trans-activation of the DNA-damage signalling protein kinase Chk2 by T-loop exchange. Embo J *25*, 3179-3190.

Olsen, J.V., Blagoev, B., Gnad, F., Macek, B., Kumar, C., Mortensen, P., and Mann, M. (2006). Global, in vivo, and site-specific phosphorylation dynamics in signaling networks. Cell *127*, 635-648.

Orr, J.W., and Newton, A.C. (1994). Requirement for negative charge on "activation loop" of protein kinase C. J Biol Chem *269*, 27715-27718.

Otwinowski, Z., and Minor, W. (1997). Processing of X-ray diffraction data collected in oscillation mode. Method Enzymol *276*, 307-326.

Pace, C.N. (1986). Determination and analysis of urea and guanidine hydrochloride denaturation curves. Methods Enzymol *131*, 266-280.

Papin, J.A., Hunter, T., Palsson, B.O., and Subramaniam, S. (2005). Reconstruction of cellular signalling networks and analysis of their properties. Nat Rev Mol Cell Biol *6*, 99-111.

Pargellis, C., Tong, L., Churchill, L., Cirillo, P.F., Gilmore, T., Graham, A.G., Grob, P.M., Hickey, E.R., Moss, N., Pav, S.*, et al.* (2002). Inhibition of p38 MAP kinase by utilizing a novel allosteric binding site. Nat Struct Biol *9*, 268-272.

Pickin, K.A., Chaudhury, S., Dancy, B.C., Gray, J.J., and Cole, P.A. (2008). Analysis of protein kinase autophosphorylation using expressed protein ligation and computational modeling. J Am Chem Soc *130*, 5667-5669.

Pike, A.C., Rellos, P., Niesen, F.H., Turnbull, A., Oliver, A.W., Parker, S.A., Turk, B.E., Pearl, L.H., and Knapp, S. (2008). Activation segment dimerization: a mechanism for kinase autophosphorylation of non-consensus sites. Embo J *27*, 704-714.

Ptacek, J., Devgan, G., Michaud, G., Zhu, H., Zhu, X., Fasolo, J., Guo, H., Jona, G., Breitkreutz, A., Sopko, R.*, et al.* (2005). Global analysis of protein phosphorylation in yeast. Nature *438*, 679-684.

Raimondi, C., and Falasca, M. (2011). Targeting PDK1 in cancer. Curr Med Chem *18*, 2763-2769.

Ramakrishnan, C., Dani, V.S., and Ramasarma, T. (2002). A conformational analysis of Walker motif A [GXXXXGKT (S)] in nucleotide-binding and other proteins. Protein Eng *15*, 783-798.

Romano, R.A., Kannan, N., Kornev, A.P., Allison, C.J., and Taylor, S.S. (2009). A chimeric mechanism for polyvalent trans-phosphorylation of PKA by PDK1. Protein Sci *18*, 1486-1497.

Ross, E.M., Maguire, M.E., Sturgill, T.W., Biltonen, R.L., and Gilman, A.G. (1977). Relationship between the beta-adrenergic receptor and adenylate cyclase. J Biol Chem *252*, 5761-5775.

Sarma, G.N., Kinderman, F.S., Kim, C., von Daake, S., Chen, L., Wang, B.C., and Taylor, S.S. (2010). Structure of D-AKAP2:PKA RI complex: insights into AKAP specificity and selectivity. Structure *18*, 155-166.

Sastri, M., Barraclough, D.M., Carmichael, P.T., and Taylor, S.S. (2005). A-kinase-interacting protein localizes protein kinase A in the nucleus. Proc Natl Acad Sci U S A *102*, 349-354.

Scheeff, E.D., Eswaran, J., Bunkoczi, G., Knapp, S., and Manning, G. (2009). Structure of the pseudokinase VRK3 reveals a degraded catalytic site, a highly conserved kinase fold, and a putative regulatory binding site. Structure *17*, 128-138.

Schindler, T., Bornmann, W., Pellicena, P., Miller, W.T., Clarkson, B., and Kuriyan, J. (2000). Structural mechanism for STI-571 inhibition of abelson tyrosine kinase. Science *289*, 1938-1942.

Schulze-Gahmen, U., De Bondt, H.L., and Kim, S.H. (1996). High-resolution crystal structures of human cyclin-dependent kinase 2 with and without ATP: bound waters and natural ligand as guides for inhibitor design. J Med Chem *39*, 4540-4546.

Song, H., Hanlon, N., Brown, N.R., Noble, M.E., Johnson, L.N., and Barford, D. (2001). Phosphoprotein-protein interactions revealed by the crystal structure of kinase-associated phosphatase in complex with phosphoCDK2. Mol Cell *7*, 615-626.

Sours, K.M., Kwok, S.C., Rachidi, T., Lee, T., Ring, A., Hoofnagle, A.N., Resing, K.A., and Ahn, N.G. (2008). Hydrogen-exchange mass spectrometry reveals activation-induced changes in the conformational mobility of p38alpha MAP kinase. J Mol Biol *379*, 1075-1093.

Steichen, J.M., Iyer, G.H., Li, S., Saldanha, S.A., Deal, M.S., Woods, V.L., Jr., and Taylor, S.S. (2010). Global consequences of activation loop phosphorylation on protein kinase A. J Biol Chem *285*, 3825-3832.

Steinberg, R.A., Cauthron, R.D., Symcox, M.M., and Shuntoh, H. (1993). Autoactivation of catalytic (C alpha) subunit of cyclic AMP-dependent protein kinase by phosphorylation of threonine 197. Mol Cell Biol *13*, 2332-2341.

Steinberg, S.F. (2012). Regulation of protein kinase d1 activity. Mol Pharmacol *81*, 284-291.

Stempka, L., Girod, A., Muller, H.J., Rincke, G., Marks, F., Gschwendt, M., and Bossemeyer, D. (1997). Phosphorylation of protein kinase Cdelta (PKCdelta) at threonine 505 is not a prerequisite for enzymatic activity. Expression of rat PKCdelta and an alanine 505 mutant in bacteria in a functional form. J Biol Chem *272*, 6805-6811.

Sunami, T., Byrne, N., Diehl, R.E., Funabashi, K., Hall, D.L., Ikuta, M., Patel, S.B., Shipman, J.M., Smith, R.F., Takahashi, I.*, et al.* (2010). Structural basis of human p70

ribosomal S6 kinase-1 regulation by activation loop phosphorylation. J Biol Chem *285*, 4587-4594.

Taylor, S.S., and Kornev, A.P. (2010). Protein kinases: evolution of dynamic regulatory proteins. Trends Biochem Sci.

Taylor, S.S., and Kornev, A.P. (2011). Protein kinases: evolution of dynamic regulatory proteins. Trends Biochem Sci *36*, 65-77.

Tholey, A., Pipkorn, R., Bossemeyer, D., Kinzel, V., and Reed, J. (2001). Influence of myristoylation, phosphorylation, and deamidation on the structural behavior of the N-terminus of the catalytic subunit of cAMP-dependent protein kinase. Biochemistry *40*, 225-231.

Torkamani, A., Kannan, N., Taylor, S.S., and Schork, N.J. (2008). Congenital disease SNPs target lineage specific structural elements in protein kinases. Proc Natl Acad Sci U S A *105*, 9011-9016.

Trevino, S.R., Scholtz, J.M., and Pace, C.N. (2007). Amino acid contribution to protein solubility: Asp, Glu, and Ser contribute more favorably than the other hydrophilic amino acids in RNase Sa. J Mol Biol *366*, 449-460.

Trevino, S.R., Scholtz, J.M., and Pace, C.N. (2008). Measuring and increasing protein solubility. J Pharm Sci *97*, 4155-4166.

Vigil, D., Blumenthal, D.K., Taylor, S.S., and Trewhella, J. (2006). Solution scattering reveals large differences in the global structures of type II protein kinase A isoforms. J Mol Biol *357*, 880-889.

Vogtherr, M., Saxena, K., Hoelder, S., Grimme, S., Betz, M., Schieborr, U., Pescatore, B., Robin, M., Delarbre, L., Langer, T.*, et al.* (2006). NMR characterization of kinase p38 dynamics in free and ligand-bound forms. Angew Chem Int Ed Engl *45*, 993-997.

Williams, M.R., Arthur, J.S., Balendran, A., van der Kaay, J., Poli, V., Cohen, P., and Alessi, D.R. (2000). The role of 3-phosphoinositide-dependent protein kinase 1 in activating AGC kinases defined in embryonic stem cells. Curr Biol *10*, 439-448.

Wilson, K.P., Fitzgibbon, M.J., Caron, P.R., Griffith, J.P., Chen, W., McCaffrey, P.G., Chambers, S.P., and Su, M.S. (1996). Crystal structure of p38 mitogen-activated protein kinase. J Biol Chem *271*, 27696-27700.

Wolanin, P.M., Thomason, P.A., and Stock, J.B. (2002). Histidine protein kinases: key signal transducers outside the animal kingdom. Genome Biol *3*, REVIEWS3013.

Wong, L., Jennings, P.A., and Adams, J.A. (2004). Communication pathways between the nucleotide pocket and distal regulatory sites in protein kinases. Acc Chem Res *37*, 304-311.

Wong, W., and Scott, J.D. (2004). AKAP signalling complexes: focal points in space and time. Nat Rev Mol Cell Biol *5*, 959-970.

Woods, V.L., Jr., and Hamuro, Y. (2001). High resolution, high-throughput amide deuterium exchange-mass spectrometry (DXMS) determination of protein binding site structure and dynamics: utility in pharmaceutical design. J Cell Biochem Suppl *Suppl 37*, 89-98.

Wu, J., Brown, S.H., von Daake, S., and Taylor, S.S. (2007). PKA type IIalpha holoenzyme reveals a combinatorial strategy for isoform diversity. Science *318*, 274-279.

Wu, J., Yang, J., Kannan, N., Madhusudan, Xuong, N.H., Ten Eyck, L.F., and Taylor, S.S. (2005). Crystal structure of the E230Q mutant of cAMP-dependent protein kinase reveals an unexpected apoenzyme conformation and an extended N-terminal A helix. Protein Sci *14*, 2871-2879.

Xu, W., Doshi, A., Lei, M., Eck, M.J., and Harrison, S.C. (1999). Crystal structures of c-Src reveal features of its autoinhibitory mechanism. Mol Cell *3*, 629-638.

Yang, J., Cron, P., Thompson, V., Good, V.M., Hess, D., Hemmings, B.A., and Barford, D. (2002). Molecular mechanism for the regulation of protein kinase B/Akt by hydrophobic motif phosphorylation. Mol Cell *9*, 1227-1240.

Yang, J., Garrod, S.M., Deal, M.S., Anand, G.S., Woods, V.L., Jr., and Taylor, S. (2005). Allosteric network of cAMP-dependent protein kinase revealed by mutation of Tyr204 in the P+1 loop. J Mol Biol *346*, 191-201.

Yang, J., Kennedy, E.J., Wu, J., Deal, M.S., Pennypacker, J., Ghosh, G., and Taylor, S.S. (2009). Contribution of non-catalytic core residues to activity and regulation in protein kinase A. J Biol Chem *284*, 6241-6248.

Yang, J., Ten Eyck, L.F., Xuong, N.H., and Taylor, S.S. (2004). Crystal structure of a cAMP-dependent protein kinase mutant at 1.26A: new insights into the catalytic mechanism. J Mol Biol *336*, 473-487.

Yang, J., Wu, J., Steichen, J.M., Kornev, A.P., Deal, M.S., Li, S., Sankaran, B., Woods, V.L., Jr., and Taylor, S.S. (2012). A conserved glu-arg salt bridge connects coevolved motifs that define the eukaryotic protein kinase fold. J Mol Biol *415*, 666-679.

Yonemoto, W., Garrod, S.M., Bell, S.M., and Taylor, S.S. (1993a). Identification of phosphorylation sites in the recombinant catalytic subunit of cAMP-dependent protein kinase. J Biol Chem *268*, 18626-18632.

Yonemoto, W., McGlone, M.L., Grant, B., and Taylor, S.S. (1997). Autophosphorylation of the catalytic subunit of cAMP-dependent protein kinase in Escherichia coli. Protein Eng *10*, 915-925.

Yonemoto, W., McGlone, M.L., and Taylor, S.S. (1993b). N-myristylation of the catalytic subunit of cAMP-dependent protein kinase conveys structural stability. J Biol Chem *268*, 2348-2352.

Zeqiraj, E., and van Aalten, D.M. (2010). Pseudokinases-remnants of evolution or key allosteric regulators? Curr Opin Struct Biol *20*, 772-781.

Zhang, F., Strand, A., Robbins, D., Cobb, M.H., and Goldsmith, E.J. (1994). Atomic structure of the MAP kinase ERK2 at 2.3 A resolution. Nature *367*, 704-711.

Zhang, P., Smith-Nguyen, E.V., Keshwani, M.M., Deal, M.S., Kornev, A.P., and Taylor, S.S. (2012). Structure and allostery of the PKA RIIbeta tetrameric holoenzyme. Science *335*, 712-716.